

University of Nevada, Reno

Auto-inhibition in Calcium-dependent Protein Kinase CPK34
Results from a Combination of Competitive and Non-competitive Mechanisms

A thesis submitted in partial fulfillment of the
requirements for the degree of Master of Science in
Biochemistry

by
Saemin Chang

Dr. Jeffrey F. Harper / Thesis Advisor

August, 2013



University of Nevada, Reno
Statewide • Worldwide

THE GRADUATE SCHOOL

We recommend that the thesis
prepared under our supervision by

SAEMIN CHANG

entitled

**Auto-inhibition in Calcium-dependent Protein Kinase CPK34 Results from a
Combination of Competitive and Non-competitive Mechanisms**

be accepted in partial fulfillment of the
requirements for the degree of

MASTER OF SCIENCE

Jeffrey F. Harper, Ph. D., Advisor

John C. Cushman, Ph. D., Committee Member

William E. Courchesne, Ph. D., Graduate School Representative

Marsha H. Read, Ph. D., Dean, Graduate School

August, 2013

Auto-inhibition in Calcium-dependent Protein Kinase CPK34 Results from a Combination of Competitive and Non-competitive Mechanisms

Abstract

Calcium-dependent protein kinases (CPKs) are Ser/Thr protein kinases that are present in plants, ciliates and apicomplexan parasites. CPKs have a novel structure in which the kinase domain is connected to a calcium-sensing calmodulin-like domain (CaM-LD). The kinase and CaM-LD are connected via an auto-inhibitory junction sequence that can block the enzyme's active site. Like calmodulin, the CaM-LD for a typical CPK contains four calcium-binding EF-hands. The kinase is activated when Ca^{2+} binding to the CaM-LD changes the enzymes conformation. This conformational change is proposed to either directly disengage the auto-inhibitor from a pseudo-substrate competitive binding interaction with the active site (model-1), or disrupt a non-competitive inhibitory structure that alters access to, or conformation of, the active site (model-2).

Here we engineered each of the four EF-hands with Ala substitutions designed to disrupt key Ca^{2+} -binding ligand interactions at positions -1 and -12 within each EF hand. The mutant enzymes were expressed and purified from *Escherichia. coli*, and then used for *in vitro* kinase assays with Syntide-2 as a substrate. All four EF-hand mutants showed a 2-fold increase in the amount of Ca^{2+} required for activation, as well as a more than 2-fold decrease in their maximum activity. These results are consistent with a model in which each EF-hand mutation created a partially inhibited enzyme that was unable to fully disengage from their auto-inhibited conformation. Interestingly, peptide substrate K_M determinations indicated that the partially autoinhibited conformations were not

equivalent for all four EF-hand mutants. For EF 1 and -2 mutants, the peptide substrate K_M for Syntide-2 was 3-fold weaker compared to WT. This is consistent with model-1 in which the auto-inhibitor can function as a competitive inhibitor with respect to a peptide substrate. In contrast, EF3 and 4 mutants showed K_M 's comparable to WT (only about 1.3-fold weaker), suggesting that these enzymes are still partially inhibited through a non-competitive mechanism. This study provides biochemical evidence that auto-inhibition in a CPK results from a combination of competitive and non-competitive mechanisms, with the N- and C-terminal lobes having kinetically distinct functions.

Additional substitutions were made in EF2 to separately test the role of all five residues that have side chains that help coordinate calcium (residue positions-1, -3, -5, -9 and -12 in EF-loop). We found that an Ala substitution of each of the five residues significantly disrupted enzyme activation. Four of the five substitutions (all but position-3) resulted in a more than 2-fold decrease in V_{max} , regardless of using high calcium concentrations. The enzymes' 50% calcium activation thresholds (K') were observed at $[Ca^{2+}] \approx 1 \mu M$ in most cases except D420A mutant (position-3). The K' of D420A mutant was observed at $[Ca^{2+}] \approx 83 \mu M$, and its activity could be restored to near wild type levels at $[Ca^{2+}] \approx 600 \mu M$. This suggests that the primary contribution of position-3 in EF2 is to simply increase calcium affinity. In contrast, mutants with Ala substitutions at the other four positions displayed reduced activity that could not be further activated by elevated $[Ca^{2+}]$. This indicates that positions-1, -5, -9 and -12 are not only important for overall calcium affinity, but that calcium binding to each position is required to promote a conformational change that disrupts auto-inhibition.

Transgenes encoding CPK34 with selected EF-hand mutations were used to create stably transformed *Arabidopsis* plants, and tested for their ability to rescue a pollen growth and fertility defect associated with a loss of, *cpk17/34* (-/-, -/-). Seed set analysis showed that Ala substitutions of position-12 in any of the four EF-hands resulted in *cpk17/34* (-/-, -/-) plants with a partial restoration of seed set. In pollen transmission assays in which rescued mutant pollen were tested in competition with wild type pollen, the EF-hand mutants provided more than 10-fold weaker transmission efficiencies compared to a control wild type *CPK34* transgene. In both seed set and pollen transmission assays, the most severely disrupted rescue potential was associated with EF2 mutations, and the least disrupted with EF3 mutations. These partial rescues are consistent with *in vitro* biochemical evidence indicating that mutant enzymes still retained partial activity, albeit with weaker calcium activation thresholds and reduced V_{\max} 's.

Using the seed set rescue assay to compare the relative effects of Ala substitutions of EF2 positions-1, -3 and -12, the weakest rescue potential occurred with a position-3 substitution, D420A. This is interesting because CPK34-D420A can attain near wild type levels of activity at high $[Ca^{2+}]$. However, at less than 1 μ M calcium, the D420A mutant has less activity than Ala substitutions of position-1 or -12 (of all EF-hand mutants). This suggests that the D420A mutant can be used as an *in vivo* gauge for calcium concentrations at the plasma membrane during pollen tube tip growth, and supports an estimate that CPK34 functions are normally being activated by Ca^{2+} signals with magnitudes of less than 1 μ M.

Contents

Abstract	i
List of Tables	vii
List of Figures	viii
1. Introduction	
1.1 Calcium-dependent protein kinases (CPKs)	1
1.2 Calmodulin-like domains (CaM-LD) of CPKs	2
1.3 The canonical structure and sequence of EF-hand	3
1.4 EF-hand mutational studies on calmodulin	4
1.5 Hypothesis for CPK activation	5
2 Material and Methods	
2.1 Plasmid constructs	6
2.2 Recombinant protein expression and purification	6
2.3 Calcium concentration measurement	7
2.4 <i>In vitro</i> kinase assays	8
2.5 Plant transformation	8
2.6 Transmission efficiency tests and seed set counting assay	8
3 Results	
3.1 Alanine substitutions at position 1 or 12 in each of the four EF-hands impair Ca-activation of CPK34	9
3.2 Each mutation of internal residues within EF2 impairs calcium activation differently	11

3.3 The influence of EF-hand mutations on active site shows paired pattern; N-terminal EF hand mutant pair has higher K_M 's than C-terminal EF-hand mutant pair	13
3.4 <i>In vivo</i> Seed Set Count Assay shows impaired rescue by EF-hand mutants and EF2 mutant shows the least seed set numbers among four EF-hand mutants	15
3.5 Transmission Efficiency Assay shows poor rescue by EF-hand mutants compared to WT, but EF3 mutant shows higher rescue among four EF-hand mutants	16
3.6 Transmission Efficiency Assay shows competitive rescue by EF-hand mutants compared to <i>cpk17/34</i> (-/-, -/-), but EF2 D420A mutant shows poor rescue in comparison with position-12 EF-hand mutants	17
4 Discussion	
4.1 Single mutation in EF-hands disrupts overall conformation	18
4.2 EF3 hand is a conduit of cooperation between N- and C-terminal	20
4.3 EF2 D420A mutant lowers calcium binding affinity only and its specific activity increases to the magnitude of WT as calcium concentration increases	22
4.4 D426A mutation lowers negative charger repulsion within EF2 and increases cooperativity	23
4.5 N426D mutation increases negative charge repulsion within EF2, but it increases cooperativity	24
4.6 Kinase assays of EF hand mutants under substrate concentration variation reveals that N- and C-terminal lobe affect auto-inhibitor differently	25

4.7 Unknown factor(s) may compensate EF3 mutant defects	26
5 Conclusion	27
References	28
Appendix A DNA sequences of plasmid constructs used in this study	59
Appendix B Calcium calibration curve with Fluo-3	72
Appendix C Calcium calibration curve with Calcium Green 5	73
Appendix D Calcium concentration measurement	74

List of Tables

Table 1. The sequence preference of the EF-hand loop	54
Table 2. Summary of mutations and their assay results	55
Table 3. Pollination transmission efficiency assay, competition with wild type	56
Table 4. Pollination transmission efficiency assay, competition with <i>cpk17/34</i>	58

List of Figures

Figure 1. Diagrammatic representation of the domain structure of CPK	34
Figure 2. Activation of CPK through intramolecular binding of the CaM-LD	35
Figure 3. Specific activities for EF-hand (1 to 4) mutants vs. calcium concentration	36
Figure 4. Calcium concentration at 50% activation, K' , of EF-hand (1 to 4) mutants	37
Figure 5. Hill coefficients for EF-hand (1 to 4) mutants	38
Figure 6. Specific activities for mutants of EF2 vs. calcium concentration	39
Figure 7. Calcium concentration at 50% activation, K' , of EF2 mutants	40
Figure 8. Hill coefficients for EF2 mutants	41
Figure 9. Specific activities for EF-hand (1 to 4) mutants vs. syntide-2 concentration	42
Figure 10. Michaelis-Menten constants, K_M , for EF-hand (1 to 4) mutants	43
Figure 11. Wild type and D420A K_M variation at different calcium concentration	44
Figure 12. Number of seeds per silique	45
Figure 13. Transmission efficiencies of EF-hand mutants	46
Figure 14. Native gel electrophoretic mobility of mutant calmodulins	47
Figure 15. Changes in side-chain conformation I	48
Figure 16. Changes in side-chain conformation II	49
Figure 17. Changes in side-chain conformation III	50
Figure 18. Hypothetical coordination model of EF2	51
Figure 19. Comparison of specific activities at low $[Ca^{2+}]$	52
Figure 20. Comparison of rescue activity of transgenes	53

1 Introduction

1.1 Calcium-dependent protein kinases (CPKs)

Calcium, as a second messenger, plays an important role in many aspects of plant growth and development, including the response of plants to biotic and abiotic stress. Response to this calcium signal is an important biological issue. In plants, there are several calcium-binding sensory proteins, including calmodulins, calcium-dependent protein kinases (CPKs), and calcineurin B-like proteins. Among them, CPKs are the best characterized and are of particular interest of this study. CPKs are serine/threonine protein kinases that are found in plants and protozoa. CPKs are structurally unique for having two distinct protein characters, a kinase and a regulatory domain, in a single peptide molecule. In addition, the N-terminal domain locates ahead of the kinase domain, and the auto-inhibitory junction domain exists between the kinase domain and the calcium-binding regulatory domain (Figure 1). The role of the N-terminal domain is not well known, but has been proposed to direct subcellular localization (Schaller and Sussman, 1988; Hrabak et al., 1996). Recently, the involvement of the N-terminal domain of tobacco CPK in substrate specificity has been reported (Ito et al., 2010). The N-terminal domain is variable in amino acid sequence and length (Cheng et al., 2002) as well as in its function. The catalytic kinase domain is responsible for phosphorylating a target protein within its signaling cascade.

The auto-inhibitory junction domain is a highly conserved 31 amino acid sequence within plant CPKs, and its function was proposed to function as an auto-inhibitor (Roberts and Harmon, 1992; Harper et al., 1993, 1994). The C-terminal calcium binding regulatory domain is highly similar to calmodulin in that it contains helix-loop-helix type EF-hand

motifs for calcium binding, thus this domain is called the calmodulin-like domain (CaM-LD). In *Arabidopsis*, 34 CPK genes were identified (Hrabak et al., 2003), of which 12 genes are expressed in pollen (Becker et al., 2003; Harper et al., 2004). Of those 12 highly expressed CPKs in pollen, CPK17 and CPK34 were found to localize on the plasma membrane of the pollen tube and were identified to have redundant activity, as indicated by the failure to detect a phenotype with single knockouts and the ability to rescue the *cpk17/34* pollen transmission defect through the expression of CPK34 alone (Myers et al., 2009).

1. 2 Calmodulin-like domain (CaM-LD) of CPKs

C-terminal domain of CPKs contains calcium-binding EF-hands resembling those found in calmodulin. These EF-hands allow the CPKs (or CaM-LD) to function as a calcium sensor. Specifically, in response to transient increases in the cellular calcium concentration, CaM-LD undergoes conformational changes that activate kinase domain to regulate other proteins by means of phosphorylation. Each EF-hand consists of a loop of 12 amino acid residues between two α -helices. A single calcium ion is bound to each EF-hand via the loop domain. In most cases, CaM-LD has four EF-hand motifs. The crystal structure of calmodulin (Babu et al., 1988) and CaM-LD (Wernimont et al., 2011) revealed that there are two distinct globular domains (N- and C-terminal lobes) and two EF-hand motifs reside in each lobe. Within each lobe, the pair of EF-hand motifs is cooperative for binding calcium (Starovasnik et al., 1992; Biekofsky et al., 1998). In addition, the cooperativity between two lobes was also reported (Mukherjea et al., 1996).

1. 3 The canonical structure and sequence of EF-hand motifs

An EF-hand, calcium-binding motif, was named after the E and F helices of parvalbumin. Parvalbumin is a calcium-binding albumin protein that is comprised of six helices, helix-A through F. Each two helices are in a pair and linked by a short loop region. Among these three pairs of helix-loop-helix motifs, the loop regions of CD and EF motifs have calcium-binding ability, whereas the AB motif does not (Kretsinger, 1976). The sequences of this calcium binding loop region and the helix-loop-helix structure are highly conserved among calcium-binding proteins. The canonical sequence of the EF-hand loop region is listed in Table 1. The number of amino acid residues in this loop region is called twelve conventionally, but the last three residues are not part of the loop and actually belong to the exiting helix (F helix). Ca^{2+} has pentagonal bipyramidal coordination geometry and requires seven coordinating groups. Five of seven coordinating groups are provided by the nine-residue loop and the remaining two come form a bidentate carboxylate ligand supplied by the side chain of an acidic amino acid located in the exiting helix (F helix). Among those twelve amino acid residues, calcium-coordinating residues are especially well conserved as acidic residues. Interestingly, in many cases, the water molecule is found on the $-X$ axis and is held by hydrogen bonds to the side chain of position-9 residue. The amino acid of the position-9 is variable, but it is conserved to have a hydrogen bond-donating side chain group. Another remarkable coordinating group is $-Y$ axis that is carbonyl oxygen of the peptide back bone of position-7. Even though the most common amino acid for this residue is Thr, this position-7 is the most variable (acidic, basic, hydrophobic, polar...) residue among the six coordinating residues.

Among non-coordinating residues within the loop, position-6 and -8 are noticeable. Gly is found at position-6 in most cases, which renders flexibility to the loop. For position-8, hydrophobic amino acids, Ile, Val, and Leu, are conserved. Peptide backbone at position-8 is hydrogen bonded to peptide backbone at position-8 of another EF-hand in a pair (Juranić et al., 2009) upon calcium binding. Position-8 is considered as a conduit for the cooperativity within a pair. The role of hydrophobic side chains at this specific residue needs further investigation.

1. 4 EF-hand mutational studies on calmodulin

Calmodulin is a Ca^{2+} binding protein that exists in all eukaryotic cells and highly conserved in its overall structure and, especially, in the sequence of its calcium binding motif, EF-hand. Calmodulin is a small cytosolic protein of which molecular weight is about 17 kd and 148 amino acids (Kretsinger, 1976; Nakayama and Kretsinger, 1994). Calmodulin senses the signal transmitted by Ca^{2+} , a secondary messenger, and relays the signal to downstream protein by binding on it. Calmodulin changes its conformation as it binds Ca^{2+} , and then it binds to its target enzyme. The downstream target protein becomes activated and signals are transduced (Cheung, 1980; Means and Dedman, 1980). Calmodulin has four EF-hands as a calcium-binding motif. These four EF-hands are grouped into two pairs, N- and C-terminal pairs. The EF-hands in each pair work cooperatively, and these two pairs are separated by two or three short helices in an apo state (Zhang et al., 1995). These short helices turn into one stretch of seven- or eight-turn helix when four calcium ions are loaded on the EF-hands (Babu et al., 1988), thus hydrophobic surface is exposed and this surface is the site for binding target proteins

(Putkey et al., 1988; VanBerkum et al., 1990; Persechini et al., 1989). The intrinsic binding affinities of EF-hand binding motifs from all four EF-hands are the same when the calmodulin is unfolded (Stigler et al., 2011; Stigler and Rief, 2012), the conformation in apo state provides the EF-hands different binding affinities. The C-terminal EF-hands (EF3 and EF4) have higher calcium-binding affinity than the N-terminal EF-hands in calmodulin (Burger et al., 1984; Linse et al., 1991). In addition, there is cooperative calcium binding on two EF-hands within a domain. However, interdomain cooperativity is found only in the presence of target protein (Ikura et al., 1989; Yazawa et al., 1987).

1. 5 Hypothesis for CPK activation

In the basal state, the auto-inhibitor functions as a pseudosubstrate and blocks the active site of CPKs. Upon Ca^{2+} stimulation, binding of calcium to CaM-LD (N-lobe) triggers a conformational change in CaM-LD, and then, intramolecular interaction between CaM-LD and auto-inhibitor is altered, subsequently, the auto-inhibitor is disengaged from the active site (Figure 2). The model shown in the figure emphasizes the different functional roles of the N- and C-terminal lobes of the CaM-LD, in which Ca^{2+} activation was shown to be dependent upon Ca^{2+} -binding EF-hands in the N-terminal lobe, but not the C-terminal lobe. These examples were found both from the studies from *P. falciparum* (Zhao et al., 1994) and *A. thaliana* (Christodoulou et al., 2004) CPK's. In this study, the goal was to characterize the interaction between the auto-inhibitor and the CaM-LD, in terms of competitive or non-competitive modes of inhibition.

2 Materials and Methods

2.1 Plasmid Constructs

For the production of GST-CPK34-6His fusion protein in *E. coli*, the clone was made as cDNA subcloned into a pGEX expression vector with a GST N-terminal affinity tag, and modified to include a C-terminal 6×His tag (Harper et al., 1994). The constructs of the EF-hand mutant fusion proteins were generated by overlap extension PCR with the primers in which suitable mutations were introduced, using the WT CPK34 fusion protein construct as a template. New suitable restriction sites were introduced by the silent mutations at each mutagenesis for selection and all amino acids are identical except for the intended mutation residue. The sequences were confirmed by DNA sequencing and the full sequences can be found in Appendix A. For plant transformation, each mutant construct was cut and inserted into the plant vector; *CPK34-promoter:[construct]-TAP2(YFP)*.

2.2 Recombinant Protein Expression and Purification

All kinase fusion proteins (including mutants) were purified as affinity sandwiches using a 6× His tag at the C-terminal end and a GST tag at the N-terminal end (Harper et al., 1994). Each protein was affinity-purified by a 6×His tag at the C-terminal end, followed by a GST tag at the N-terminal end, using Ni-NTA Superflow (Qiagen, Valencia, CA) and Glutathion HiCap Matrix (Qiagen, Valencia, CA), respectively.

2. 3 Calcium concentration measurement

Calcium concentration of kinase assay buffers was measured using two calcium dyes, Fluo-3 (for less than 1 μM) and Calcium Green 5 (for over 1 μM) because the calcium concentration range was wider than the range of any of single dye. Calcium calibration buffer kit (Molecular Probes, Eugene, OR, USA) was used to make two series of standard calcium concentration buffers for two dyes, respectively. A standard calcium calibration curve from each series was drawn and calcium concentration of kinase reaction buffer was calculated from the fitting function of the curve. Buffer 10 and 11 were measured with both dyes and the calcium concentrations of each buffer from two series were found compatible. A total 8 of buffers (buffer #1 and #7-13) were used for kinase assay. The samples of kinase reaction buffer were prepared as kinase assays performed, but protein was not included. Calibration curves and the concentration of assay buffers are show in Appendix B, C, and D.

2. 4 *In vitro* kinase assays

Kinase activity assays were performed basically as described (Cohen et al., 2006). A typical reaction volume was 50 μl and combined by 10 μl of each of the following five components; Water, kinase reaction buffer (with varying Ca^{2+} concentration, Tris-HCl 100 mM, MgCl_2 50 mM, EGTA 5 mM, pH 7.5), BSA (2.5 mg/ml) or BSA (2.5 mg/ml) +Syntide-2 (500 μM), CPK-fusion protein (0.01 $\mu\text{g}/\mu\text{l}$ in enzyme dilution buffer containing 20 mM Tris-HCl, 10% Glycerine, pH 7.5), and ATP (1.5 mM + 2.0 μCi $^{33}\text{P}[\gamma\text{-ATP}]$). Briefly, kinase reactions were started by adding 10 μl of ATP (final concentration of 300 μM ATP plus 2.0 μCi $^{33}\text{P}[\gamma\text{-ATP}]$) to a reaction that consisted of the

other four components. This reaction was allowed to proceed at RT for 16 min and was stopped by spotting a 20 μ l aliquot onto P81 phosphocellulose chromatography paper (GE Healthcare Biosciences, Piscataway, NJ, USA) and immediately immersing into 75 mM phosphoric acid. Filters were further washed four times with 250 ml of 75 mM phosphoric acid for 15 minutes (each) with gentle agitation. After washing, the filters were rinsed with 70% EtOH and air-dried. Dry filters were submerged in Optiphase Supermix (Perkin Elmer, Waltham, MA, USA) and ^{33}P counts were determined by a scintillation counter (MicroBeta TriLux, Perkin Elmer, Waltham, MA, USA). To calculate specific activities in nmol P incorporated/min/mg enzyme, the total amount of ^{33}P label in reactions was determined by counting a 20 μ l aliquot of a sample reaction that was dried on filter paper and left unwashed.

2. 5 Plant transformation

Transformation of *Arabidopsis thaliana* (ecotype Col-0) were done through a floral dip protocol using *Agrobacterium tumefaciens* strain GV 3101 containing the helper plasmid pSoup (Clough and Bent, 1998).

2. 6 Transmission efficiency tests and seed set counting assay

Mutant CPK constructs were transformed into a plant line, *cpk 17-5(-/-) / 34-1(+/-)*, in which Basta resistance marker associated with the 34-1 allele. In this background, all of the pollen will have a *cpk17-5(-)* genotype, and half will also have a *cpk34-1(-)* mutation. Because the *cpk34-1* allele has linked Basta-resistance marker in the T-DNA insertion, the transmission frequency of the *cpk17-5/34-1* pollen can be assayed by scoring

offspring for the presence of Basta-resistance. These assays were done by crossing pollen to a female *cpk17-2 (-/-)/34-2 (-/-)*. By using another *cpk17/34* double knockout as a female recipient, any offspring that resulted from a male transmission of the Basta-resistance would have a double knockout background of *cpk17-5/17-1, 34-2/34-1*. Representative offspring were genotyped from each cross to insure the absence of unanticipated cross pollination from other plants, and rescued plant lines were grown up to evaluate their seed set levels.

3 Results

3.1 Alanine substitutions at position 1 or 12 in each of the four EF-hands impair Ca-activation of CPK34

To determine the relative importance of each of the four EF-hands in the calmodulin-like regulatory domain, the acidic residues in positions-1 and -12 of each EF-hand were independently substituted with an Ala. For example, EF-hand 1 was mutated to have either a D382A (position-1) or E393A (position-12) substitution (Figure 1). All eight mutant enzymes showed more than a 2-fold reduction in V_{max} compared to wild type (Figure 3), and were fully activated around 4 μ M calcium concentration. There was very little additional increase in activity observed by increasing calcium concentration to 100 μ M. The greatest reduction in V_{max} resulted from mutations in EF-hands 1 and 3 in the N- and C-terminal lobes, respectively. For example, Ala substitutions in position 1 in both EF-1 and -3 (respectively, D382A and D454A) resulted in an approximately 10-fold reduction in V_{max} (at 4 or 100 μ M), which indicates that disruptions of calcium binding in both the N- and C-terminal lobes can impair activation to an equivalent degree. A

calcium response for the activation of a wild type CPK34 showed a sigmoid curve (Figure 3). This is consistent with the presence of a calmodulin-like domain in which four EF-hands bind calcium in a cooperative manner (Christodoulou et al., 2004). In the assay conditions used here, the activation of wild type CPK34 showed a K' of 0.6 μM , and a Hill coefficient of 4.5 (Figure 3 and 4). In comparison, all eight mutations resulted in decreased sensitivities to calcium, with EF-3 mutations being the most disruptive (K' of 1.3 μM , Hill coefficient 1.8). While calcium sensitivities were decreased for all eight mutations, the magnitudes of the disruptions did not correlate with their relative decreases in V_{max} . For example, while both EF-1 and -3 mutations resulted in the most severe decreases in V_{max} , EF-1 mutants resulted small shift in K' (from 0.6 μM of WT to 0.9 μM), whereas EF-3 mutants resulted the largest shift (to 1.3 μM). These results indicate that calcium binding to each of the four EF-hands plays a critical role in enzyme activation. However, because none of mutants could be restored to full activity by simply increasing calcium concentrations to 100 μM , the defects associated with Ala substitutions of positions-1 and -12 do more than simply weaken calcium affinity. The evidence here indicates that positions-1 and -12 in all four EF-hands are important for calcium binding as well as a subsequent conformational change required for full activation of the enzyme. While each of the coordinating positions in an EF-hand are expected to contribute to the calcium-binding affinity, a subset of residues are also expected to be essential for transforming the calcium-binding interaction into a subsequent conformational change that activates the enzyme.

3. 2 Each mutation of internal residues within EF2 impairs calcium activation differently

To further investigate the role of different calcium-coordinating residues within an EF-hand, EF-hand 2 with 3 substitutions at positions-3, -5, and -9, were engineered independently and in combination. EF-2 was chosen for more extensive analysis because mutations of positions-1 and -12 (D418A and E429A) resulted in mutant enzymes with high specific activities, thus, difference between mutants might be more easily observed in case that additional mutants would generate very little change with respect to one another. In addition, EF-2 resulted in intermediate level of Hill coefficients and K' 's compared to other mutants. This intermediate starting point was considered ideal, as it provided the expectation that further mutations in EF-hand 2 could result in further decreases or relative increase. First of all, the EF-hand 2 mutants that showed the most severe decrease in V_{max} was one in which all five positions involved in coordinating calcium were substituted with alanines (aka. 5 A's in Figure 6). The activity of this enzyme was approximately 10-fold lower than either of the single substitutions at position-1 or -12. Because the activity was so low, it was not possible to quantify a K' or Hill coefficient. This low activity emphasizes that complete disruption of key calcium binding coordination sites in just one EF-hand is sufficient to effectively inactivated the enzyme. With one exception (D420A), all other single Ala substitutions resulted in mutant enzymes with reductions in V_{max} similar to what was observed for Ala substitutions of positions-1 and -12. The K' and Hill coefficients were also very similar, suggesting that positions-1, -5, -9, and -12 all functioned in an equivalent way to help bind calcium and change the conformation of the regulatory domain. In contrast, the

position-3 substitution of D420A showed decreases in calcium sensitivity, but failed to show a clear change in V_{\max} . The V_{\max} appeared to increase to near wild type levels as calcium concentration was further increased from 300 and 600 μM at same time, the K' was approximate 82-fold higher than that for a position 1 substitution, and the Hill coefficient was calculated to be less than 1. This is consistent with the hypothesis that position-3 is critical to calcium affinity, but less important than the other 5 positions for the subsequent structural changes that change the conformation of the regulatory domain and release the enzyme from auto-inhibition. To determine if we could also modify position-12 to partially weaken the calcium affinity without changing the V_{\max} , we engineered an E429D substitution to shorten the length of the acidic side chain by the distance of one carbon atom. Surprisingly this “1-carbon” shortening was just as disruptive as completely eliminating the acidic side group with an E429A substitution, as evidenced by a similar decrease in V_{\max} and Hill coefficients, as well as equivalent increases in the K' . To determine if we could increase calcium affinity, position-5 was substituted with an N422D to replace the predicted polar interaction between Asn and calcium, with a stronger charge – charge interaction. This mutation increased the cooperativity of the calcium response, as shown by an increase in the Hill coefficient from 4.5 to almost 6. However, the overall V_{\max} was still reduced by nearly 2-fold. This suggests that while the N422D might have enhanced calcium binding, it nevertheless failed to mediate the optimal conformational change required to fully activate the enzyme. The position-5 and -12 are in opposite ends of Z axis in pentagonal bipyramidal calcium coordination (Figure 18). Thus the mutant, N422D+E429D, has both increasing and decreasing factors for calcium affinity in the EF2 at same time. Specific activity, K' ,

and Hill coefficient of this double mutant were obtained in mid-range between two single mutants, N422D and E429D. These opposite effects seemed to compromise each other without further disruption of conformation.

3.3 The influence of EF-hand mutations on active site shows paired pattern; N-terminal EF-hand mutant pair has higher K_M 's than C-terminal EF-hand mutant pair.

To investigate the effect of regulatory CaM-LD on active site, four mutants representing each EF-hand, E393A (EF1), E429A (EF2), E465A (EF3), and E500A (EF4), were chosen to perform kinase activity assay at fixed calcium concentration (100 μM for full activity) and with varied substrate concentration (from zero to 200 μM). Each of these mutants has the mutation on its position-12 on one of four EF-hands. The position-12 residue provides calcium ion two carboxylate oxygens as a bidentate ligand on $-Z$ axis and behaves as a lid in the binding pocket (Beckingham, 1991). Thus, mutation on this residue reduces calcium-binding affinity and enzyme activity effectively. The activation curves of this assay are hyperbolic which reaches to plateau at about [Syntide-2] = 100 μM (Figure 9). The activity of EF2 mutant seems increasing slightly more as the substrate concentration increases toward 200 μM , but it does not seem to increase far more close to WT curve. To determine if each of the four EF-hands has equivalent mechanistic functions in regulating auto-inhibition, the apparent peptide substrate K_M 's, the Michaelis-Menten constants, of these mutant enzymes were evaluated (Figure 10). While the N-terminal lobe (EF1 and -2) mutants resulted in K_M 's that were more than 4-5 fold higher than wild type, the C-terminal lobe mutations (FE hand 3 and 4) resulted in

K_M 's that were only marginally increased (1.3-fold). This difference indicates that the way in which mutant versions of the N- and C-terminal lobes mediate a partial auto-inhibition is different, despite that fact these mutations can decrease the V_{max} to equivalent degrees.

The peptide substrate K_M was also determined for the mutant with an EF2 D420A substitution in position-3. In contrast to position-12 Ala substitutions, the position-3 D420A was the only mutation found in this study that appeared to simply decrease the calcium sensitivity, without a dramatic affect on V_{max} . This allowed us to assay the mutant enzyme with an expanded range of calcium concentrations and correlate different activation states with changes in the peptide substrate K_M (Figure. 11). In a weakly activated state of low calcium concentration, $[Ca^{2+}] = 0.88 \mu M$, the mutant enzyme showed a peptide substrate K_M that was 5-fold higher than wild type. This high K_M is similar to that observed for the EF2 mutant with a position 12 Ala substitution. However, when the position-3 D420A mutant was further activated by higher calcium concentration, 1.6 μM and 100 μM , the K_M shifted towards a wild type concentration. This is consistent with a model in which position-3 functions primarily to increase calcium affinity, as opposed to positions-1, -5, -9, and -12 in which the calcium ligand interactions are also important for mediating subsequent conformational changes. Results of kinase activity assays are summarized in Table 2.

3. 4 *In vivo* Seed Set Count Assay shows impaired rescue by EF-hand mutants and EF2 mutant shows the least seed set numbers among four EF-hand mutants

To evaluate the biological effects of different CPK34 EF-hand mutations on pollen tubes growth *in vivo*, selected mutants were stably transformed into plants, and tested for their ability to rescue a near sterile pollen phenotype associated with a double loss of function mutation *cpk17/34* (-/-, -/-) for two redundant CPKs, 17 and 34. At least ten independent transgenic plant lines were isolated for each mutant. The assays used to evaluate a transgene's ability to rescue the phenotype included, quantifying seed set in each silique and comparing pollen transmission in competition with either wild type pollen or non-rescued mutant pollen.

The average seed number per silique was determined (Figure 12). Wild type siliques normally have 50 to 60 seeds. In contrast, siliques from a *cpk17/34* knockout are usually empty, but those knockout siliques contain around one or two seeds per silique. As a positive control, *cpk17/34* plants rescued by a wild type CPK34-GFP transgene were found to have near wild type levels of seed set. As a negative control, a CPK34 transgene harboring a double substitution at position-12 in EF3 and -4 was previously shown to provide no significant increase in seed set (Myers et al., 2009). By contrast, Figure 10 shows that transgenes harboring only a single substitutions at position-12 in any of four EF-hands were able to provide a partial restoration of seed set to approximately 20 to 50 %. This indicates that the mutant enzymes retained enough function to restore most of seed set deficiency in a *cpk17/34* knockout in spite of more than 2-fold reduction in V_{max} , and a reduced calcium sensitivity. The weakest seed set restoration for any of the position-12 mutations was observed for plants rescued by EF2 D429A. To confirm that it

was not just a unique feature of position-12, plant lines rescued with a position 1 Ala substitution (EF2 D418A) were also assayed, and found to have a similar low level of seed set. The most significant decrease in seed set observed for any of single substitution mutation analyzed was for EF2 D420A (position-3 in EF2). In biochemical assays, this mutant enzyme was the exception that showed a decrease in calcium sensitivity, but still retained a near normal Vmax at very high calcium levels. While the seed set did appear to be slightly better than a non-rescued *cpk17/34*, it was equivalent to the seed set resulting from rescues by an EF2 mutant harboring a 5 Ala substitution at position-1, -3, -5, -9, and -12 (EF2 5A's). This suggests that the functional impact of EF2 D420A alone is just as severe as including four other substitutions that would eliminate all side chain calcium ligand interactions.

3. 5 Transmission Efficiency Assay shows poor rescue by EF-hand mutants compared to WT, but EF3 mutant shows higher rescue among four EF-hand mutants

Figure 13 shows results from pollen transmission assays. In these assays, a perfect rescue of the *cpk17/34* pollen infertility phenotype would result in 33% of the F1 offspring showing Basta-resistance. The reason for 33% instead of 50% is that only 3 of the 4 possible meiotic products have the potential for transmission. This is because any *cpk17/34* pollen without a rescue transgene is effectively sterile and will not produce offspring. As a positive control, a wild type CPK34 transgene was observed to provide around 30% transmission. In contrast, relatively poor transmission frequencies were observed using transgenes harboring EF-hand mutations. Of the CPK34 mutants with

position-12 Ala substitutions, EF3 E465A showed the highest average transmission at 2.3% (average of four best lines among 17 plant lines, Figure 13), which was still 15-fold lower than the expected transmission frequency. The average of all plant lines is still the highest at 0.9% among the four EF-hand mutants (Table 3). The worst rescue of pollen transmission was 0.24% (of four highest plant lines, 0.10% for all 15 lines) observed for EF2 E429A, which is 140-fold lower than expected. This indicates that a CPK34 with position-12 Ala substitutions in any of the 4 EF-hands dramatically reduces its ability to compete with wild type pollen at some point during the pollen tube growth and fertilization.

3. 6 Transmission Efficiency Assay shows competitive rescue by EF-hand mutants compared to *cpk17/34* (-/-, -/-), but EF2 D420A mutant shows poor rescue in comparison with position-12 EF-hand mutants

A second type of pollen transmission assay was used to compare how well mutant pollen with a rescue construct could compete against a non-rescued mutant pollen (Table 4). In this assay, plant lines that are homozygous for *cpk17/34* and hemizygous for the transgene, were both used in reciprocal crosses and allowed to self fertilize. Since mutant pollen only show rare transmission events, this competition assay represents the most sensitive test to determine if a transgene provides any competitive advantage. As a negative control, the segregation of a vector only transgene was observed to provide no competitive advantage, and showed 50% expected transmission frequencies in reciprocal crosses, and 75% expected transmission frequency in self-fertilization. In contrast, representative plant lines partially rescued by EF-hand position-12 Ala substitutions, all

hemizygous transgenes showed 99 to 100% transmission through the male, indicating that pollen harboring a partially functional CPK34 EF-hand mutant was much more competitive than a mutant pollen without any “rescue activity”.

While the seed set assays did not provide a confident measurement of rescue for EF2 mutants with a position-3 substitution, EF2 D420A, the sensitivity of a mutant vs. rescued mutant segregation distortion assay was able to confirm a low level of rescue potential. In hemizygous plants allowed to self fertilize, two EF2 D420A lines showed average 92% transmission to F1 progeny (75% expected).

On the other hand, the five alanine substituted mutant (EF2 5A's) that was indistinguishable from EF2 D420A mutant in seed set assay, showed only 76% in self fertilization transmission frequency (75% expected) which is similar to vector only and indicates no CPK activity. These results indicate that the activity of EF2 D420A (position 3 mutant) is less than the position-12 mutant (E429A), but it is more active than the five-Ala-substituted mutant (position-1, -3, -5, -9, and -12). While a self fertilization assay was able to detect a measurable rescue, our attempt to examine the segregation in a pollen outcross failed, despite attempting more than 10 outcrosses for each line. This is consistent with a very weak level of rescue mediated by these EF2 mutants.

4 Discussion

4.1 Single mutation in EF-hands disrupts overall conformation

The sigmoid shape of the CPK activation curves depending on calcium concentration (Figure. 2) indicates that there is cooperativity among its calcium binding sites. In

addition the different maximum specific activity plateaus that were achieved at high calcium concentrations (over 2 μM) suggest that the mutation disrupts not only calcium binding affinity, but also overall conformation of protein for activation. If the mutation reduces only the binding affinity to calcium, the activities of mutants would have increased to that of WT at high concentration of calcium. The example of calmodulin in which a single mutation in the EF-hand loop disrupts overall folding of calmodulin was reported (Maune et al., 1992) and shown in Figure 14. In this example, neutral glutamine (Q) or positively charged lysine (K) substituted negatively charged glutamic acid (E) of position-12 in each EF-hand calcium-binding loop. As expected, positive calcium loaded WT and mutants moved more slowly toward the anode than unloaded proteins. Also neutral glutamine substituted mutants moved faster than positive lysine substituted series except for the EF4 mutants. However, two unexpected results were obtained. First, the less negative mutants showed higher, at least similar, mobility than WT towards the anode. Second, the four EF-hand mutants within either the Q or K mutant series showed different mobility. These two unexpected results suggested that single mutations on the calcium-binding loop of the EF-hand might cause an overall conformational change in calmodulin. In CPKs where CaM-LD is attached to the kinase domain via auto-inhibitory junction domain, single mutation on the EF-hand calcium-binding loops might cause the conformational change in regulatory calmodulin-like domain in both apo and holo states. The conformation of mutant CaM-LD might be unfavorable to remove the auto-inhibitory junction domain from the active site in the kinase domain, compared to WT. Thus, the specific activities of mutants were observed to be lower than those of WT.

4. 2 EF3 hand is a conduit of cooperation between N- and C-terminal

Based on the knowledge that C-terminal EF-hands have higher calcium affinities than N-terminal EF-hands (Burger et al., 1984; Linse et al., 1991), EF3 and EF4 hands are supposed to bind calcium ahead in EF1 and EF2 mutants. And then, one of the EF-hand in N-terminal lobe binds calcium. Probably, the non-mutated EF-hand might bind first and then, helps its partner to bind calcium, even though the partner is a mutated EF-hand. The smaller Hill coefficient of the EF2 mutant indicates that mutation in EF2-hand affects the calcium-binding affinity of the EF1-hand is greater than the reverse. This result was also shown earlier in the binding affinity study of mutant calmodulins (Starovasnik et al., 1992). The reason can be explained by NMR structural studies in which the isoleucines (the eighth residue among 12 loop residues) of EF1- and EF3-hands change their $H\alpha$ - $C\alpha$ - $C\beta$ - $H\beta$ conformation from gauche to trans by rotating the bond between $C\alpha$ and $C\beta$ upon calcium binding, whereas the conformation of isoleucines in EF2- and EF4-hands remain in trans in both absence and presence of calcium (Figure 15) (Biekofsky et al., 1998). This “gauche-to-trans” transition was observed only in NMR structural studies. These isoleucines of EF1- and EF3-hands change their conformation upon calcium binding to their partners (EF2 and EF4, respectively), not by binding to their own loops. EF1 of cTnC (cardiac troponin C) does not bind Ca^{2+} but showed rotation of Ile36 (in EF1) upon calcium binding to EF2 (Biekofsky et al., 1998). Ile27 (in EF1) of E31Q mutant (EF1 mutant) of calmodulin also showed conformational change (Starovasnik et al., 1992) upon calcium binding to EF2. In the other hand, E140Q (mutant in EF4) of the C-terminal domain of calmodulin did not show conformational rotation on Ile100 (in EF3) even with calcium bound on EF3 (Evenäs et al., 1997). These examples

of rotation and half-loaded states are depicted in Figure 16 and 17. These results could explain smaller Hill coefficients of EF2 mutants in comparison with EF1 mutants. This was possible because C-terminal lobe are supposed to be loaded already with calcium before the N-terminal lobe was loaded, so the mutational effect of N-terminal lobe on the calcium binding to C-terminal lobe might be negligible. But the comparison for EF-hands in C-terminal lobe is more complicated because calcium binding on any of the C-terminal lobes affects not only its partner, but also N-terminal EF-hands. Our results show that the Hill coefficients of EF3 mutants were larger than those of EF4 mutants, which should be reversed if the “gauche-to-trans” rotation is the only factor for the Hill coefficient of the C-terminal lobe. The small Hill coefficients of the EF3 mutants (both D454A and E465A, position-1 and -12, respectively) indicate that EF3 has more important role in conformational change of CaM-LD by relaying cooperation between N- and C-terminal as well as EF3 and EF4 hands. As shown in the X-ray structures of Ca-loaded and Ca-unloaded apicomplexan CPKs (Wernimont et al., 2010, 2011), a helix between EF2 and EF3 hands bends into two helices upon calcium binding. This bending motion is supposed to be a conduit between N- and C-terminal cooperation, which controls calcium binding to EF3 rather than to EF4. This hypothesis must be confirmed by further structural studies.

The isoleucines in EF-hand loops form a stable pairing of two EF-hands within a domain (Juranić et al., 2009), but the influence of the conformational change of hydrophobic isoleucine (sometimes valine or leucine) in EF1 and EF3 to overall conformation of the protein needs to be elucidated further.

4. 3 EF2 D420A mutant lowers calcium binding affinity only and its specific activity increases to the magnitude of WT as calcium concentration increases

Further mutational studies were performed within EF2. Among 12 EF-hand amino acid residues, 6 calcium coordinating amino acid residues were mutated into alanine one-by-one. In these mutant series, the D420A mutant (the third residue among 6 coordinating residues) showed a different pattern of activity compared with the other mutants. The activities of wild type and all other mutants increased as calcium concentration increased and then reached a plateau (Figure 6). But the D420A mutant did not reach a plateau and it kept increasing toward the maximum activity of wild type at around 600 μM . In another set of assays with increasing substrate concentration at fixed calcium concentrations (i.e., 0.88, 1.6, and 100 μM), the K_M 's of each set decreased close to the level of WT (Figure 11) as calcium concentration increases. Not like other mutants, D420A is considered to recover wild type native conformation for activation at higher calcium concentrations, even though it has weak activity due to low calcium-binding affinity at low calcium concentration. In this mutant, the mutation lowers calcium binding affinity only, it does not disrupt the overall conformation in the apo state significantly, and then, it recovers the fully active conformation of WT as calcium concentration increases. The roles of this residue, D420, are coordinating Ca^{2+} on Y axis, and, additionally, hydrogen-bonding to water molecule that coordinates Ca^{2+} on $-X$ axis (Waltersson et al., 1993). The first residue that locates next to the E-helix and the last residue that belongs in the beginning of the F-helix seems the most important to control the fully active conformation. Therefore, as long as the first and the last residues keep the E- and F- helix in position upon calcium binding and the $-X$ axis water molecule is held

by D426, the D420A mutation only lowers the binding affinity and does not disrupt overall structure.

The transgene plant with D420A (EF2 loop position-3) mutant provided lower numbers in seed set than four position-12 mutants and one position-1 mutant; E393A-EF1, E429A-EF2, E465A-EF3, E500A-EF4, and D418A-EF2 (Figure 12). The results from pollen transmission assay showed that the competence with the pollen harboring *cpk17/34* (-/-, -/-) was inferior to those four position-12 mutants (92% for D420A vs. 99-100% for other four mutants, 75% expected, Table 4). Whereas four position-12 mutants showed 100% in the reciprocal crosses, indicating that the pollen from these mutant constructs are highly competitive than the pollen harboring the *cpk17/34* (-/-, -/-), the D420A mutant failed to obtain seeds in the reciprocal crosses, like the negative control (vector only). In addition, the specific activity of D420A mutant is smaller than EF1 E393A, EF2 E429A, EF3 E465A, and EF4 E500A at $[Ca^{2+}] < 1.0 \mu M$. Combining these results, the calcium concentration in the pollen tube (tip region) is considered below 1.0 μM . This result is consistent with previously reported measurement (Iwano et al., 2009).

4. 4 D426A mutation lowers negative charged repulsion within EF2 and increases cooperativity

Another residue that is holding the water molecule of the -X axis ligand, D426, also plays an interesting role. This residue is holding a water molecule to coordinate Ca^{2+} on the -X axis, which is also held by D420. So, the repulsion between negatively charged D420 and D426 is released by mutating D426 into alanine. And this release of the negative charge repulsion stabilizes the conformation around the EF2 binding pocket and,

as long as the $-X$ axis water molecule is held by D420, the EF2 D426A shows higher cooperativity than WT. But this loss of one negative charge also reduces the binding affinity, so K' is still higher and specific activity is lower than WT.

4.5 N426D mutation increases negative charge repulsion within EF2, but it increases cooperativity

On the contrary, in the N422D mutant, the addition of negative charge into the calcium-binding loop increases the cooperativity. Apparently, there is an addition of negative charge that might cause repulsion within the binding loop. Thus, reduction of cooperativity was expected. But the N422D mutation increases the binding affinity to calcium and this increased binding affinity wins over the unfavorable effect of negative charge build-up within the loop. Thus, the cooperativity and K' appear close to WT. Even though the maximum specific activity is still lower than WT, it is still the highest among all the mutants surveyed. The reason N422D mutant shows a positive effect towards cooperativity with negative charge build-up within the binding loop might be answered with its location that is in the middle of the loop (position-9). This position is considered quite flexible compared to D418, D420, and D426 that are closely connected to adjacent E- and F-helix of EF2. Therefore, the N422D mutant might find its environment better able to compensate the negative charge build-up and only show its increased calcium-binding affinity.

4. 6 Kinase assays of EF-hand mutants under substrate concentration variation reveals that N- and C-terminal lobe affect auto-inhibitor differently

The activity of CPK34 WT and four EF-hand mutants; EF1(E393A), EF2(E429A), EF3(E465A), and EF4(E500A) were assayed at 100 μM of calcium, and increasing concentration of substrate, syntide-2, from 0 to 200 μM (Figure 9). The pattern of specific activity revealed hyperbolic rather than sigmoidal curves. This hyperbolic pattern indicates that there is no cooperativity in substrate binding. The activities reached a maximum at about 50 μM of syntide-2. Even though WT and EF2(E429A) mutant showed a slight increase to $[\text{Syntide-2}] = 200 \mu\text{M}$, their increment was not large and was expected to reach a plateau soon outside of the range of assays tested, $[\text{Syntide-2}] = 200 \mu\text{M}$. In this assay, the mutation on each mutant is inhibiting the phosphorylation activity on the substrate by altering the interaction between the CaM-LD and the auto-inhibitor. These results were applied to the Michaelis-Menten equation to obtain Michaelis-Menten constant, K_M (Figure 10), which would provide information about the inhibition mode of these mutants. The Michaelis-Menten constants of EF1 and EF2 mutants are more than three-fold higher than that of WT. On the contrary, the K_M 's of EF3 and EF4 mutants are similar in magnitude with WT. These results indicate that the mutations in EF1 and EF2 behave as competitive inhibitors and the mutations on EF3 and EF4 inhibit kinase domain in a noncompetitive mode. The auto-inhibitor domain is obviously a competitive inhibitor because it locates on the substrate-binding site in apo state. The EF1 and the EF2 are close to the auto-inhibitor domain in sequence and space, and they are connected to the auto-inhibitor directly, thus they can be considered as one "extended auto-inhibitor domain". Therefore, the mutations on these EF-hands reinforce the inhibiting ability of

the auto-inhibitor and act as a competitive inhibitor for substrate binding site. On the other hand, the C-terminal lobe, the EF3 and the EF4 hands, is not part of the “extended auto-inhibitor domain” and is connected to EF2 via one long helix (24 amino acid residues, in calcium unloaded state). And this helix bends into two helices and conformational change occurs upon calcium binding to EF3 and EF4 (Figure 2) (Wernimont et al., 2011). This bending motion might be not favored if the C-terminal lobe has mutations that reduce calcium-binding affinity. Therefore, calcium binding by the N-terminal EF-hands, and the removal of the auto-inhibitor from the active site is delayed sequentially. Thus, the EF3 and the EF4 mutants show noncompetitive inhibition mode.

4. 7 Unknown factor(s) may compensate EF3 mutant defects

In vitro kinase activity assay results showed that the mutation on EF3 disrupts the activity of the enzyme severely; smaller specific activities, higher K' , and lower Hill coefficient than other three mutant EF-hands. But *in vivo* seed set count and transmission efficiency assays showed that the EF3 mutant had higher activity than other EF-hand mutants. This discrepancy has allegedly come from the difference between *in vitro* reaction condition in which only the enzyme, ATP, Ca^{2+} , and syntide-2 react in free solution, and the cytosol in a compact environment where more factors are expected (e.g. membrane, ATP carrier, real protein substrate...) to affect enzyme behavior. Something unknown that compensates off and undergirds the vulnerable EF3 mutant defects is expected to exist for the EF3 mutant plant to show better *in vivo* result. Further investigation is required to find out this unknown factor(s).

5 Conclusion

In this study, we found that the N- and C-terminal lobes affect auto-inhibitor differently.

The auto-inhibitor of CPK34 with a single mutation on one of the EF-hands in the N-terminal lobe showed competitive inhibition mode, however, when the mutation is in the C-terminal lobe, the non-competitive inhibition mode was shown (Figure 10).

Actual calcium level in pollen tube tip was found to be under 1 μM by combining the results from two assays; 1) the pollen transmission efficiency assay (Table 4) in which EF2 D420A mutant (mutation on position-3) showed weaker activity than four position-12 mutants of E393A (EF1), E429A (EF2), E465A (EF3), and E500A (EF4), 2) *in vitro* kinase activity assay in which D420A mutant showed lower activity than the above four mutants at $[\text{Ca}^{2+}] < 1 \mu\text{M}$ (Figure 19).

Comparison of rescuing activities of the transgenes tested is summarized in Figure 20.

CPK34 WT showed good results in rescuing *cpk17/34* (-/-, -/-) plant, but it produced less seed set number than WT *Arabidopsis* plant. Plants that have the transgenes of position-12 mutant showed more seed set numbers and pollen of these plants had higher transmission efficiency than D420A (position-3) mutant (100% vs. 92%). But these position-12 mutant transgene plants showed less seed set numbers than WT transgene plant. D420A transgene is positioned in “Poor rescue”, because pollen of D420A transgene plant had higher transmission efficiency than EF2-5A transgene plant (92% vs. 76%).

References

- Babu, Y.S., Bugg, C.E., and Cook, W.J.** (1988). Structure of calmodulin refined at 2.2 Å resolution. *Journal of molecular biology* **204**: 191–204.
- Becker, D., Boavida, L.C., Carneiro, J., Haury, M., and Feijo, A.** (2003). Transcriptional profiling of *Arabidopsis* tissues. *Plant physiology* **133**: 713–725.
- Beckingham, K.** (1991). Use of site-directed mutations in the individual calcium-binding sites of calmodulin to examine calcium-induced conformational changes. *The Journal of biological chemistry* **266**: 6027–6030.
- Biekofsky, R.R., Martin, S.R., Browne, J.P., Bayley, P.M., and Feeney, J.** (1998). Ca²⁺ coordination to backbone carbonyl oxygen atoms in calmodulin and other EF-hand proteins: ¹⁵N chemical shifts as probes for monitoring individual-site Ca²⁺ coordination. *Biochemistry* **37**: 7617–7629.
- Burger, D., Cox, J.A., Comte, M., and Stein, E.A.** (1984). Sequential conformational changes in calmodulin upon binding of calcium. *Biochemistry* **23**: 1966–1971.
- Cheng, S., Willmann, M.R., Chen, H., and Sheen, J.** (2002). Calcium signaling through protein kinases . The *Arabidopsis* calcium-dependent protein kinase gene family. *Plant physiology* **129**: 469–485.
- Cheung, W.Y.** (1980). Calmodulin plays a pivotal role in cellular regulation. *Science* **207**: 19–27.
- Christodoulou, J., Malmendal, A., Harper, J.F., and Chazin, W.J.** (2004). Evidence for differing roles for each lobe of the calmodulin-like domain in a calcium-dependent protein kinase. *The Journal of biological chemistry* **279**: 29092–29100.

- Clough, S.J. and Bent, A.F.** (1998). Floral dip : a simplified method for *Agrobacterium*-mediated transformation of *Arabidopsis thaliana*. **16**: 735–743.
- Evenäs, J., Thulin, E., Malmendal, a, Forsén, S., and Carlström, G.** (1997). NMR studies of the E140Q mutant of the carboxy-terminal domain of calmodulin reveal global conformational exchange in the Ca^{2+} -saturated state. *Biochemistry* **36**: 3448–57.
- Harper, J.F., Binder, B.M., and Sussmans, M.R.** (1993). Calcium and lipid regulation of an *Arabidopsis* protein kinase expressed in *Escherichia coli*. *Biochemistry* **32**: 3282–3290.
- Harper, J.F., Breton, G., and Harmon, A.** (2004). Decoding Ca^{2+} signals through plant protein kinases. *Annual review of plant biology* **55**: 263–288.
- Harper, J.F., Huang, J.F., and Lloyd, S.J.** (1994). Genetic identification of an autoinhibitor in CDPK, a protein kinase with a calmodulin-like domain. *Biochemistry* **33**: 7267–7277.
- Hrabak, E.M., Chan, C.W.M., Gribskov, M., Harper, J.F., Choi, J.H., Halford, N., Luan, S., Nimmo, H.G., Sussman, M.R., Thomas, M., Walker-simmons, K., Zhu, J., and Harmon, A.C.** (2003). The *Arabidopsis* CDPK-SnRK superfamily of protein kinases. *Plant physiology* **132**: 666–680.
- Hrabak, E.M., Dickmann, L.J., Satterlee, J.S., and Sussman, M.R.** (1996). Characterization of eight new members of the calmodulin-like domain protein kinase gene family from *Arabidopsis thaliana*. *Plant molecular biology* **31**: 405–412.
- Ikura, M., Hasegawa, N., Aimoto, S., Yazawa, M., Yagi, K., and Hikichi, K.** (1989). ^{113}Cd -NMR evidence for cooperative interaction between amino- and carboxy-

- terminal domains of calmodulin. *Biochemical and Biophysical Research Communications* **161**: 1233–1238.
- Ito, T., Nakata, M., Fukazawa, J., Ishida, S., and Takahashi, Y.** (2010). Alteration of substrate specificity: the variable N-terminal domain of tobacco Ca^{2+} -dependent protein kinase is important for substrate recognition. *The Plant cell* **22**: 1592–1604.
- Iwano, M., Entani, T., Shiba, H., Kakita, M., Nagai, T., Mizuno, H., Miyawaki, A., Shoji, T., Kubo, K., Isogai, A., and Takayama, S.** (2009). Fine-tuning of the cytoplasmic Ca^{2+} concentration is essential for pollen tube growth. *Plant physiology* **150**: 1322–34.
- Juranić, N., Atanasova, E., Macura, S., and Prendergast, F.G.** (2009). Directly observed hydrogen bonds at calcium-binding-sites of calmodulin in solution relate to affinity of the calcium-binding. *Journal of inorganic biochemistry* **103**: 1415–1418.
- Kretsinger, R.H.** (1976). Calcium-binding proteins. *Annual review of biochemistry* **45**: 239–266.
- Linse, S., Helmersson, A., and Forsén, S.** (1991). Calcium binding to calmodulin and its globular domains. *The Journal of biological chemistry* **266**: 8050–8054.
- Maune, J.F., Klee, C.B., and Beckingham, K.** (1992). Ca^{2+} binding and conformational change in two series of point mutations to the individual Ca^{2+} -binding sites of calmodulin. *The Journal of biological chemistry* **267**: 5286–5295.
- Means, A.R. and Dedman, J.R.** (1980). Calmodulin - an intracellular calcium receptor. *Nature* **285**: 73–77.

- Mukherjea, P., Maune, J.F., and Beckingham, K.** (1996). Interlobe communication in multiple calcium-binding site mutants of *Drosophila* calmodulin. *Protein science* **5**: 468–77.
- Myers, C., Romanowsky, S.M., Barron, Y.D., Garg, S., Azuse, C.L., Curran, A., Davis, R.M., Hatton, J., Harmon, A.C., and Harper, J.F.** (2009). Calcium-dependent protein kinases regulate polarized tip growth in pollen tubes. *The Plant journal : for cell and molecular biology* **59**: 528–539.
- Nakayama, S. and Kretsinger, R.H.** (1994). Evolution of the EF-hand family of proteins. *Annu. Rev. Biophys. Biomol. Struct.* **23**: 473–507.
- Persechini, A., Blumenthal, D.K., Jarrett, H.W., Klee, C.B., Hardy, D.O., and Kretsinger, R.H.** (1989). The effects of deletions in the central helix of calmodulin on enzyme activation and peptide binding. *The Journal of biological chemistry* **264**: 8052–8058.
- Putkey, J.A., Ono, T., VanBerkum, M.F.A., and Means, A.R.** (1988). Functional significance of the central helix in calmodulin. *The Journal of biological chemistry* **263**: 11242–11249.
- Roberts, D.M. and Harmon, A.C.** (1992). Calcium-modulated proteins: targets of intracellular calcium signals in higher plants. **43**: 375–414.
- Schaller, G.E. and Sussman, M.R.** (1988). Phosphorylation of the plasma membrane H^+ -ATPase of oat roots by a calcium-stimulated protein kinase. *Planta* **173**: 509–518.

- Starovasnik, M.A., Su, D.R., Beckingham, K., and Klevit, R.E.** (1992). A series of point mutations reveal interactions between the calcium-binding sites of calmodulin. *Protein science* **1**: 245–253.
- Stigler, J. and Rief, M.** (2012). Calcium-dependent folding of single calmodulin molecules. *Proceedings of the National Academy of Sciences of the United States of America* **109**: 17814–17819.
- Stigler, J., Ziegler, F., Gieseke, A., Gebhardt, J.C.M., and Rief, M.** (2011). The complex folding network of single calmodulin molecules. *Science (New York, N.Y.)* **334**: 512–516.
- VanBerkum, M.F.A., George, S.E., and Means, A.R.** (1990). Calmodulin activation of target enzymes. *The Journal of biological chemistry* **265**: 3750–3756.
- Waltersson, Y., Linse, S., Brodin, P., and Grundström, T.** (1993). Mutational effects on the cooperativity of Ca²⁺ binding in calmodulin. *Biochemistry* **32**: 7866–7871.
- Wernimont, A.K., Amani, M., Qiu, W., Pizarro, J.C., Artz, J.D., Lin, Y.-H., Lew, J., Hutchinson, A., and Hui, R.** (2011). Structures of parasitic CDPK domains point to a common mechanism of activation. *Proteins* **79**: 803–20.
- Wernimont, A.K., Artz, J.D., Finerty, P., Lin, Y.-H., Amani, M., Allali-Hassani, A., Senisterra, G., Vedadi, M., Tempel, W., Mackenzie, F., Chau, I., Lourido, S., Sibley, L.D., and Hui, R.** (2010). Structures of apicomplexan calcium-dependent protein kinases reveal mechanism of activation by calcium. *Nature structural & molecular biology* **17**: 596–601.

Yazawa, M., Ikura, M., Hikichi, K., Ying, L., and Yagi, K. (1987). Communication between two globular domains of calmodulin in the presence of mastoparan or caldesmon fragment. *The Journal of biological chemistry* **262**: 10951–10954.

Zhang, M., Tanaka, T., and Ikura, M. (1995). Calcium-induced conformational transition revealed by the solution structure of apo calmodulin. *Nature structural biology* **2**: 758–767.

Zhao, Y., Pokutta, S., Maurer, P., Lindt, M., Franklin, R.M., and Kappes, B. (1994). Calcium-binding properties of a calcium-dependent protein kinase from *Plasmodium falciparum* and the significance of individual calcium-binding sites for kinase activation. *Biochemistry* **33**: 3714–3721.

Figures

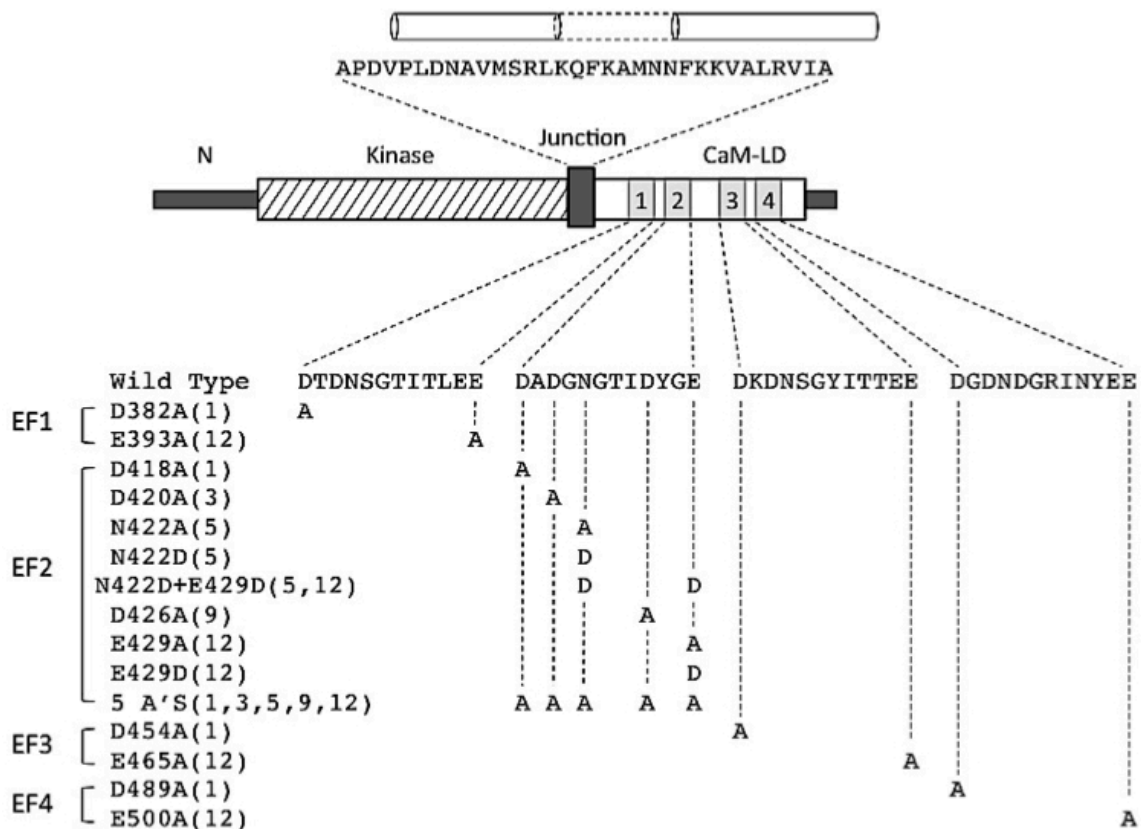


Figure 1. Diagrammatic representation of the domain structure of CPK and mutation residues.

Calcium-binding EF-hands within CaM-LD are indicated as gray boxes and sequences of WT and each mutants are shown. Auto-inhibitor sequence in junction domain is shown.

Its secondary structure is one long helix in inactivated state and it bends into two helix in activated state according to (Wernimont et al., 2011)

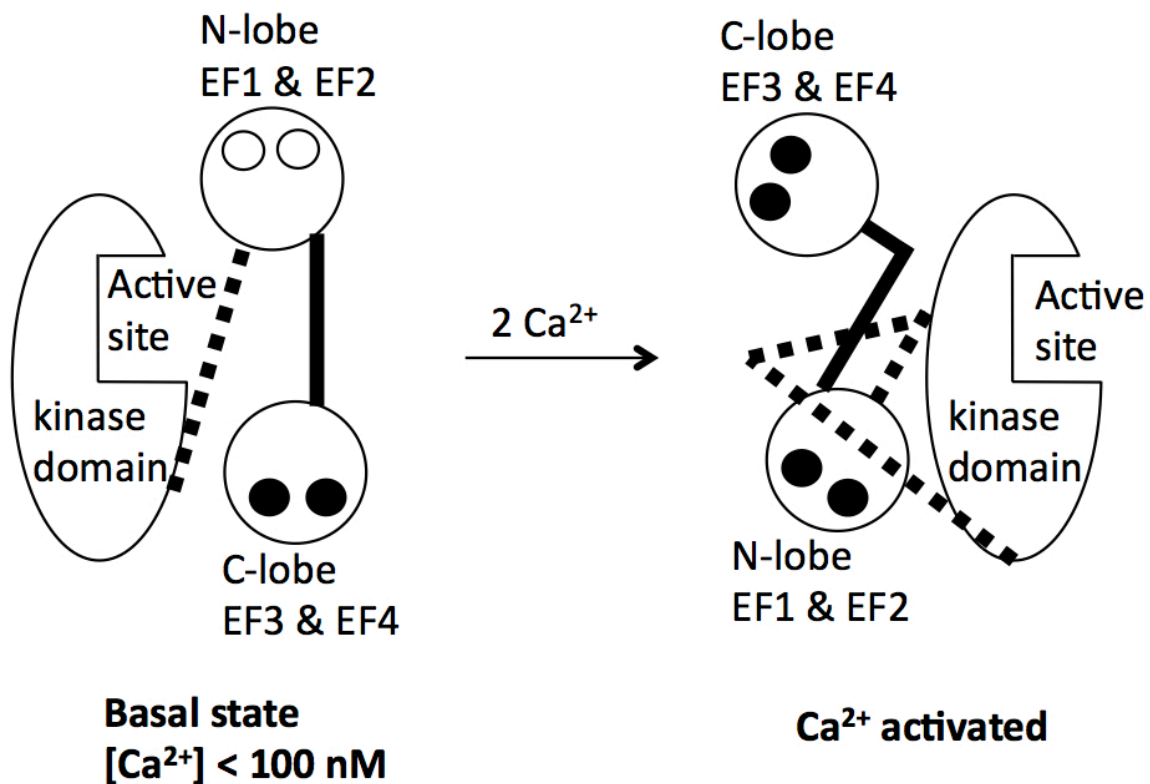


Figure 2. Activation of CPK through intramolecular binding of the CaM-LD.

C-terminal lobe (EF3 and EF4) is already Ca^{2+} -loaded at basal state ($[Ca^{2+}] < 100 \text{ nM}$).

Empty circles represent un-loaded EF-hands and black circles represent Ca^{2+} -loaded EF-hands. A dotted line between kinase domain and N-lobe indicate an α -helix that bends into three helices at Ca^{2+} -activated state. Active site is blocked by this α -helix in which the auto-inhibitor domain is included. The auto-inhibitor domain is disengaged from the active site at fully Ca^{2+} -loaded. A Thick line between N-lobe and C-lobe indicate an α -helix that bends into two helices at Ca^{2+} -activated state. (Redrawn from Wernimont et al., 2011, Figure 1)

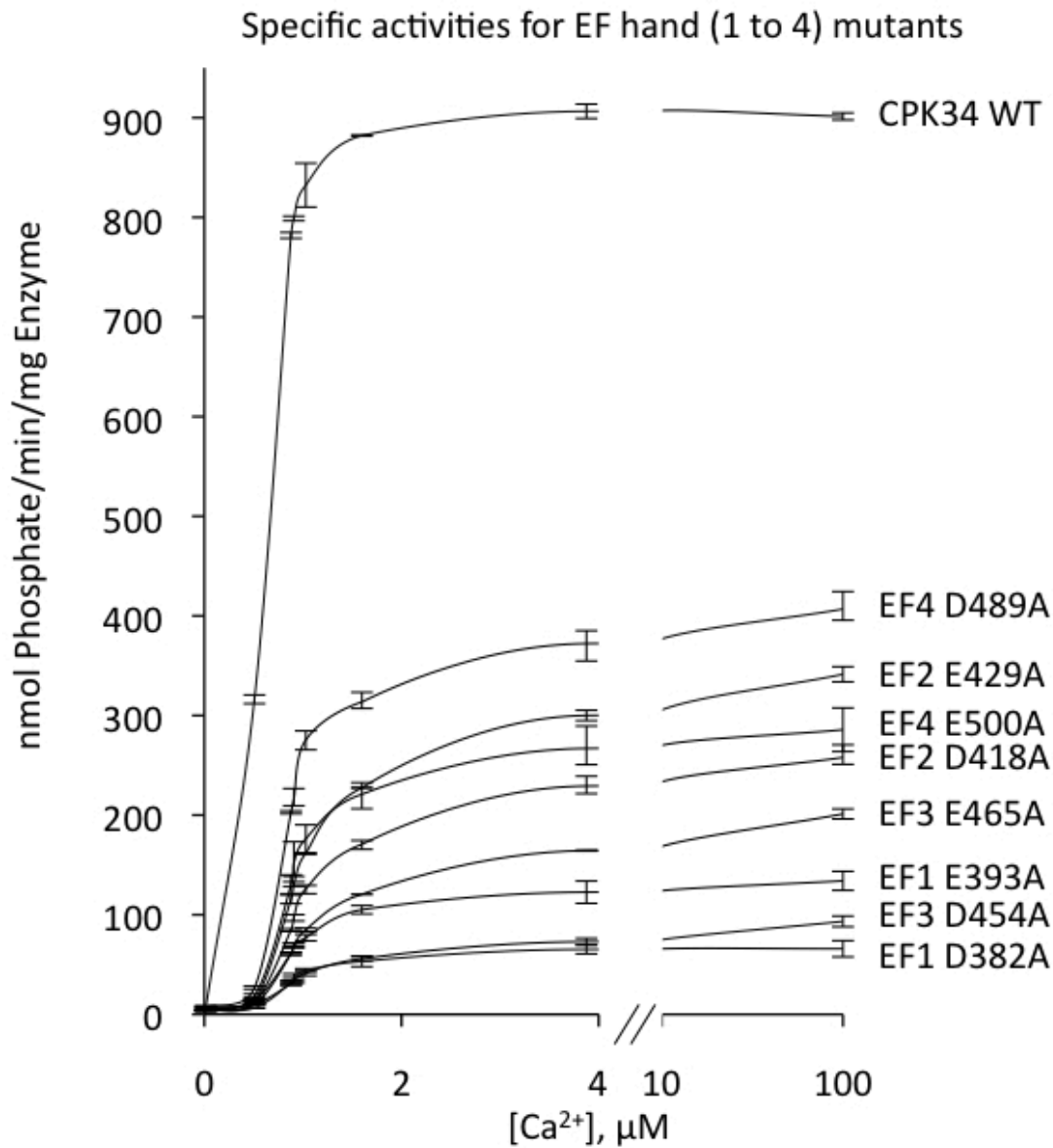


Figure 3. Specific activities for EF-hand (1 to 4) mutants vs. calcium concentration.

Sigmoid curves were obtained, which is indicating cooperativity among calcium binding sites. The activity of WT is 2-10 fold bigger than mutants. Error bars represent minimum and maximum values of more than two assays of more than two independent protein expressions.

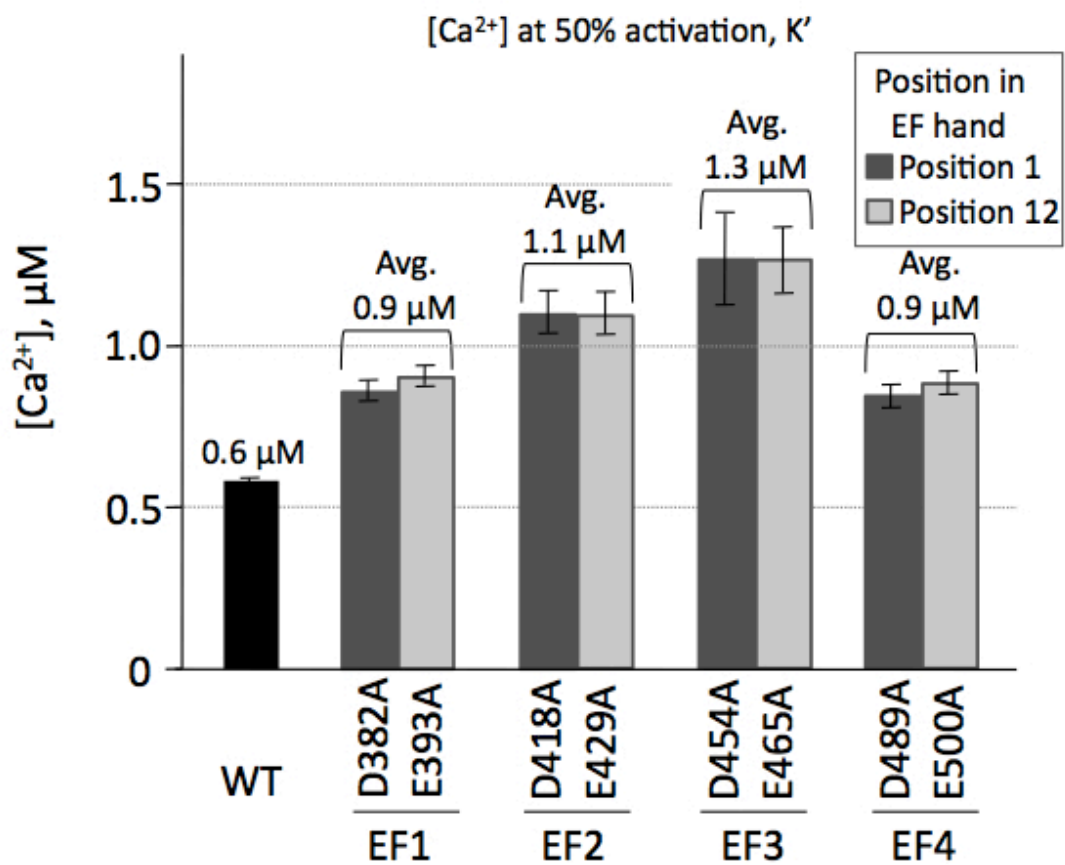


Figure 4. Calcium concentration at 50% activation, K', of EF-hand (1 to 4) mutants. Error bars represent standard errors provided by Origin® for parameters, K'.

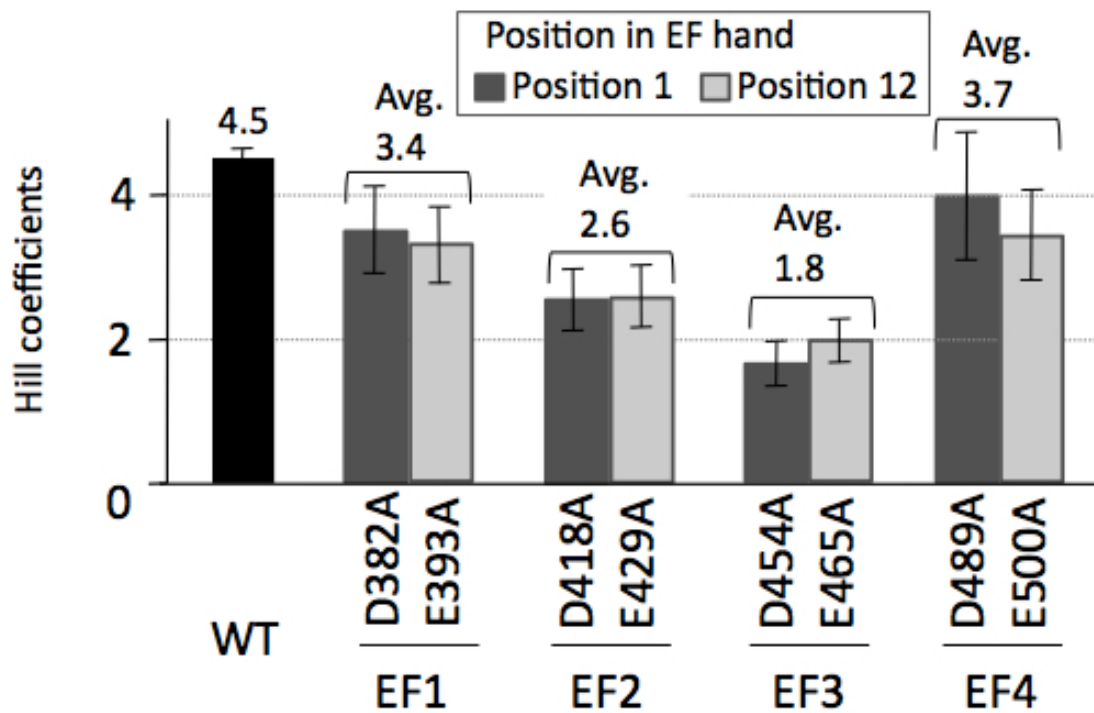


Figure 5. Hill coefficients for EF-hand (1 to 4) mutants. Error bars represent standard errors provided by Origin® for parameters, Hill coefficients.

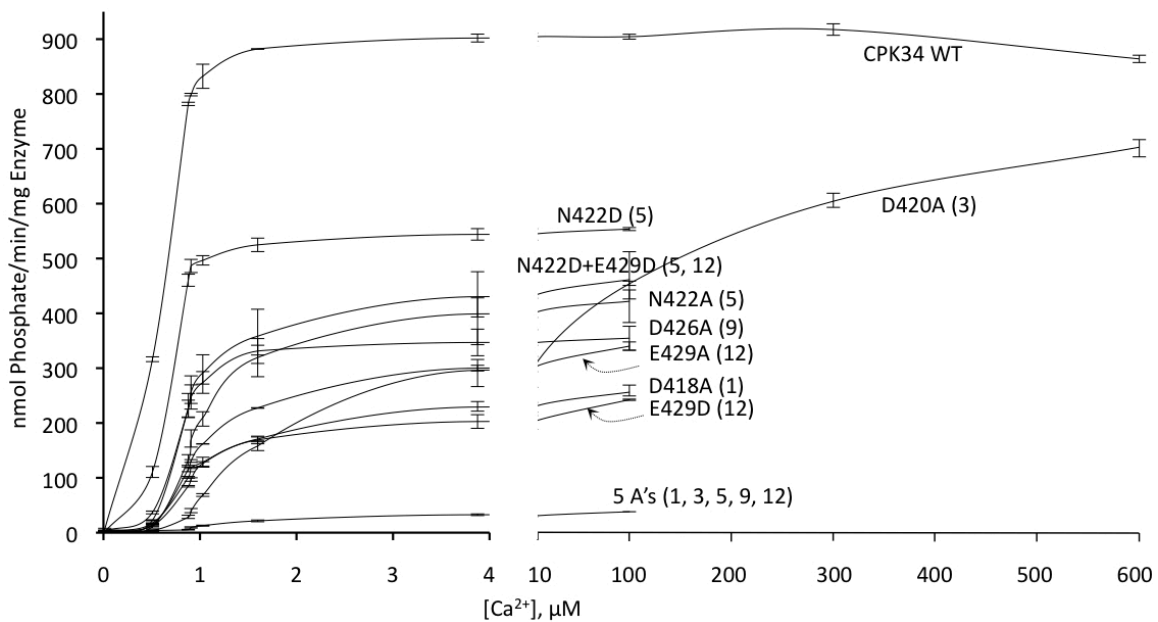


Figure 6. Specific activities for mutants of EF2 vs. calcium concentration. Sigmoid curves were obtained, which is indicating cooperativity among calcium binding sites. The activity of WT is 3-10 fold bigger than mutants. Specific activities of WT and D420A. The activity of D420A increases close to WT at high $[Ca^{2+}]$. Error bars represent minimum and maximum values of more than two assays of more than two independent protein expressions.

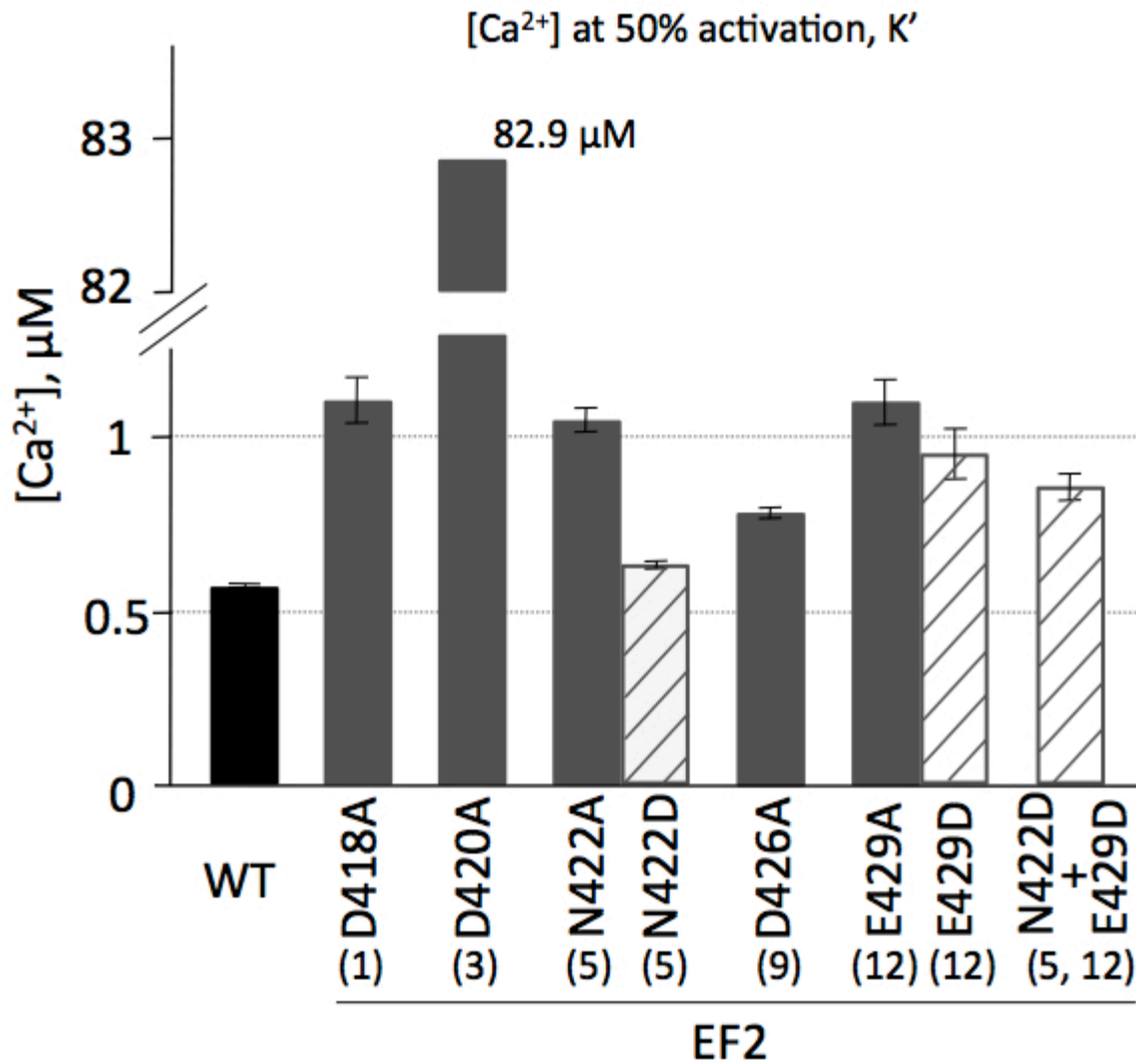


Figure 7. Calcium concentration at 50% activation, K', of EF2 mutants. Error bars represent standard errors provided by Origin® for parameters, K' and Hill coefficients. Numbers in parentheses are the residual numbers in Ca-binding loop.

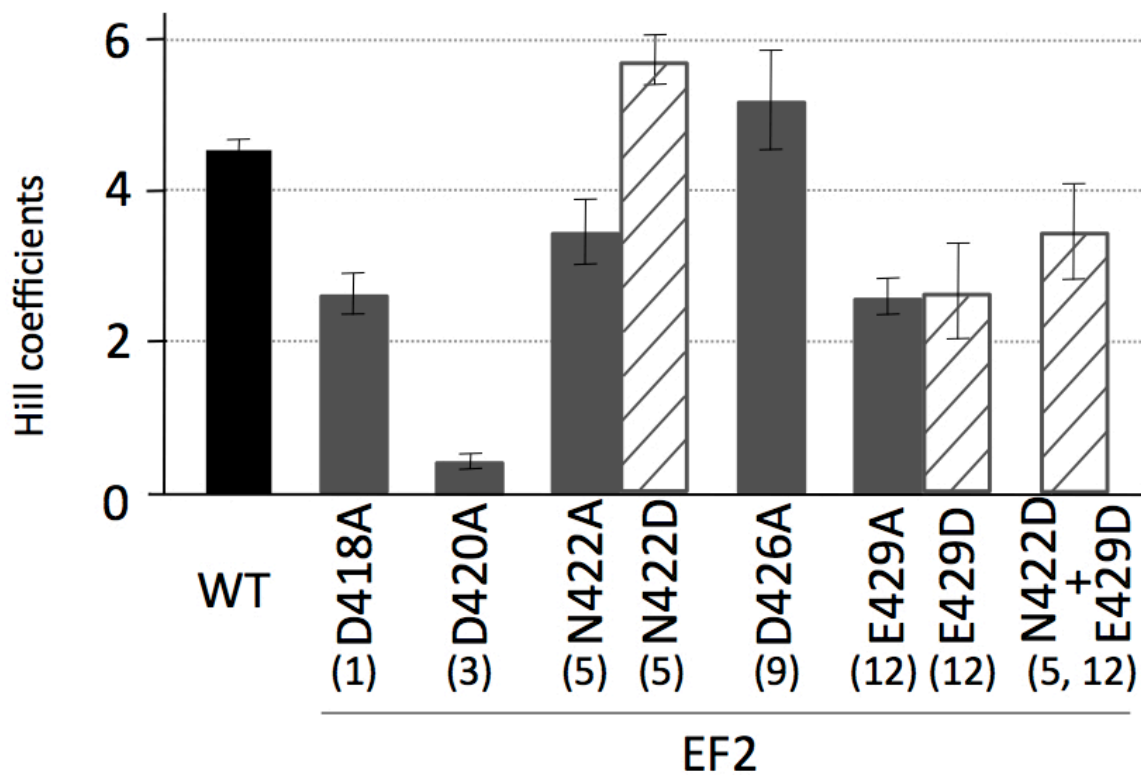


Figure 8. Hill coefficients for EF2 mutants. Error bars represent standard errors provided by Origin® for parameters, K' and Hill coefficients. Numbers in parentheses are the residual numbers in Ca-binding loop.

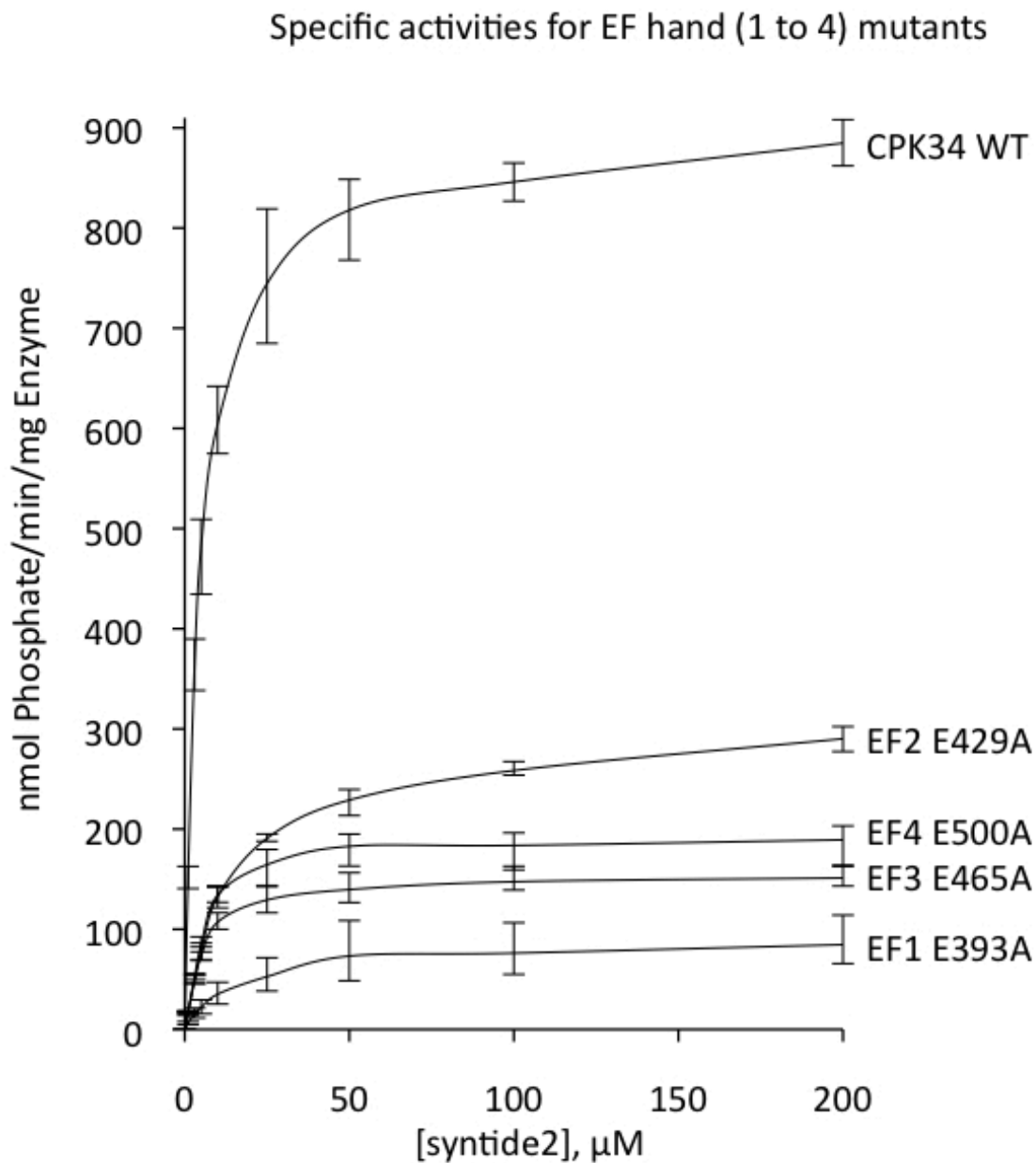


Figure 9. Specific activities for EF-hand (1 to 4) mutants vs. syntide-2 concentration. The activity of WT is 2-10 fold bigger than mutants. Error bars represent minimum and maximum values of more than two assays of more than two independent protein expressions.

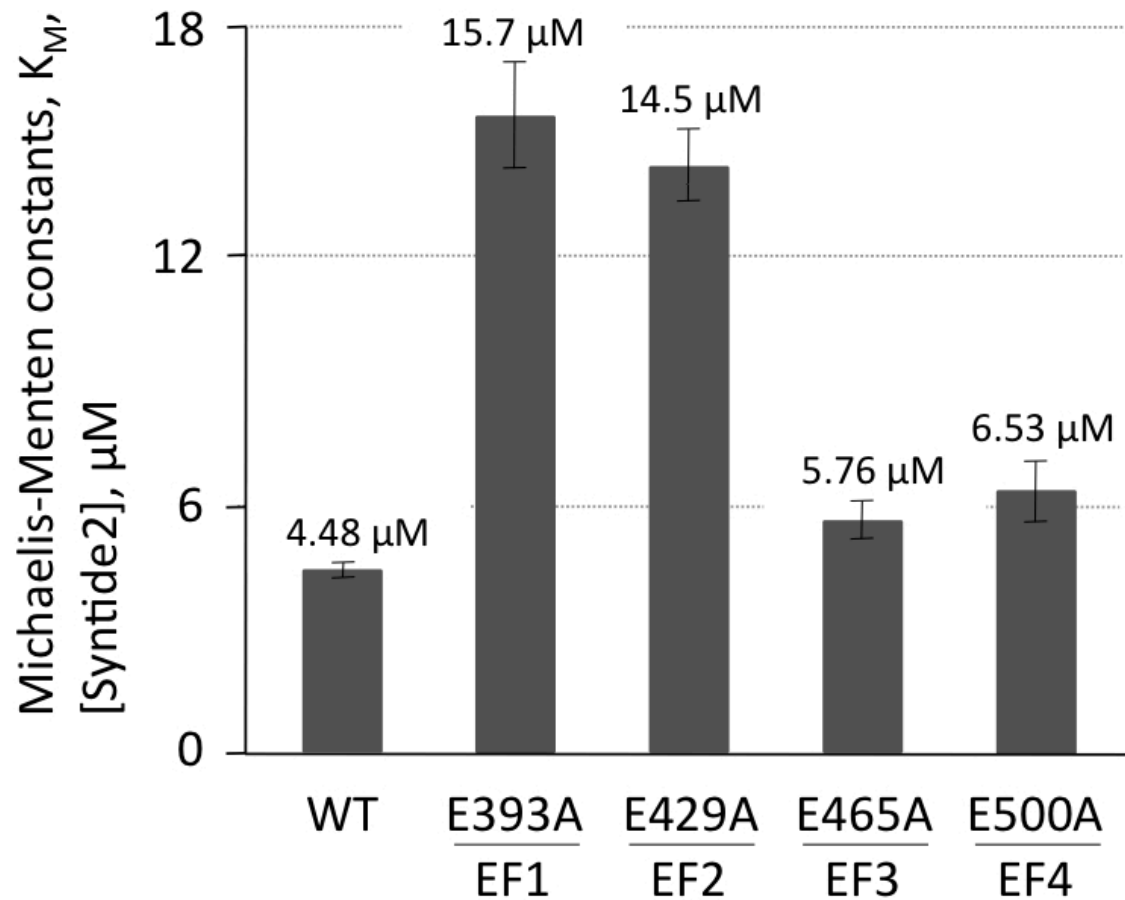


Figure 10. Michaelis-Menten constants, K_M , for EF-hand (1 to 4) mutants at $[\text{Ca}^{2+}] = 100 \mu\text{M}$. EF1 and EF2 mutants require [syntide2] 2-3 times more than WT, EF3 and EF4 mutants. Error bars represent standard errors provided by Prism5® for parameter, K_M .

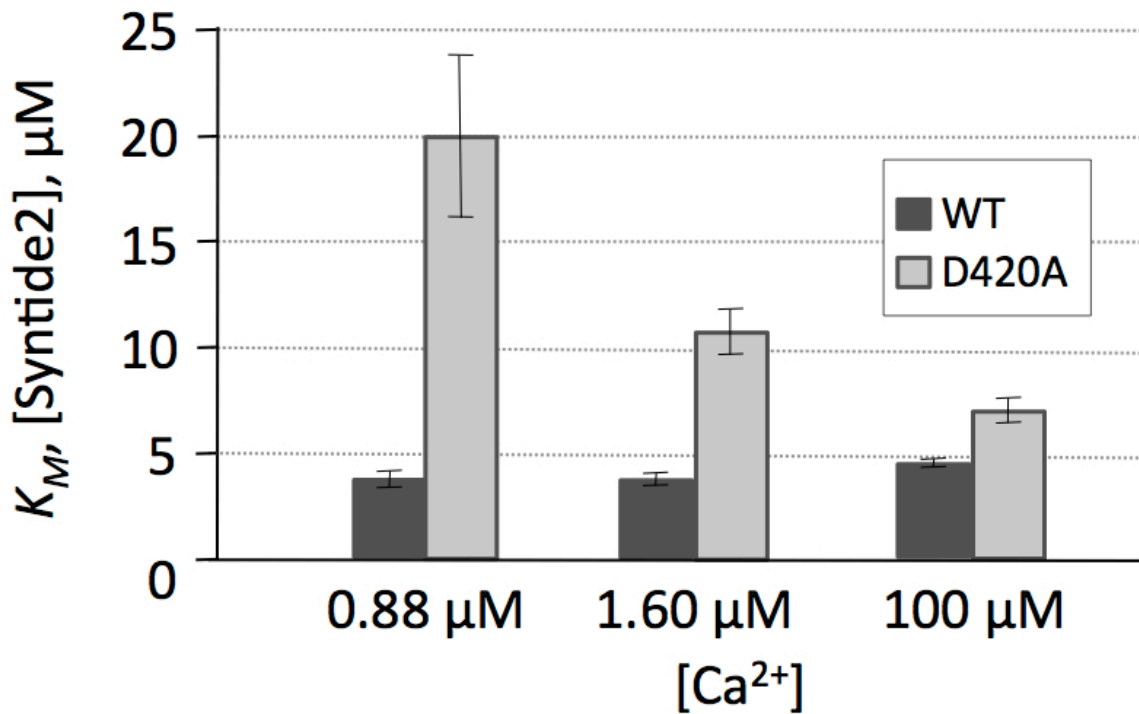


Figure 11. Wild type and D420A K_M variation at different calcium concentration. K_M of D420A decreases close to WT as $[\text{Ca}^{2+}]$ increases. Error bars represent standard errors provided by Prism5® for parameter, K_M .

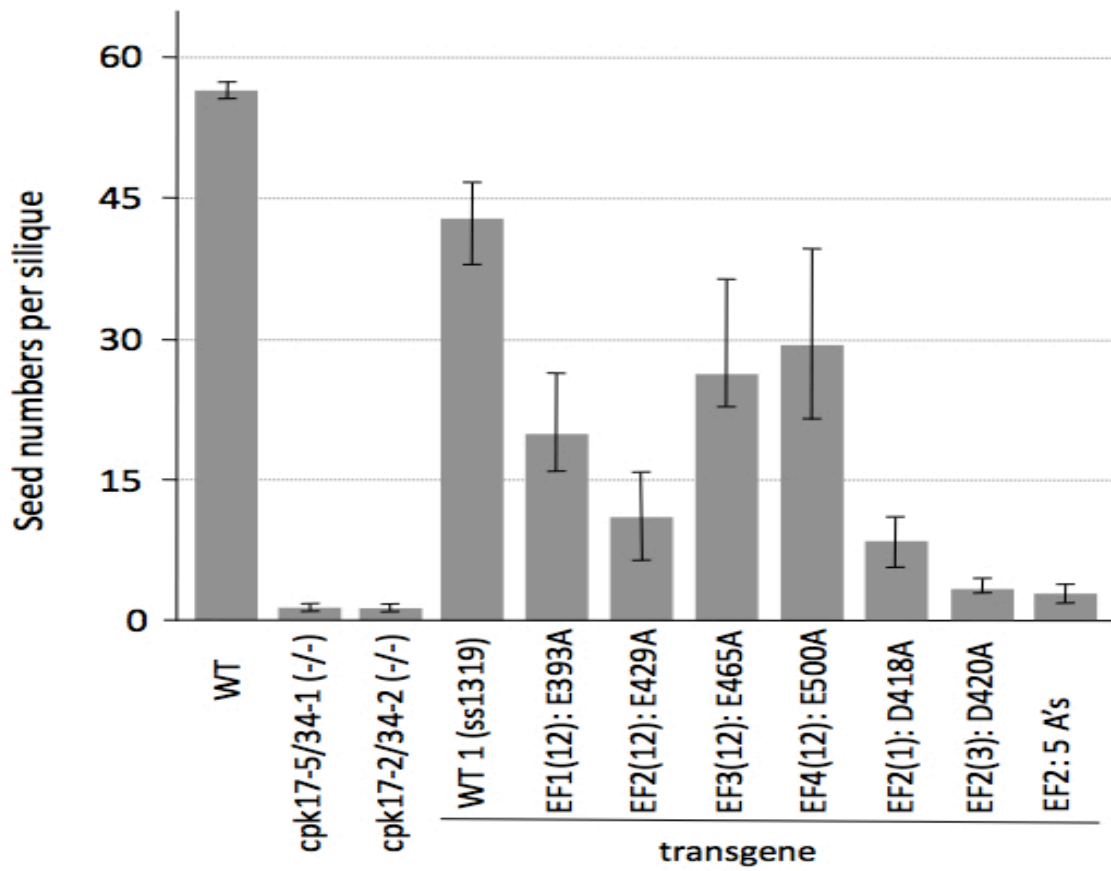


Figure 12. Number of seeds per silique from wild type, knock outs, and rescued by WT and mutants. cpk17-5/34-1 (-/-) (ss997), cpk17-2/34-2 (-/-) (ss992H), WT rescue 1; ss1319. The numbers in parenthesis in mutants of transgenes indicated the position of the mutation within each EF-hand. EF2: 5 A's; five alanine substitutions within EF2 hand on calcium coordinating residues, D418(1), D420(3), N422(5), D426(9), and E429(12). Error bars indicate maximum and minimum numbers from 4 independent lines (EF1: ss1677, 1678, 1684, 1686, EF2: ss1687, 1689, 1690, 1692, EF3: ss1693, 1695, 1703, 1704, EF4: ss1707, 1708, 1710, 1714, D418A: ss1716, 1719, 1720, 1723). For EF2 D420A, three lines were tested (ss2107, 2109, 2110). For EF2 5As, eleven lines were tested (ss2007-2017)

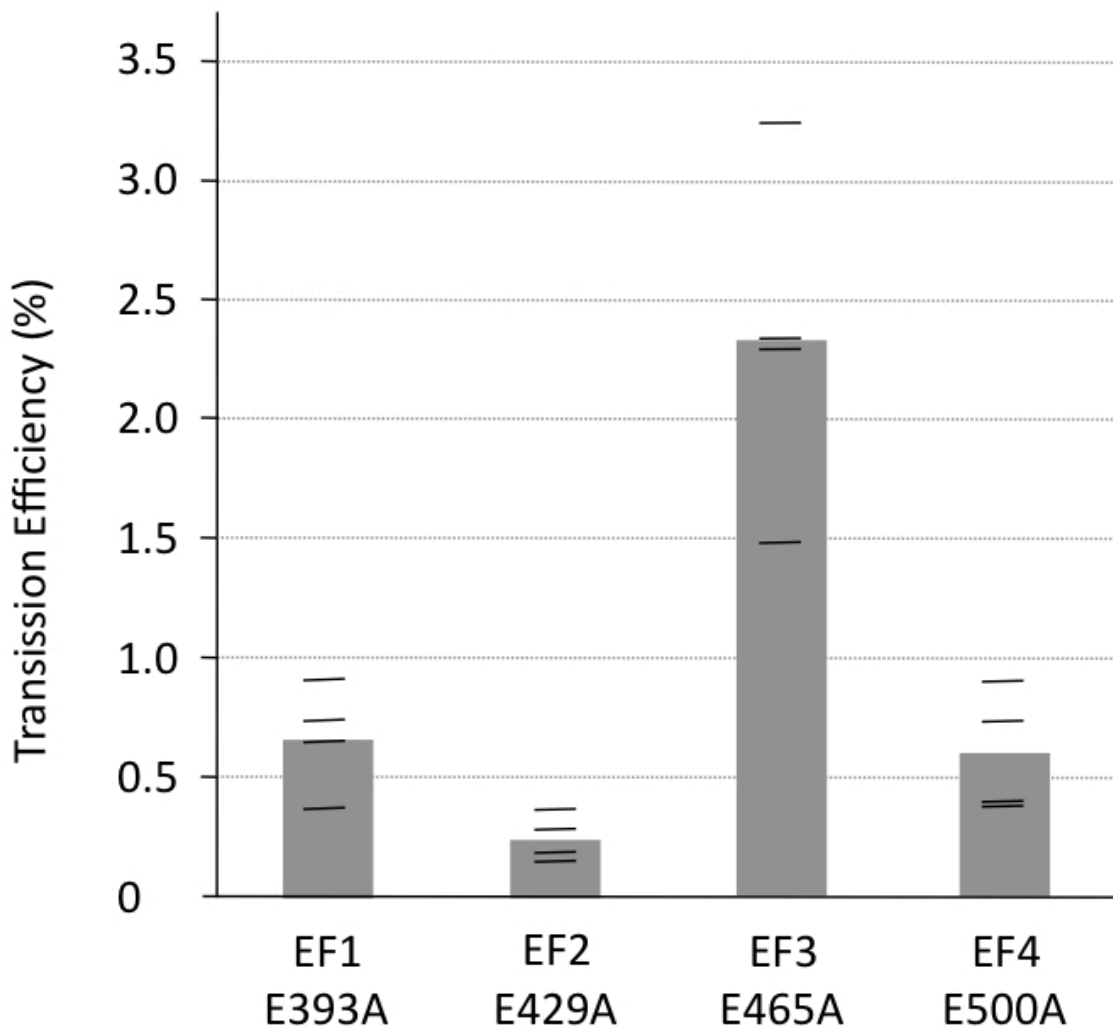


Figure 13. Transmission efficiencies of EF-hand mutants. Columns indicate the average of four best transmission efficiencies per each mutant. Four lines in each column indicate individual transmission efficiencies. EF3 is statistically different from other three at the 0.01 level by Tukey-HSD model. Transmission efficiencies of all other plant lines tested are listed in Table 2.

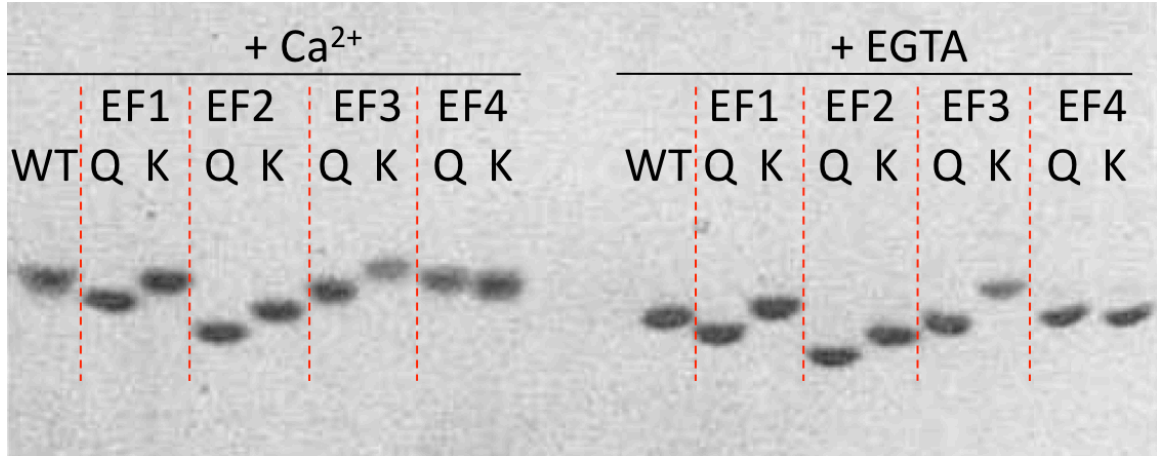


Figure 14. Native gel electrophoretic mobility of mutant calmodulins from *Drosophila melanogaster*. (Figure 3 in (Maune et al., 1992)) Position-12, Glu was mutated to neutral Gln (Q) or positive Lys (K).

In both apo state (+EGTA) and calcium-loaded state (+Ca²⁺), the mobility towards the anode of neutral Q series mutant (which carries one less negative charge than the WT) was as great or greater than that of wild type calmodulin. In addition, each EF-hand mutant showed different mobility in comparison within both Q- and K-series mutant groups (in both +EGTA and +Ca²⁺). These results indicate that overall conformational change is caused by a single mutation.

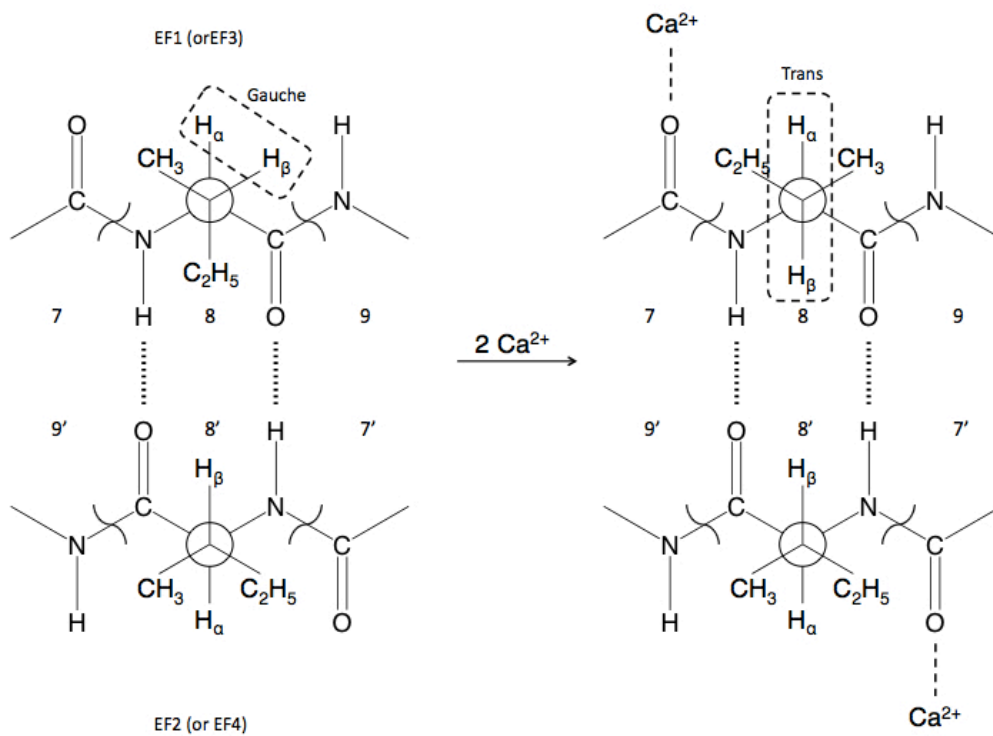


Figure 15. Changes in side-chain conformation of position-8 upon calcium binding to both EF1 and EF2 (or EF3 and EF4) in a pair. Dihedral conformation of H_α - C_α - C_β - H_β transits from gauche to trans. (redrawn from Biekofsky et al. (1998) Figure. 2A)

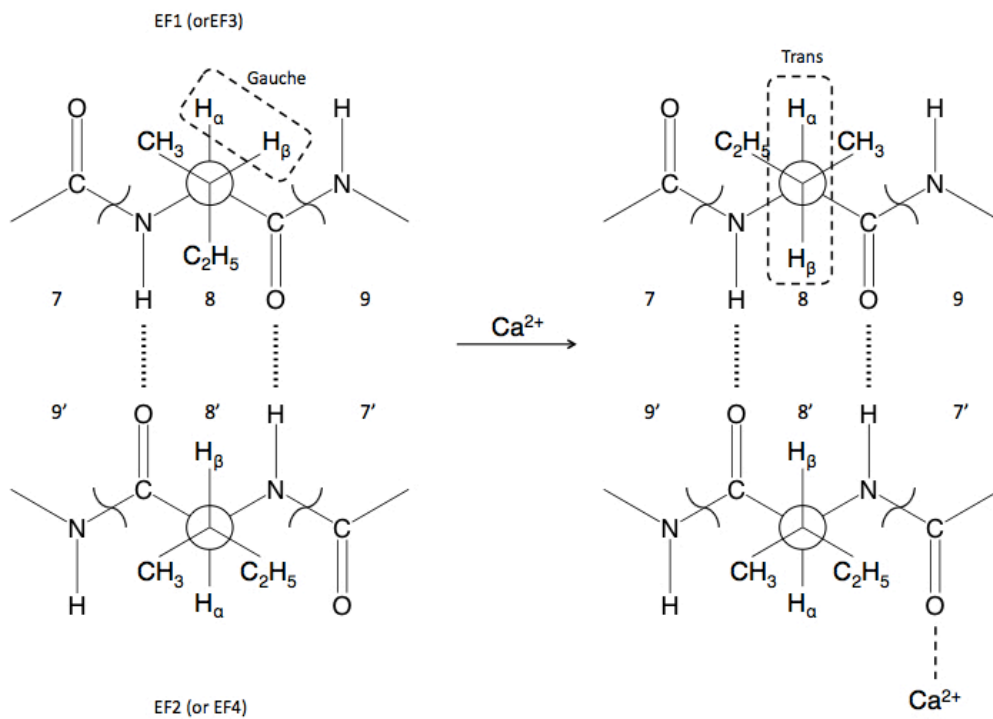


Figure 16. Changes in side-chain conformation of position-8 upon calcium binding to only EF2 (or EF4) in a pair. Dihedral conformation of H_α- C_α- C_β- H_β transits from gauche to trans. (redrawn from Biekofsky et al. (1998) Figure. 2B)

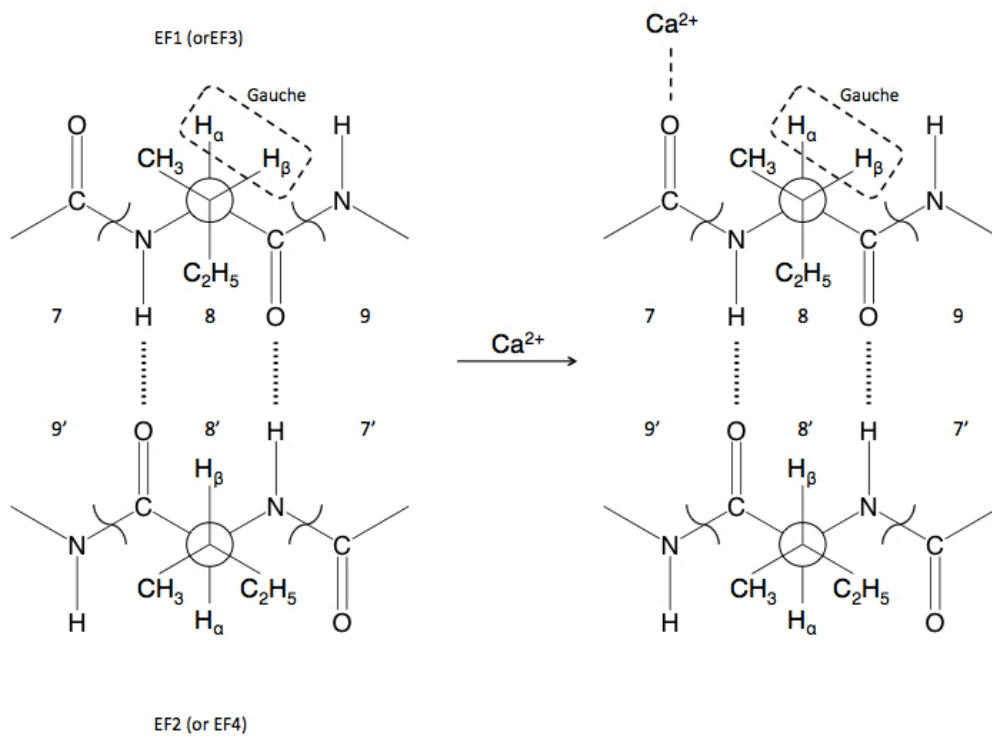


Figure 17. Changes in side-chain conformation of position-8 upon calcium binding to only EF1 (or EF3) in a pair. Dihedral conformation of $\text{H}\alpha\text{-C}\alpha\text{-C}\beta\text{-H}\beta$ maintains gauche. (redrawn from Bickofsky et al. (1998) Figure. 2C)

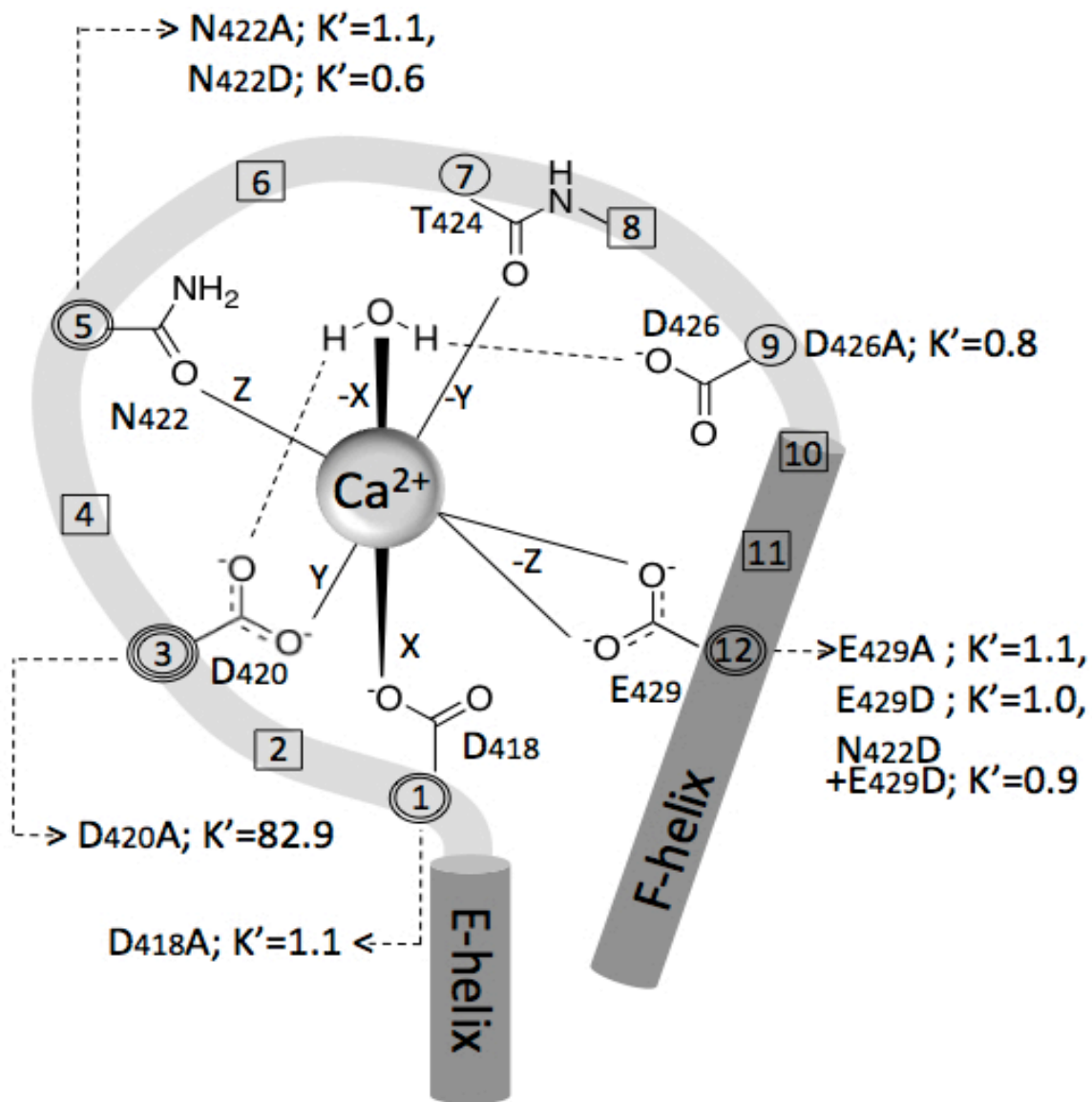


Figure 18. Hypothetical coordination model of EF2 modified from Waltersson et al. (1993). The position-3 and -9 residues hold water molecule to $-X$ ligand. The numbers with circles indicate six ligand residues. The last three residues belong to the first turn of F-helix. X, Y, Z, and $-Z$ ligands coordinate through the side chains of the residues whereas $-Y$ ligand coordinates through the carbonyl oxygen of backbone. D420 coordinates not only Ca^{2+} but also water molecule which is the $-X$ ligand. This water molecule is held by D426 as well. K' of each mutant is shown.

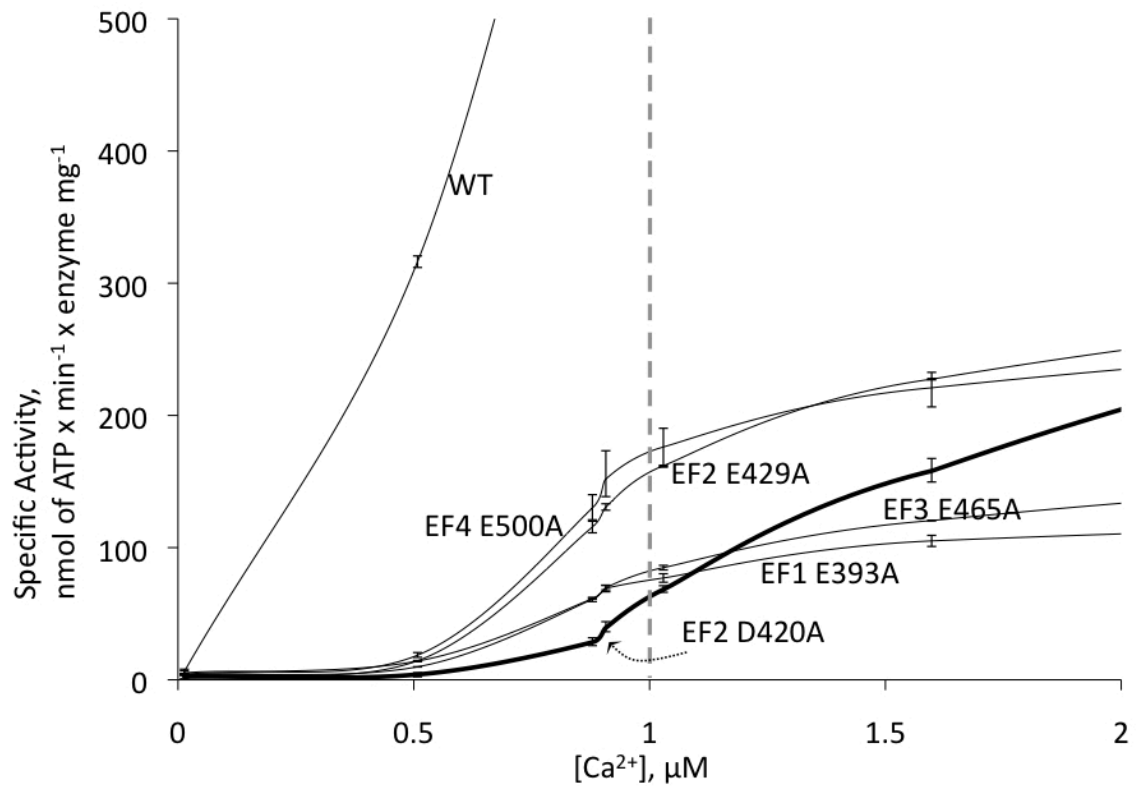


Figure 19. Comparison of specific activities at low [Ca²⁺]. EF2 D420A (position-3) showed weaker activity than other four position-12 mutants at [Ca²⁺] < 1 μM.

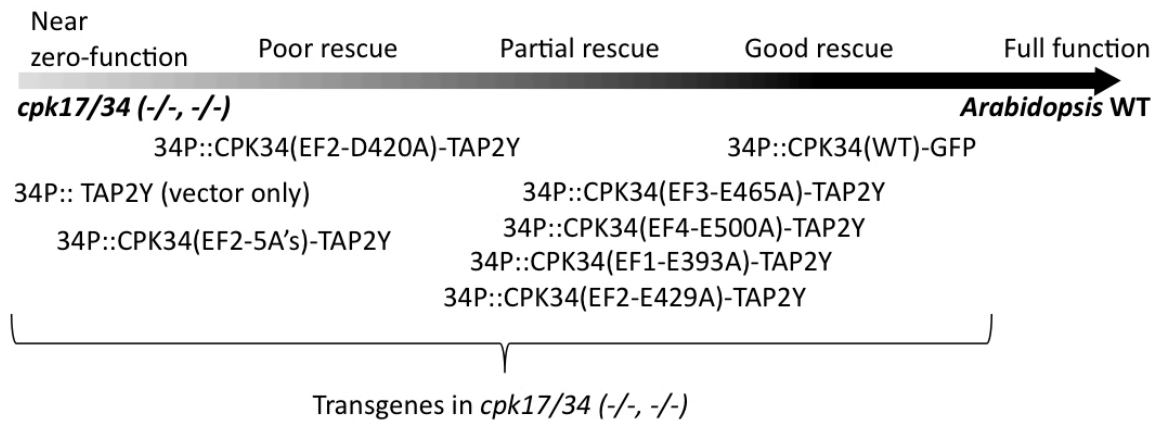


Figure 20. Comparison of rescue activity of transgenes. **Good rescue;** the plant that has WT transgene showed less seed set number than *Arabidopsis* WT. **Partial rescue;** Plants that have the transgenes of position-12 mutant showed more seed set numbers and pollen of these plants had higher transmission efficiency than D420A (position-3) mutant (100% vs. 92%). But these position-12 mutant transgene plants showed less seed set numbers than WT transgene plant. **Poor rescue;** pollen of D420A transgene plant had higher transmission efficiency than EF2-5A transgene plant (92% vs. 76%).

Tables

EF-loop position	1	2	3	4	5	6	7	8	9	10	11	12
coordinating ligand	X sc		Y sc		Z sc		-Y bb		-X sc*			-Z sc2
most common	Asp 100%	Lys 29%	Asp 76%	Gly 56%	Asp 52%	Gly 96%	Thr 23%	Ile 68%	Asp 32%	Phe 23%	Glu 29%	Glu 92%
also frequently observed		Ala Gln Thr Val Ile Ser Glu Arg	Asn	Lys Arg Asn	Ser Asn		Phe Lys Gln Tyr Glu Arg	Val Leu	Ser Thr Glu Asn Gly Gln	Tyr Ala Thr Leu Glu Lys	Asp Lys Ala Pro Asn	Asp

Table 1. The sequence preference of the EF-hand loop. The Ca²⁺ ligands are indicated by both their position in the EF-loop and in the coordinating array with whether or not coordination occurs via the side chain (sc) or through the backbone (bb) indicated below. The asterisk (*) highlights the ligand typically provided by a water molecule that is hydrogen-bonded to the side chain of the amino acid found at position-9. Also noted in the table are the most common amino acids at each position, with their corresponding percentage of occurrence, and those that occur with a frequency greater than 5% in known EF-loops. This table is redrawn from Gifford et al., 2007, figure 3A.

EF Hands	Substitution	Position in loop	Coordinating axis	V _{max}	K'	Hill Coeff.	K _M **
1	D382A	1	X	64.5	0.86	3.50	
	E393A	12	-Z	127.4	0.91	3.33	15.67
2	D418A	1	X	247.6	1.10	2.60	
	D420A	3	Y	950*	82.9*	0.46*	
	N422A	5	Z	410.4	1.05	3.45	
	N422D	5	Z	541.2	0.64	5.71	
	N422D + E429D	5	Z + -Z	437.9	0.86	3.47	
	D426A	9	-X	346.4	0.78	5.52	
	E429A	12	-Z	326.1	1.10	2.62	14.45
	E429D	12	-Z	225.0	0.95	2.66	
	5 A's	1, 3, 5, 9, and 12	X, Y, Z, -X, and -Z	40.1	1.62	2.05	
3	D454A	1	X	90.7	1.27	1.65	
	E465A	12	Z	194.3	1.27	1.98	5.76
4	D489A	1	X	378.5	0.85	3.98	
	E500A	12	Z	271.7	0.89	3.49	6.53
	WT			899.6	0.58	4.54	

Table 2. Summary of mutations and their assay results. V_{max}, K' and Hill coefficients are assayed at [Syntide-2] = 200 μM and [Ca²⁺] ranges from zero to 100 μM. *assay results of the [Ca²⁺] range up to 600 μM. **Assays at [Ca²⁺] = 100 μM.

	Plant line	TG in Male	Basta ^f	Total N	Observed
WT	Total 4	34P::CPK34-GFP	287	942	30.47
	1319		75	239	31.38
	1320		54	192	28.13
	2127		77	266	28.95
	TL12514		81	245	33.06
EF 1	Total 14	34P::CPK34(E393A)-TAP2Y	20	7055	0.28
	1677		4	618	0.65
	1683		2	551	0.36
	1684		5	553	0.90
	1686		3	407	0.74
	TL 13868 b		1	121	0.83
	TL 13869 c		1	866	0.12
	TL 13870 d		1	901	0.11
	TL 13871 e		1	547	0.18
	TL 13872 f		1	347	0.29
	TL 13875 i		1	497	0.20
	TL 13875 j		0	541	0
	TL 13878 l		0	489	0
	TL 13879 m		0	363	0
	TL 13881 o		0	254	0
EF 2	Total 15	34P::CPK34(E429A)-TAP2Y	10	10408	0.10
	1687		2	718	0.28
	1688		1	683	0.15
	1689		3	833	0.36
	1692		2	1099	0.18
	TL 13894		0	495	0
	TL 13896		0	371	0
	TL 13882 a		0	141	0
	TL 13883 b		0	477	0
	TL 13885 d		0	30	0
	TL 13886 e		0	1060	0
	TL 13887 f		0	394	0
	TL 13889 h		1	1002	0.10
	TL 13890 i		0	1203	0
	TL 13891 j		1	1110	0.09
	TL 13892 k		0	792	0

Continued on next page

EF 3	Total 17	34P::CPK34(E465A)-TAP2Y	62	6875	0.90
	1693		6	406	1.48
	1695		10	308	3.25
	1700		18	770	2.34
	1703		6	261	2.30
	TL 13916		3	817	0.37
	TL 13897 a		1	50	2.00
	TL 13898 b		0	17	0
	TL 13899 c		2	692	0.29
	TL 13900 d		0	150	0
	TL 13901 e		3	377	0.80
	TL 13903 g		3	668	0.45
	TL 13904 h		0	344	0
	TL 13905 i		5	782	0.64
	TL 13906 j		0	210	0
	TL 13908 l		0	161	0
	TL 13909 m		3	298	1.01
	TL 13910 n		2	564	0.35
EF 4	Total 16	34P::CPK34(E500A)-TAP2Y	21	9131	0.23
	1706		5	685	0.73
	1710		7	781	0.90
	1713		1	253	0.40
	1714		2	521	0.38
	TL 13932		0	453	0
	TL 13919 b		2	1594	0.13
	TL 13920 c		0	336	0
	TL 13921 d		0	591	0
	TL 13922 e		2	629	0.32
	TL 13923 f		1	413	0.24
	TL 13926 i		0	634	0
	TL 13929 l		1	469	0.21
	TL 13930 m		0	335	0
	TL 13925 h		0	1208	0
	TL 13926 i		0	229	0

Table 3. Pollination transmission efficiency assay, competition with wild type.

Female line in this assay is *cpk17-2/34-2* (-/-, -/-). Male line is *cpk17-5/34-1* (-/-, +/-,

Basta^r). Theoretical expected % is 33.3 for all cases. Averages of all plant lines tested are

listed in the first row at each section. Four best plant lines used to draw figure 13, are

shown in bold. Each individual line is indicated under the four best lines.

Construct	Male	Female	Hyg-R	Total N	Observed %	Expected %
Vector only; 34P-TAP2Y	col	vector	105	195	53.8	50
	vector	<i>17/34, -/-</i>	0	More than 10 crosses	0	50
	Het. Self		648	850	76.2	75
EF1 E393A	col	EF1 E393A	168	324	51.9	50
	EF1 E393A	<i>17/34, -/-</i>	47	47	100.0	50
	Het. Self		334	338	98.8	75
EF2 E429A	col	EF2 E429A	270	509	53.0	50
	EF2 E429A	<i>17/34, -/-</i>	12	12	100.0	50
	Het. Self		748	758	98.7	75
EF3 E465A	col	EF3 E465A	110	200	55.0	50
	EF3 E465A	<i>17/34, -/-</i>	46	46	100.0	50
	Het. Self		295	295	100.0	75
EF4 E500A	col	EF4 E500A	69	135	51.1	50
	EF4 E500A	<i>17/34, -/-</i>	245	245	100.0	50
	Het. Self		754	758	99.5	75
EF2 D420A	col	EF2 D420A	88	168	52.4	50
	EF2 D420A	<i>17/34, -/-</i>	0	More than 10 crosses	0	50
	Het. Self		569	618	92.1	75
EF2 5A's	Het. Self		1369	1810	75.6	75

Table 4. Pollination transmission efficiency assay, competition with *cpk17/34*. Four position-12 mutants showed competitive frequency against *17/34 (-/-)* in reciprocal crosses and self-fertilization. But D420A (position-3 EF2) showed less activity than position-12 mutants and better activity than EF2 5A's of which result was close to negative control (vector only).

Appendix A. DNA sequences of plasmid constructs used in this study

GST-CPK34(WT)-6His in pGEX vector.

CPK34 (**BOLD**) starts with ATG following GST (**BLUE**) and ends with a TGA downstream of a 6-His (**blue lower case**) coding site. XhoI and XbaI restriction sites (**yellow lower case**) are located between GST and CPK34, and between CPK34 and 6-His, respectively. Stop codon (**TGA**) after 6-His is highlighted as yellow.

```

ACGTTATCGACTGCACGGTGCACCAATGCTTCTGGCGTCAGGCAGCCATCGGAAGCTGTGGTATGGCTGTG
CAGGTTCGTAAATCACTGCATAATTCGTGTGCGTCAAGGCGCACTCCCGTTCTGGATAATGTTTTTTCGCC
GACATCATAACGGTTCTGGCAAATATTCTGAAATGAGCTGTTGACAATTAATCATCGGCTCGTATAATGTG
TGGAATTGTGAGCGGATAACAATTTACACACAGGAAACAGTATTCATGTCCCCTATACTAGGTTATTGGAAA
ATTAAGGGCCTTGTGCAACCCACTCGACTTCTTTTGGAAATATCTTGAAGAAAAATATGAAGAGCATTGTGA
TGAGCGCGATGAAGGTGATAAATGGCGAAACAAAAAGTTTGAATTGGGTTTGGAGTTTCCCAATCTTCCTT
ATTATATTGATGGTGTATGTTAAATTAACACAGTCTATGGCCATCATACTGTTATATAGCTGACAAGCACAAC
ATGTTGGGTGGTTGTCCAAAAGAGCGTGCAGAGATTTCAATGCTTGAAGGAGCGGTTTTGGATATTAGATA
CGGTGTTTTCGAGAATTGCATATAGTAAAGACTTTGAAACTCTCAAAGTTGATTTTTCTTAGCAAGCTACCTG
AAATGCTGAAAATGTTGCAAGATCGTTTTATGTCATAAAACATATTTAAATGGTGATCATGTAACCCATCCT
GACTTCATGTTGTATGACGCTCTTGATGTTGTTTTATACATGGACCCAATGTGCCTGGATGCGTTCCCAAA
ATTAGTTTGTTTTTAAAAACGTATTGAAGCTATCCACAAATTGATAAGTACTTGAATCCAGCAAGTATA
TAGCATGGCCTTTGCAGGGCTGGCAAGCCACGTTTGGTGGTGGCGACCATCCTCCAAAATCGGATCTGGTT
CCGCGTGGATCTCGTGCATCTGTTGGATCCATGGAATTCctcgagATGGGAAATTGTTGCTCTCATGG
AAGAGATTGAGATGATAACAAAGAAGAACCAGGGCCGGAAAATGGAGGCGGGGTTGGTGGCCGCTGAAG
CCTCTGTTAGAGCTTCTAAACACCCGCCAGCATCTCCTCCTCCTGCAACCAAAACAAGGACCAATAGGACCT
GTCTTAGGGCGCAACATGGAAGATGTAAGAGCTCATATACATTGGGTAAGGAGCTAGGTCTGGACAGTT
TGGGGTGACTCATCTCTGCACGCAAAAGGCCAGGGGCTGCAATTCGCTTGAAGACCATTGCTAAAAGGA
AGCTCGTGAACAAAGAAGACATTGAGGATGTGAGAAGGGAGGTGCAGATTATGCATCACTTGACC GGTCAG
CCAAACATTGTGGAGCTTAAAGGAGCGTATGAGGATAAGCATTCTGTGCATTTGGTTATGGAGCTTTGCGC
GGGAGGTGAGTTGTTTCGACAGGATTATCGCAAAGGGACATTATTCGGAGAGAGCTGCAGCCTCGTTACTAC
GGACGATTGTGCAGATTATCCATACTTGCCATTCCATGGGGGTTATCCACAGGGACTTGAAGCCTGAGAAC
TTTTTGTGCTTAGCAAGGATGAGAATTCTCCTCTGAAAGCCACCGACTTCGGGTTATCCGTGTTCTACAA
ACCAGGAGAGGTGTTCAAAGACATTGTGGGAAGTGCTTATTACATTGCACCAGAGGTGTTGAGGAGGAAGT
ATGGACCAGAGGCTGATATTTGGAGCATTGGTGTCTGTTGTATATCCTCCTGTGTGGTGTTCACCTTTT
TGGGCTGAGTCAGAGAATGGGATTTTTCAATGCCATCCTAAGTGGACAGGTTGATTTTTCAAGCGATCCATG
GCCAGTCATCTCACCACAGGCAAAAGACCTCGTTAGGAAGATGCTCAACTCTGATCCAAAACAAAGATTAA
CCGCTGCTCAAGTTCTCAATCATCCATGGATCAAGGAGGATGGAGAAGCACCGGATGTTTCTTGGACAAAT
GCAGTGATGTCTAGGCTCAAGCAGTTCAAAGCAATGAACAACTTTAAGAAAAGTTGCTTTACGGGTGATAGC
CGGGTGCTTATCAGAGGAAGAAATCATGGGGTTAAAAGAGATGTTCAAAGGAATGGACACTGACAACAGTG
GAACATAAATCTTGAGGAACTAAGACAGGGACTTGCTAAGCAAGGTACAAGTTTATCCGAATACGAAGTC
CAGCAACTAATGGAAGCTGCTGATGCGGACGGTAATGGAAACAATAGACTATGGGGAGTTTCATTGCGACTAC
AATGCACATCAACAGGCTCGACAGAGAAGAGCATCTCTACTCAGCCTTCAAACATTTGACAAAAGACAACA
GTGGATATATCAACGGAAGAGCTAGAGCAAGCCCTTCGGGAGTTTGGCATGAACGATGGCAGAGACATT
AAGGAAATCATTTCTGAGGTTGATGGAGACAATGATGGGCGGATAAACTACGAGGAATTTGTGGCGATGAT
GAGAAAAGGAAACCCAGATCCTAATCCTAAGAAGCGGCGTGAACCTATCATTCAAAGGTGGCGGtctagaCC
CGGGAATGcatcaccatcaccatcacGGATCCTGAATTGATCGATAGAGCTCAAGCTTAATTCATCGTGACT
GACTGACGATCTGCCTCGCGGTTTTCGGTGATGACGGTGAAAACCTCTGACACATGCAGCTCCCGGAGACG
GTCACAGCTTGTCTGTAAGCGGATGCCGGGAGCAGACAAGCCCGTCAGGGCGCGTCAGCGGGTGTGGCGG
GTGTCGGGGCGCAGCCATGACCCAGTCACGTAGCGATAGCGGAGTGTATAATTTTGAAGACGAAAGGGCC
TCGTGATACGCCTATTTTTATAGGTTAATGTCATGATAATAATGGTTTTCTTAGACGTCAGGTGGCACTTTT
CGGGGAAATGTGCGCGGAACCCCTATTTGTTTTATTTTTCTAAATACATTCAAATATGTATCCGCTCATGAG
ACAATAACCCTGATAAATGCTTCAATAAATTTGAAAAAGGAAGAGTATGAGTATTCAACATTTCCGTGTGCG
CCCTTATCCCTTTTTGCGGCATTTTTGCCTTCTGTTTTTGTCTCACCAGAAACGCTGGTGAAGATAAA
GATGCTGAAGATCAGTTGGGTGCACGAGTGGGTTACATCGAACTGGATCTCAACAGCGGTAAGATCCTTGA
GAGTTTTTCGCCCCGAAGAAGCTTTTCCAATGATGAGCACTTTTAAAGTTCTGCTATGTGGCGGGTATTAT
CCCGTGTGACGCCGGCAAGAGCAACTCGGTCGCCGCATACACTATTCTCAGAATGACTTGGTTGAGTAC
TCACCAGTCACAGAAAAGCATCTTACGGATGGCATGACAGTAAGAGAATTATGCAGTGCTGCCATAACCAT

```

GAGTGATAACACTGCGGCCAACTTACTTCTGACAACGATCGGAGGACCGAAGGAGCTAACCGCTTTTTTGC
 ACAACATGGGGGATCATGTAACCTGCCTTGATCGTTGGGAACCGGAGCTGAATGAAGCCATACCAAACGAC
 GAGCGTGACACCACGATGCCTGCAGCAATGGCAACAACGTTGCGCAAACCTATTAACCTGGCGAACTACTTAC
 TCTAGCTTCCCGGCAACAATTAATAGACTGGATGGAGGCGGATAAAGTTGCAGGACCCTTCTGCGCTCGG
 CCCTTCCGGCTGGCTGGTTTTATTGCTGATAAATCTGGAGCCGGTGAGCGTGGGTCTCGCGGTATCATTGCA
 GCACTGGGGCCAGATGGTAAGCCCTCCCGTATCGTAGTTATCTACACGACGGGGAGTCAGGCAACTATGGA
 TGAACGAAATAGACAGATCGCTGAGATAGGTGCCTCACTGATTAAGCATTGGTAACCTGTGACACCAAGTTT
 ACTCATATATACTTTAGATTGATTTAAAACCTCATTTTTTAATTTAAAAGGATCTAGGTGAAGATCCTTTTT
 GATAATCTCATGACCAAATCCCTTAACGTGAGTTTTTCGTTCCACTGAGCGTCAGACCCCGTAGAAAAGAT
 CAAAGGATCTTCTTGAGATCCTTTTTTTCTGCGCGTAATCTGCTGCTTGCAAACAAAAAACACCCTAC
 CAGCGGTGGTTTTGTTTGGCGGATCAAGAGCTACCAACTCTTTTTCCGAAGGTAACCTGGCTTCAGCAGAGCG
 CAGATACCAAATACTGTCCTTCTAGTGTAGCCGTAGTTAGGCCACCACTTCAAGAACTCTGTAGCACCGCC
 TACATACCTCGCTCTGCTAATCCTGTTACCAGTGGCTGCTGCCAGTGGCGATAAGTCGTGTCTTACCGGGT
 TGGACTCAAGACGATAGTTACCAGGATAAGGCGCAGCGGTGGGCTGAACGGGGGGTTCGTGCACACAGCCC
 AGCTTGGAGCGAACGACCTACACCGAACTGAGATACCTACAGCGTGAGCTATGAGAAAGCGCCACGCTTCC
 CGAAGGGGAGAAAGGCGGACAGGTATCCGGTAAGCGGCAGGGTTCGGAACAGGAGAGCGCACGAGGGGAGCTTC
 CAGGGGGAAACGCCTGGTATCTTTATAGTCTGTGCGGGTTTTCGCCACCTCTGACTTGAGCGTCGATTTTTG
 TGATGCTCGTCAGGGGGGCGGAGCCTATGGAAAAACGCCAGCAACGCGGCCTTTTTACGGTTCCTGGCCTT
 TTGCTGGCCTTTTGGCTCACATGTTCTTTCTGCGTTATCCCCTGATTCTGTGGATAACCGTATTACCGCCT
 TTGAGTGAGCTGATACCGCTCGCCGACGCCGAAACGAGCGCAGCGAGTCAGTGAGCGAGGAAGCGGAA
 GAGCGCCTGATGCGGTATTTTTCTCCTTACGCATCTGTGCGGTATTTTACACCCGATAAATCCGACACCAT
 CGAATGGTGCAAACCTTTTCGCGGTATGGCATGATAGCGCCCGAAGAGAGTCAATTCAGGGTGGTGAATG
 TGAACCAGTAACGTTATACGATGTGCGCAGAGTATGCCGGTGTCTCTTATCAGACCGTTTTCCCGCTGGTG
 AACCAGGCCAGCCACGTTTTCTGCGAAAACGCGGAAAAAGTGAAGCGGCGATGGCGGAGCTGAATTACAT
 TCCCAACCGCGTGGCACAACAACCTGGCGGGCAAACAGTCGTTGCTGATTGGCGTTGCCACCTCCAGTCTGG
 CCCTGCACGCGCCGTCGCAAATTTGTCGCGGCGATTAAATCTCGCGCCGATCAACTGGGTGCCAGCGTGGTG
 GTGTGATGGTAGAACGAAGCGGCGTGAAGCCTGTAAAGCGGCGGTGCACAATCTTCTCGCGCAACGCGT
 CAGTGGGCTGATCATTAACTATCCGCTGGATGACCAGGATGCCATTGCTGTGGAAGCTGCCTGCACTAATG
 TTCCGGCGTTATTTCTTGATGTCTCTGACCAGACACCCATCAACAGTATTATTTTTCTCCCATGAAGACGGT
 ACGCGACTGGGCGTGGAGCATCTGGTTCGATTGGGTACCAGCAAATCGCGCTGTTAGCGGGCCCATTAAG
 TTCTGTCTCGGCGCGTCTGCGTCTGGCTGGCTGGCATAAATATCTCACTCGCAATCAAATTCAGCCGATAG
 CGGAACGGGAAGGCGACTGGAGTGCCATGTCCGGTTTTCAACAAACCATGCAAATGCTGAATGAGGGCATC
 GTTCCCACCTGCGATGCTGGTTGCCAACGATCAGATGGCGCTGGGCGCAATGCGCGCCATTACCGAGTCCGG
 GCTGCGCGTGGTGGGATATCTCGGTAGTGGGATACGACGATAACGAAGACAGCTCATGTTATATCCCGC
 CGTTAACACCATCAAACAGGATTTTTCGCCTGCTGGGGCAAACAGCGTGGACCCTTGCTGCAACTCTCT
 CAGGGCCAGGCGGTGAAGGGCAATCAGCTGTTGCCCGTCTCACTGGTGAAAAGAAAAACCACCCTGGCGCC
 CAATACGCAAACCGCCTCTCCCCGCGGTTGGCCGATTCAATTAATGCAGCTGGCAGCAGAGGTTTTCCCGAC
 TGGAAAGCGGGCAGTGAGCGCAACGCAATTAATGTGAGTTAGCTCACTCATTAGGCACCCAGGCTTTACA
 CTTTATGCTTCCGGCTCGTATGTTGTGTGGAATTGTGAGCGGATAACAATTTACACAGGAAACAGCTATG
 ACCATGATTACGATTCACTGGCCGTCGTTTTACAACGTCGTGACTGGGAAAACCTGGCGTTACCCAACCT
 TAATCGCCTTGCAGCACATCCCCCTTTGCCAGCTGGCGTAATAGCGAAGAGGCCCGCACCGATCGCCCTT
 CCCAACAGTTGCGCAGCCTGAATGGCGAATGGCGCTTTGCCTGGTTTTCCGGCACCAAGCGGTGCCGGAA
 AGCTGGCTGGAGTGGGATCTTCCCTGAGGCCGATACTGTCGTGCTCCCTCAAACCTGGCAGATGCACGGTTA
 CGATGCGCCCATCTACACCAACGTAACCTATCCATTACGGTCAATCCGCCGTTTTGTTCCACGGAGAATC
 CGACGGGTTGTTACTCGCTCACATTTAATGTTGATGAAAGCTGGCTACAGGAAGGCCAGACGCGAATTATT
 TTTGATGGCGTTGGAATT

GST-CPK34(D382A)-6His in pGEX vector; mutation in EF1, from GST to stop codon (TGA) is shown. CPK34(D382A) (**BOLD**) starts with ATG following GST and ends with a TGA downstream of a 6-His (**blue lower case**) coding site. XhoI and XbaI restriction sites (**yellow lower case**) are located between GST and CPK34(D382A), and between CPK34(D382A) and 6-His, respectively. Stop codon (**TGA**) after 6-His is highlighted as yellow.

**ATGTCCCCTATACTAGGTTATTGGAAAAATTAAGGGCCTTGTGCAACCCACTCGACTTCTTTTGGAAATATCT
 TGAAGAAAAATATGAAGAGCATTGTATGAGCGCGATGAAGGTGATAAATGGCGAAAACAAAAAGTTTGAAT**

TGGGTTTGGAGTTTCCCAATCTTCCTTATTATATTGATGGTGATGTTAAATTAACACAGTCTATGGCCATC
 ATACGTTATATAGCTGACAAGCACAACATGTTGGGTGGTTGTCCAAAAGAGCGTGCAGAGATTTCAATGCT
 TGAAGGAGCGGTTTTGGATATTAGATACGGTGTTCGAGAATTGCATATAGTAAAGACTTTGAAACTCTCA
 AAGTTGATTTTTCTTAGCAAGCTACCTGAAATGCTGAAAATGTTTGAAGATCGTTTATGTCATAAAACATAT
 TTAATGGTGATCATGTAACCCATCCTGACTTCATGTTGTATGACGCTCTTGATGTTGTTTTATACATGGA
 CCCAATGTGCCTGGATGCGTTCCCAAAATTAGTTTGTGTTTTAAAAACGTATTGAAGCTATCCCACAAATTG
 ATAAGTACTTGAAATCCAGCAAGTATATAGCATGGCCTTTGCAGGGCTGGCAAGCCACGTTTGGTGGTGGC
 GACCATCTCCAAAATCGGATCTGGTCCGCGTGGATCTCGTCGTGCATCTGTTGGATCCATGGAATTC**ct**
cgagATGGGAAATTTGGTCTCTCATGGAAGAGATT**CAGATGATAACAAAGAAGAACC**GAGGCCGAAAATG
 GAGCGGCGGTGTTGGTGCCGCTGAAGCCTCTGTTAGAGCTTCTAAACACCCGCCAGCATCTCCTCCTCCT
 GCAACCAAAACAAGGACCAATAGGACCTGTCTTAGGGCGACCAATGGAAGATGTAAAGAGCTCATATACATT
 GGGTAAGGAGCTAGGTCGTGGACAGTTTGGGGTGACTCATCTCTGCACGCAAAAGGCCACGGGGCTGCAAT
 TCGCTTGAAGACCATTGCTAAAAGGAAGCTCGTGAACAAAGAAGACATTGAGGATGTGAGAAGGGAGGTG
 CAGATTATGCATCACTTGACCGGT**CAGCCAAACATTGTGGAGCTTAAAGGAGCGTATGAGGATAAGCATT**
TGTGCATTTGGTTATGGAGCTTTGCGCGGGAGGTGAGTTGTTCGACAGGATTATCGCAAAGGGACATTATT
 CGGAGAGAGCTGCAGCCTCGTTACTACGGACGATTGTGCAGATTATCATACTTGCATTCCATGGGGGTT
 ATCCACAGGGACTTGAAGCCTGAGAACTTTTTGGTCTTAGCAAGGATGAGAATTTCTCCTCTGAAAGCCAC
 CGACTTCGGGTTATCCGTGTTCTACAAACCAGGAGAGGTGTTCAAAGACATTGTGGGAAGTGCTTATTACA
 TTGCACCAGAGGTGTTGAGGAGGAAGTATGGACCAGAGGCTGATATTTGGAGCATTGGTGTATGTTGTAT
 ATCCTCTGTGTGGTGTCCACCTTTTTGGGCTGAGTCAGAGAATGGGATTTTTCAATGCCATCCTAAGTGG
 ACAGTTTGTATTTTTCAAGCGATCCATGGCCAGTCACTCACACAGGCAAAAGACCTCGTTAGGAAGATGC
 TCAACTCTGATC AAAAACAAGATTAACCGCTGCTCAAGTTCTCAATCATCATGGATCAAGGAGGATGGA
 GAAGCACCGGATGTTCTCTTGACAATGCAGTGATGTCTAGGCTCAAGCAGTTCAAAGCAATGAACAACCTT
 TAAGAAAGTTGCTTTACGGGTGATAGCCGGGTGCTTATCAGAGGAAGAAATCATGGGGTAAAAGAGATGT
 TCAAAGGAATGGCCACTGACAACAGTGGTACCATAACTCTTGAGGAACTAAGACAGGGACTTGCTAAGCAA
 GGTACAAGTTATCCGAATACGAAGTCCAGCAACTAATGGAAGCTGCTGATGCGGACGGTAATGGAACAAT
 AGACTATGGGGAGTTT**CATTGCAGCTACAATGCACATCAACAGGCTCGACAGAGAAGAGCATCTCTACTCAG**
CCTTCCAACACTTTGACAAAGACAACAGTGGATATATCACAACGGAAGAGCTAGAGCAAGCCCTTCGGGAG
TTTGGCATGAACGATGGCAGAGACATTAAGGAAATCATTCTGAGGTTGATGGAGACAATGATGGGCGGAT
AAACTACGAGGAATTTGTGGCGATGATGAGAAAAGGAAACCAGATCCTAATCCTAAGAAGCGGCGTGAAC
TATCATTCAAAGGTGGCGGtctagaCCCGGGAATG**catcaccatcaccatcac**GGATCCT**GATGA**

GST-CPK34(E393A)-6His in pGEX vector; mutation in EF1, from GST to stop codon (TGA) is shown.
 CPK34(E393A) (**BOLD**) starts with ATG following GST and ends with a TGA downstream of a 6-His
 (blue lower case) coding site. XhoI and XbaI restriction sites (yellow lower case) are located between GST
 and CPK34(E393A), and between CPK34(E393A) and 6-His, respectively. Stop codon (TGA) after 6-His
 is highlighted as yellow.

ATGTCCCTATACTAGGTTATTGGAAAATTAAGGGCCTTGTGCAACCCACTCGACTTCTTTTTGGAATATCT
 TGAAGAAAAATATGAAGAGCATTGTTGATGAGCGCGATGAAGGTGATAAATGGCGAAAACAAAAGTTTGAAT
 TGGGTTTGGAGTTTCCCAATCTTCCTTATTATATTGATGGTGATGTTAAATTAACACAGTCTATGGCCATC
 ATACGTTATATAGCTGACAAGCACAACATGTTGGGTGGTTGTCCAAAAGAGCGTGCAGAGATTTCAATGCT
 TGAAGGAGCGGTTTTGGATATTAGATACGGTGTTCGAGAATTGCATATAGTAAAGACTTTGAAACTCTCA
 AAGTTGATTTTTCTTAGCAAGCTACCTGAAATGCTGAAAATGTTTGAAGATCGTTTATGTCATAAAACATAT
 TTAATGGTGATCATGTAACCCATCCTGACTTCATGTTGTATGACGCTCTTGATGTTGTTTTATACATGGA
 CCCAATGTGCCTGGATGCGTTCCCAAAATTAGTTTGTGTTTTAAAAACGTATTGAAGCTATCCCACAAATTG
 ATAAGTACTTGAAATCCAGCAAGTATATAGCATGGCCTTTGCAGGGCTGGCAAGCCACGTTTGGTGGTGGC
 GACCATCTCCAAAATCGGATCTGGTCCGCGTGGATCTCGTCGTGCATCTGTTGGATCCATGGAATTC**ct**
cgagATGGGAAATTTGGTCTCTCATGGAAGAGATT**CAGATGATAACAAAGAAGAACC**GAGGCCGAAAATG
 GAGCGGCGGTGTTGGTGCCGCTGAAGCCTCTGTTAGAGCTTCTAAACACCCGCCAGCATCTCCTCCTCCT
 GCAACCAAAACAAGGACCAATAGGACCTGTCTTAGGGCGACCAATGGAAGATGTAAAGAGCTCATATACATT
 GGGTAAGGAGCTAGGTCGTGGACAGTTTGGGGTGACTCATCTCTGCACGCAAAAGGCCACGGGGCTGCAAT
 TCGCTTGAAGACCATTGCTAAAAGGAAGCTCGTGAACAAAGAAGACATTGAGGATGTGAGAAGGGAGGTG
 CAGATTATGCATCACTTGACCGGT**CAGCCAAACATTGTGGAGCTTAAAGGAGCGTATGAGGATAAGCATT**
TGTGCATTTGGTTATGGAGCTTTGCGCGGGAGGTGAGTTGTTCGACAGGATTATCGCAAAGGGACATTATT

CGGAGAGAGCTGCAGCCTCGTTACTACGGACGATTGTGCAGATTATCCATACTTGCCATTCCATGGGGGTT
 ATCCACAGGGACTTGAAGCCTGAGAACTTTTTGTTGCTTAGCAAGGATGAGAATTCTCCTCTGAAAGCCAC
 CGACTTCGGGTTATCCGTGTTCTACAAACAGGAGAGGTGTTCAAAGACATTGTGGGAAGTGCTTATTACA
 TTGCACCAGAGGTGTTGAGGAGGAAGTATGGACCAGAGGCTGATATTTGGAGCATTGGTGTATGTTGTAT
 ATCCTCCTGTGTGGTGTTCACCTTTTTGGGCTGAGTCAGAGAATGGGATTTTCAATGCCATCCTAAGTGG
 ACAGGTTGATTTTTCAAGCGATCCATGGCCAGTCATCTCACCACAGGCAAAAGACCTCGTTAGGAAGATGC
 TCAACTCTGATCCAAAACAAAGATTAACCGCTGCTCAAGTTCTCAATCATCCATGGATCAAGGAGGATGGA
 GAAGCACCGGATGTTCTCTTGACAATGCAGTGTCTAGGCTCAAGCAGTTCAAAGCAATGAACAACCTT
 TAAGAAAGTTGCTTTACGGGTGATAGCCGGGTGCTTATCAGAGGAAGAAATCATGGGGTTAAAAGAGATGT
 TCAAAGGAATGGCACTGACAACAGTGGTACCATAACTCTTGAGGCACTAAGACAGGGACTTGCTAAGCAA
 GGTACAAGTTATCCGAATACGAAGTCCAGCAACTAATGGAAGCTGCTGATGCGGACGGTAATGGAACAAT
 AGACTATGGGGAGTTCATTGCAGCTACAATGCACATCAACAGGCTCGACAGAGAAGAGCATCTCTACTCAG
 CCTTCCAACACTTTGACAAAGACAACAGTGGATATATCACAACGGAAGAGCTAGAGCAAGCCCTTCGGGAG
 TTTGGCATGAACGATGGCAGAGACATTAAGGAAATCATTTCTGAGGTTGATGGAGACAATGATGGGCGGAT
 AAACCTACGAGGAATTTGTGGCGATGATGAGAAAAGGAAACCAGATCCTAATCCTAAGAAGCGGCGTGAAC
 TATCATTCAAAGGTGGCGGtctagaCCCGGAATGcatcaccatcaccatcacGGATCCTGA

GST-CPK34(D418A)-6His in pGEX vector; mutation in EF2, from GST to stop codon (TGA) is shown. CPK34(D418A) (**BOLD**) starts with ATG following GST and ends with a TGA downstream of a 6-His (blue lower case) coding site. XhoI and XbaI restriction sites (yellow lower case) are located between GST and CPK34(D418A), and between CPK34(D418A) and 6-His, respectively. Stop codon (TGA) after 6-His is highlighted as yellow.

ATGTCCCCTATACTAGGTTATTGGAAAATTAAGGGCCTTGTGCAACCCACTCGACTTCTTTTGAATATCT
 TGAAGAAAAATATGAAGAGCATTGTATGAGCGCGATGAAGGTGATAAATGGCGAAACAAAAAGTTTGAAT
 TGGGTTTGGAGTTTCCCAATCTTCTTATTATATTGATGGTGTATGTTAAATTAACACAGTCTATGGCCATC
 ATACGTTATATAGCTGACAAGCACAACATGTTGGGTGGTGTCCAAAAGAGCGTGCAGAGATTTCAATGCT
 TGAAGGAGCGGTTTTGGATATTAGATACGGTGTTCGAGAATTGCATATAGTAAAGACTTTGAAACTCTCA
 AAGTTGATTTTCTTAGCAAGCTACCTGAAATGCTGAAAATGTTTGAAGATCGTTTATGTCATAAAACATAT
 TTAATGGTGTATCATGTAACCCATCCTGACTTCATGTTGTATGACGCTCTTGATGTTGTTTTATACATGGA
 CCAATGTGCCTGGATGCGTTCCAAAATTAGTTTGTGTTTTAAAAACGTATTGAAGCTATCCACAAATTG
 ATAAGTACTTTGAAATCCAGCAAGTATATAGCATGGCCTTTGCAGGGCTGGCAAGCCACGTTTGGTGGTGGC
 GACCATCCTCCAAAATCGGATCTGGTTCGCGTGGATCTCGTCTGTCATCTGTTGGATCCATGGAATTCct
 cgagATGGGAAATGTTGCTCTCATGGAAGAGATTGAGATGATAACAAAGAAGAACCAGGAGCCGGAAAATG
 GAGGCGGCGGTGTTGGTGCCGCTGAAGCCTCTGTTAGAGCTTCTAAACACCCGCAAGCATCTCCTCCTCCT
 GCAACCAAACAAGGACCAATAGGACCTGTCTTAGGGCGCAATGGAAGATGTAAGAGCTCATATACATT
 GGGTAAGGAGCTAGGTCTGGACAGTTTTGGGTGACTCATCTCTGCACGAAAAGGCCACGGGGCTGCAAT
 TCGCTTGCAAGACCATTGCTAAAAGGAAGCTCGTGAACAAAGAAGACATTGAGGATGTGAGAAGGGAGGTG
 CAGATTATGCATCACTTGACCGGTGAGCCAAAATTGTTGGAGCTTAAAGGAGCGTATGAGGATAAGCATT
 TGTGCATTTGGTTATGGAGCTTTGCGCGGGAGGTGAGTTGTTGACAGGATTATCGCAAAGGGACATTATT
 CGGAGAGAGCTGCAGCCTCGTTACTACGGACGATTGTGCAGATTATCCATACTTGCCATTCCATGGGGGTT
 ATCCACAGGGACTTGAAGCCTGAGAACTTTTTGTTGCTTAGCAAGGATGAGAATTCTCCTCTGAAAGCCAC
 CGACTTCGGGTTATCCGTGTTCTACAAACAGGAGAGGTGTTCAAAGACATTGTGGGAAGTGCTTATTACA
 TTGCACCAGAGGTGTTGAGGAGGAAGTATGGACCAGAGGCTGATATTTGGAGCATTGGTGTATGTTGTAT
 ATCCTCCTGTGTGGTGTTCACCTTTTTGGGCTGAGTCAGAGAATGGGATTTTCAATGCCATCCTAAGTGG
 ACAGGTTGATTTTTCAAGCGATCCATGGCCAGTCATCTCACCACAGGCAAAAGACCTCGTTAGGAAGATGC
 TCAACTCTGATCCAAAACAAAGATTAACCGCTGCTCAAGTTCTCAATCATCCATGGATCAAGGAGGATGGA
 GAAGCACCGGATGTTCTCTTGACAATGCAGTGTCTAGGCTCAAGCAGTTCAAAGCAATGAACAACCTT
 TAAGAAAGTTGCTTTACGGGTGATAGCCGGGTGCTTATCAGAGGAAGAAATCATGGGGTTAAAAGAGATGT
 TCAAAGGAATGGCACTGACAACAGTGGTACCATAACTCTTGAGGAACTAAGACAGGGACTTGCTAAGCAA
 GGTACAAGTTATCCGAATACGAAGTCCAGCAACTAATGGAAGCTGCTGCGCGGACGGTAATGGAACAAT
 AGACTATGGGGAGTTCATTGCAGCTACAATGCACATCAACAGGCTCGACAGAGAAGAGCATCTCTACTCAG
 CCTTCCAACACTTTGACAAAGACAACAGTGGATATATCACAACGGAAGAGCTAGAGCAAGCCCTTCGGGAG
 TTTGGCATGAACGATGGCAGAGACATTAAGGAAATCATTTCTGAGGTTGATGGAGACAATGATGGGCGGAT

**AAACTACGAGGAATTTGTGGCGATGATGAGAAAAGGAAACCCAGATCCTAATCCTAAGAAGCGGCGTGAAC
TATCATTCAAAGGTGGCGGtctagaCCCGGAATGcatcaccatcaccatcacGGATCC**TGA****

GST-CPK34(E429A)-6His in pGEX vector; mutation in EF2, from GST to stop codon (TGA) is shown. CPK34(E429A) (**BOLD**) starts with ATG following GST and ends with a TGA downstream of a 6-His (blue lower case) coding site. XhoI and XbaI restriction sites (yellow lower case) are located between GST and CPK34(E429A), and between CPK34(E429A) and 6-His, respectively. Stop codon (**TGA**) after 6-His is highlighted as yellow.

ATGTCCCCTATACTAGGTTATTGGAAAATTAAGGGCCTTGTGCAACCCACTCGACTTCTTTTGGAAATATCT
TGAAGAAAAATATGAAGAGCATTGTATGAGCGCGATGAAGGTGATAAATGGCGAAACAAAAAGTTTGAAT
TGGGTTTGGAGTTTCCAATCTTCCTTATTATATTGATGGTGATGTTAAATTAACACAGTCTATGGCCATC
ATACGTTATATAGCTGACAAGCACAACATGTTGGGTGGTTGTCCAAAAGAGCGTGCAGAGATTTCAATGCT
TGAAGGAGCGGTTTTGGATATTAGATACGGTGTTCGAGAATTGCATATAGTAAAGACTTTGAAACTCTCA
AAGTTGATTTTCTTAGCAAGCTACCTGAAATGCTGAAAATGTTTGAAGATCGTTTATGTCATAAAACATAT
TTAAATGGTGATCATGTAACCCATCTGACTTCATGTTGTATGACGCTCTTGATGTTGTTTTATACATGGA
CCCAATGTGCCTGGATGCGTTCCCAAAATTAGTTTGTTTTAAAAAACGTATTGAAGCTATCCACAAATTG
ATAAGTACTTGAAATCCAGCAAGTATATAGCATGGCCTTTGCAGGGCTGGCAAGCCACGTTTGGTGGTGGC
GACCATCTCCAAAATCGGATCTGGTTCCGCGTGGATCTCGTCTGTCATCTGTTGGATCCATGGAATTCct
cgagATGGGAAATTTGTTGCTCTCATGGAAGAGATTAGATGATAACAAAGAAGAACCAGGAGCCGGAAAATG
GAGGCGGCGGTGTTGGTGCCGCTGAAGCCTCTGTTAGAGCTTCTAAACACCCGCCAGCATCTCCTCCTCCT
GCAACCAACAAGGACCAATAGGACCTGTCTTAGGGCGACCAATGGAAGATGTAAGAGCTCATATACATT
GGGTAAAGGACTAGGTCGTGGACAGTTTGGGTGACTCATCTCTGCACGCAAAAGGCCACGGGGCTGCAAT
TCGCTTGCAAGACATTGCTAAAAGGAAGCTCGTGAAACAAAGAAGACATTGAGGATGTGAGAGGGGAGGTG
CAGATTATGCATCACTTGACCGGTGAGC AAA CATTGTGGAGCTTAAAGGAGCGTATGAGGATAAGCATT
TGTGCATTTGGTTATGGAGCTTTGCGCGGGAGGTGAGTTGTTGACAGGATTATCGCAAAGGGACATTATT
CGGAGAGAGCTGCAGCCTCGTTACTACGGACGATTGTGCAGATTATCCATACTTGCCATTCCATGGGGGTT
ATCCACAGGGACTTGAAGCCTGAGAACTTTTTGTTGCTTAGCAAGGATGAGAATTCTCCTCTGAAAGCCAC
CGACTTCGGGTTATCCGTGTTCTACAAACCAGGAGAGGTGTTCAAAGACATTGTGGGAAGTGCTTATTACA
TTGCACCAGAGGTGTTGAGGAGGAAGTATGGACCAGAGGCTGATATTTGGAGCATTGGTGTGATGTTGTAT
ATCCTCCTGTGTGGTGTTCACCTTTTTGGGCTGAGTCAGAGAATGGGATTTTCAATGCATCCTAAGTGG
ACAGGTTGATTTTTCAAGCGATCCATGGCCAGTCATCTCACACAGGCAAAAGACCTCGTTAGGAAGATGC
TCAACTCTGATCCAAAACAAAGATTAACCGCTGCTCAAGTTCTCAATCATCCATGGATCAAGGAGGATGGA
GAAGCACCGGATGTTTCTCTTGACAATGCAGTGATGTCTAGGCTCAAGCAGTTCAAAGCAATGAACAATT
TAAGAAAATTGCTTTACGGGTGATAGCCGGTGCTTATCAGAGGAAGAAATCATGGGGTTAAAAGAGATGT
TCAAAGGAATGGCACTGACAACAGTGAACATAACTCTTGAGGAACTAAGACAGGGACTTGCTAAGCAA
GGTACAAGTTATCCGAATACGAAGTCCAGCAACTAATGGAAGCTGCTGATGCGGAGCGTAATGGAACAT
AGACTATGGGGCGTTTATTGAGCTACAATGCACATCAACAGGCTCGACAGAGAAGAGCATCTCTACTCAG
CCTTCCAACACTTTGACAAAGACAACAGTGGATATATCACAACGGAAAGAGCTAGAGCAAGCCCTTCGGGAG
TTTGGCATGAACGATGGCAGAGACATTAAGGAAATCATTCTGAGGTTGATGGAGACAATGATGGGCGGAT
AAACTACGAGGAATTTGTGGCGATGATGAGAAAAGGAAACCCAGATCCTAATCCTAAGAAGCGGCGTGAAC
TATCATTCAAAGGTGGCGGtctagaCCCGGAATGcatcaccatcaccatcacGGATCC**TGA**

GST-CPK34(D454A)-6His in pGEX vector; mutation in EF3, from GST to stop codon (TGA) is shown. CPK34(D454A) (**BOLD**) starts with ATG following GST and ends with a TGA downstream of a 6-His (blue lower case) coding site. XhoI and XbaI restriction sites (yellow lower case) are located between GST and CPK34(D454A), and between CPK34(D454A) and 6-His, respectively. Stop codon (**TGA**) after 6-His is highlighted as yellow.

ATGTCCCCTATACTAGGTTATTGGAAAATTAAGGGCCTTGTGCAACCCACTCGACTTCTTTTGGAAATATCT
TGAAGAAAAATATGAAGAGCATTGTATGAGCGCGATGAAGGTGATAAATGGCGAAACAAAAAGTTTGAAT
TGGGTTTGGAGTTTCCAATCTTCCTTATTATATTGATGGTGATGTTAAATTAACACAGTCTATGGCCATC
ATACGTTATATAGCTGACAAGCACAACATGTTGGGTGGTTGTCCAAAAGAGCGTGCAGAGATTTCAATGCT
TGAAGGAGCGGTTTTGGATATTAGATACGGTGTTCGAGAATTGCATATAGTAAAGACTTTGAAACTCTCA

AAGTTGATTTTCTTAGCAAGCTACCTGAAATGCTGAAAATGTTTGAAGATCGTTTATGTCATAAAACATAT
 TTAAATGGTGATCATGTAACCCATCCTGACTTCATGTTGTATGACGCTCTTGATGTTGTTTTATACATGGA
 CCAATGTGCCTGGATGCGTTCCCAAATAGTTTGTGTTTTAAAAACGTATTGAAGCTATCCACAAATTG
 ATAAGTACTTGAAATCCAGCAAGTATATAGCATGGCCTTTGCAGGGCTGGCAAGCCACGTTTGGTGGTGGC
 GACCATCCTCCAAAATCGGATCTGGTTCCGCGTGGATCTCGTCGTGCATCTGTTGGATCCATGGAATTC**ct**
cgagATGGGAAATTGTTGCTCTCATGGAAGAGATTAGATGATAACAAAGAAGAACCAGGAGCCGGAAAATG
 GAGGCGGCGGTGTTGGTGCCGCTGAAGCCTCTGTTAGAGCTTCTAAACACCCGCCAGCATCTCCTCCTCCT
 GCAACCAAACAAGGACCAATAGGACCTGTCTTAGGGCGACCAATGGAAGATGTAAGAGAGCTCATATACATT
 GGGTAAGGAGCTAGGTCGTGGACAGTTTGGGGTGACTCATCTCTGCACGCAAAAGGCCACGGGGCTGCAAT
 TCGCTTGCAAGACCATTGCTAAAAGGAAGCTCGTGAAACAAAGAAGACATTGAGGATGTGAGAAGGGAGGTG
 CAGATTATGCATCACTTGACCGGTGAGCCAAAACATTGTGGAGCTTAAAGGAGCGTATGAGGATAAGCATT
 TGTGCATTTGGTTATGGAGCTTTGCGCGGGAGGTGAGTTGTTGACAGGATTATCGCAAAGGGACATTATT
 CGGAGAGAGCTGCAGCCTCGTTACTACGGACGATTGTGCAGATTATCCATACTTGCCATTCCATGGGGGTT
 ATCCACAGGGACTTGAAGCCTGAGAACTTTTTGTTGCTTAGCAAGGATGAGAATTCTCCTCTGAAAGCCAC
 CGACTTCGGGTTATCCGTGTTCTACAAACCAGGAGAGGTGTTCAAAGACATTGTGGGAAGTGCTTATTACA
 TTGCACAGAGGTGTTGAGGAGGAAGTATGGACAGAGGCTGATATTTGGAGCATTGGTGTATGTTGTAT
 ATCCTCCTGTGTGGTGTTCACCTTTTTGGGCTGAGTCAGAGAATGGGATTTTCAATGCCATCCTAAGTGG
 ACAGGTTGATTTTTCAAGCGATCCATGGCCAGTCATCTCACCACAGGCAAAAGACCTCGTTAGGAAGATGC
 TCAACTCTGATCCAAAACAAAGATTAACCGCTGCTCAAGTTCTCAATCATCCATGGATCAAGGAGGATGGA
 GAAGACCCGGATGTTCTCTTGACAATGCAGTGTATCTAGGCTCAAGCAGTTCAAAGCAATGAACAACCTT
 TAAGAAAGTTGCTTTACGGGTGATAGCCGGTGCTTATCAGAGGAAGAAATCATGGGGTTAAAAGAGATGT
 TCAAAGGAATGGACACTGACAACAGTGAACATAACTCTTGAGGAACTAAGACAGGGACTTGCTAAGCAA
 GGTACAAGTTATCCGAATACGAAGTCCAGCAACTAATGGAAGCTGCTGATGCGGACGGTAATGGAACAAT
 AGACTATGGGGAGTTCATTGCAGCTACAATGCACATCAACAGGCTCGACAGAGAAGAGCATCTCTACTCAG
 CCTTCCAACACTTCGCGAAAGACAACAGTGGATATATCACAACGGAAGAGCTAGAGCAAGCCCTTCGGGAG
 TTTGGCATGAACGATGGCAGAGACATTAAGGAAATCATTTCTGAGGTTGATGGAGACAATGATGGGCGGAT
 AAACACAGGAAATTTGTGGCGATGATGAGAAAAGGAAACCAGATCCTAATCCTAAGAAGCGGCGTGAAC
 TATCATTCAAAGGTGGCGG**ctctaga**CCCGGGAATG**catcaccatcaccatcac**GGATCCTGA

GST-CPK34(E465A)-6His in pGEX vector; mutation in EF3, from GST to stop codon (TGA) is shown.
 CPK34(E465A) (**BOLD**) starts with ATG following GST and ends with a TGA downstream of a 6-His
 (blue lower case) coding site. XhoI and XbaI restriction sites (yellow lower case) are located between GST
 and CPK34(E465A), and between CPK34(E465A) and 6-His, respectively. Stop codon (TGA) after 6-His
 is highlighted as yellow.

ATGTCCCTATACTAGGTTATTGGAAAATTAAGGGCCTTGTGCAACCCACTCGACTTCTTTTGGAAATATCT
 TGAAGAAAAATATGAAGAGCATTGTTGATGAGCGCGATGAAGGTGATAAATGGCGAAACAAAAAGTTTGAAT
 TGGGTTTGGAGTTTCCAATCTTCTTATTATATTGATGGTGATGTTAAATTAACACAGTCTATGGCCATC
 ATACGTTATATAGCTGACAAGCACAACATGTTGGGTGGTTGTCCAAAAGAGCGTGCAGAGATTTCAATGCT
 TGAAGGAGCGGTTTTGGATATTAGATACGGTGTTCGAGAATTGCATATAGTAAAGACTTTGAAACTCTCA
 AAGTTGATTTTCTTAGCAAGCTACCTGAAATGCTGAAAATGTTTGAAGATCGTTTATGTCATAAAACATAT
 TTAAATGGTGATCATGTAACCCATCCTGACTTCATGTTGTATGACGCTCTTGATGTTGTTTTATACATGGA
 CCAATGTGCCTGGATGCGTTCCCAAATAGTTTGTGTTTTAAAAACGTATTGAAGCTATCCACAAATTG
 ATAAGTACTTGAAATCCAGCAAGTATATAGCATGGCCTTTGCAGGGCTGGCAAGCCACGTTTGGTGGTGGC
 GACCATCCTCCAAAATCGGATCTGGTTCCGCGTGGATCTCGTCGTGCATCTGTTGGATCCATGGAATTC**ct**
cgagATGGGAAATTGTTGCTCTCATGGAAGAGATTAGATGATAACAAAGAAGAACCAGGAGCCGGAAAATG
 GAGGCGGCGGTGTTGGTGCCGCTGAAGCCTCTGTTAGAGCTTCTAAACACCCGCCAGCATCTCCTCCTCCT
 GCAACCAAACAAGGACCAATAGGACCTGTCTTAGGGCGACCAATGGAAGATGTAAGAGAGCTCATATACATT
 GGGTAAGGAGCTAGGTCGTGGACAGTTTGGGGTGACTCATCTCTGCACGCAAAAGGCCACGGGGCTGCAAT
 TCGCTTGCAAGACCATTGCTAAAAGGAAGCTCGTGAAACAAAGAAGACATTGAGGATGTGAGAAGGGAGGTG
 CAGATTATGCATCACTTGACCGGTGAGCCAAAACATTGTGGAGCTTAAAGGAGCGTATGAGGATAAGCATT
 TGTGCATTTGGTTATGGAGCTTTGCGCGGGAGGTGAGTTGTTGACAGGATTATCGCAAAGGGACATTATT
 CGGAGAGAGCTGCAGCCTCGTTACTACGGACGATTGTGCAGATTATCCATACTTGCCATTCCATGGGGGTT
 ATCCACAGGGACTTGAAGCCTGAGAACTTTTTGTTGCTTAGCAAGGATGAGAATTCTCCTCTGAAAGCCAC
 CGACTTCGGGTTATCCGTGTTCTACAAACCAGGAGAGGTGTTCAAAGACATTGTGGGAAGTGCTTATTACA

TTGCACCAGAGGTGTTGAGGAGGAAGTATGGACCAGAGGCTGATATTTGGAGCATTGGTGTTCATGTTGTAT
 ATCCTCCTGTGTGGTGTCCACCTTTTTGGGCTGAGTCAGAGAATGGGATTTTCAATGCCATCCTAAGTGG
 ACAGGTTGATTTTTCAAGCGATCCATGGCCAGTCATCTCACCACAGGCAAAAGACCTCGTTAGGAAGATGC
 TCAACTCTGATCCAAAACAAAGATTAACCGCTGCTCAAGTTCTCAATCATCCATGGATCAAGGAGGATGGA
 GAAGCACCGGATGTTTCTTGGACAATGCAGTGATGTCTAGGCTCAAGCAGTTCAAAGCAATGAACAACCTT
 TAAGAAAAGTTGCTTTACGGGTGATAGCCGGGTGCTTATCAGAGGAAGAAATCATGGGGTTAAAAGAGATGT
 TCAAAGGAATGGACACTGACAACAGTGGAACCATAACTCTTGAGGAACTAAGACAGGGACTTGTCAAGCAA
 GGTACAAGGTTATCCGAATACGAAGTCCAGCAACTAATGGAAGCTGCTGATGCGGACGGTAATGGAACAAT
 AGACTATGGGGAGTTTATTGACGCTACAATGCACATCAACAGGCTCGACAGAGAAGAGCATCTCTACTCAG
 CCTTCCAACACTTTTGACAAAAGACAACAGTGGATATATCACAACGGAAGCGCTAGAGCAGGCCTTACGGGAG
 TTTGGCATGAACGATGGCAGAGACATTAAGGAAATCATTTCTGAGGTTGATGGAGACAATGATGGGCGGAT
 AAACCTACGAGGAATTTGTGGCGATGATGAGAAAAGGAAACCCAGATCCTAATCCTAAGAAGCGGCGTGAAC
 TATCATTCAAAGGTGGCGGtctagaCCCGGGAATGcatcaccatcaccatcacGGATCCTGA

GST-CPK34(D489A)-6His in pGEX vector; mutation in EF4, from GST to stop codon (TGA) is shown.
 CPK34(D489A) (**BOLD**) starts with ATG following GST and ends with a TGA downstream of a 6-His
 (blue lower case) coding site. XhoI and XbaI restriction sites (yellow lower case) are located between GST
 and CPK34(D489A), and between CPK34(D489A) and 6-His, respectively. Stop codon (TGA) after 6-His
 is highlighted as yellow.

ATGTCCCCTATACTAGGTTATTGGAAAATTAAGGGCCTTGTGCAACCCACTCGACTTCTTTTGGAAATATCT
 TGAAGAAAAATATGAAGAGCATTGTATGAGCGCGATGAAGGTGATAAATGGCGAAAACAAAAGTTTGAAT
 TGGGTTTGGAGTTTCCCAATCTTCTTATTATATTGATGGTGATGTTAAATTAACACAGTCTATGGCCATC
 ATACGTTATATAGCTGACAAGCACAACATGTTGGGTGTTGCTCCAAAAGAGCGTGCAGAGATTTCAATGCT
 TGAAGGAGCGGTTTTGGATATTAGATACGGTGTTCGAGAATTGCATATAGTAAAGACTTTGAAACTCTCA
 AAGTTGATTTTTCTTAGCAAGCTACCTGAAATGCTGAAAATGTTTGAAGATCGTTTTATGTCATAAAACATAT
 TTAAATGGTGATCATGTAACCCATCCTGACTTCATGTTGTATGACGCTCTTGATGTTGTTTTATACATGGA
 CCAATGTGCCTGGATGCGTTCCCAAAATTAGTTTGTTTTTAAAAACGTATTGAAGCTATCCACAAATTG
 ATAAGTACTTGAAATCCAGCAAGTATATAGCATGGCCTTTCAGGGCTGGCAAGCCACGTTTGGTGGTGGC
 GACCATCCTCCAAAATCGGATCTGGTTCCGCGTGGATCTCGTCTGCATCTGTTGGATCCATGGAATTCct
 cgagATGGGAAATTGTTGCTCTCATGGAAGAGATTAGATGATAACAAAGAAGAACCAGAGGCCGAAAATG
 GAGGCGGCGGTGTTGGTGCCTGAAAGCCTCTGTTAGAGCTTCTAAACACCCGCCAGCATCTCCTCCTCCT
 GCAACCAAAACAAGGACCAATAGGACCTGTCTTAGGGCGACCAATGGAAGATGTAAAGAGCTCATATACATT
 GGGTAAGGAGCTAGGTCGTGGACAGTTTGGGGTGACTCATCTCTGCACGCAAAAGGCCACGGGGCTGCAAT
 TCGTTGCAAGACCATTGCTAAAAGGAAGCTCGTGAACAAAGAAGACATTGAGGATGTGAGAAGGGAGGTG
 CAGATTATAGCATCACTTACCGGTGAGCAACATTGTTGGAGCTTAAAGGAGCGTATGAGGATAAGCATTTC
 TGTGCATTTGGTTATGGAGCTTTGCGCGGGAGGTGAGTTGTTTCGACAGGATTATCGAAAGGGACATTATT
 CGGAGAGAGCTGCAGCCTCGTTACTACGGACGATTGTGCAGATTATCCATACTTGCCATTCCATGGGGGTT
 ATCCACAGGGACTTGAAGCCTGAGAACTTTTTGTTGCTTAGCAAGGATGAGAATTCCTCTGAAAGCCAC
 CGACTTCGGGTTATCCGTGTTCTACAAACCAGGAGAGGTGTTCAAAGACATTGTGGGAAGTGCTTATTACA
 TTGCACCAGAGGTGTTGAGGAGGAAGTATGGACCAGAGGCTGATATTTGGAGCATTGGTGTTCATGTTGTAT
 ATCCTCCTGTGTGGTGTCCACCTTTTTGGGCTGAGTCAGAGAATGGGATTTTCAATGCCATCCTAAGTGG
 ACAGGTTGATTTTTCAAGCGATCCATGGCCAGTCATCTCACCACAGGCAAAAGACCTCGTTAGGAAGATGC
 TCAACTCTGATCCAAAACAAAGATTAACCGCTGCTCAAGTTCTCAATCATCCATGGATCAAGGAGGATGGA
 GAAGCACCGGATGTTTCTTGGACAATGCAGTGATGTCTAGGCTCAAGCAGTTCAAAGCAATGAACAACCTT
 TAAGAAAAGTTGCTTTACGGGTGATAGCCGGGTGCTTATCAGAGGAAGAAATCATGGGGTTAAAAGAGATGT
 TCAAAGGAATGGACACTGACAACAGTGGAACCATAACTCTTGAGGAACTAAGACAGGGACTTGTCAAGCAA
 GGTACAAGGTTATCCGAATACGAAGTCCAGCAACTAATGGAAGCTGCTGATGCGGACGGTAATGGAACAAT
 AGACTATGGGGAGTTTATTGACGCTACAATGCACATCAACAGGCTCGACAGAGAAGAGCATCTCTACTCAG
 CCTTCCAACACTTTTGACAAAAGACAACAGTGGATATATCACAACGGAAGAGCTAGAGCAAGCCTTACGGGAG
 TTTGGCATGAACGATGGCAGAGACATTAAGGAAATGATATCTGAGGTTGCTGGAGACAATGATGGGCGGAT
 AAACCTACGAGGAATTTGTGGCGATGATGAGAAAAGGAAACCCAGATCCTAATCCTAAGAAGCGGCGTGAAC
 TATCATTCAAAGGTGGCGGtctagaCCCGGGAATGcatcaccatcaccatcacGGATCCTGA

GST-CPK34(E500A)-6His in pGEX vector; mutation in EF4, from GST to stop codon (TGA) is shown. CPK34(E500A) (**BOLD**) starts with ATG following GST and ends with a TGA downstream of a 6-His (blue lower case) coding site. XhoI and XbaI restriction sites (yellow lower case) are located between GST and CPK34(E500A), and between CPK34(E500A) and 6-His, respectively. Stop codon (TGA) after 6-His is highlighted as yellow.

```

ATGTCCCCTATACTAGGTTATTGGAAAATTAAGGGCCTTGTGCAACCCACTCGACTTCTTTTGGAAATATCT
TGAAGAAAAATATGAAGAGCATTGTATGAGCGCGATGAAGGTGATAAATGGCGAAAACAAAAAGTTTGAAT
TGGGTTTGGAGTTTCCCAATCTTCCTTATTATATTGATGGTGTATGTTAAATTAACACAGTCTATGGCCATC
ATACGTTATATAGCTGACAAGCACAACATGTTGGGTGGTTGTCCAAAAGAGCGTGCAGAGATTTCAATGCT
TGAAGGAGCGGTTTTGGATATTAGATACGGTGTTCGAGAATTGCATATAGTAAAGACTTTGAAACTCTCA
AAGTTGATTTTCTTAGCAAGCTACCTGAAATGCTGAAAATGTTTGAAGATCGTTTATGTCATAAAACATAT
TTAAATGGTGATCATGTAACCCATCCTGACTTCATGTTGTATGACGCTCTTGATGTTGTTTTATACATGGA
CCCAATGTGCCTGGATGCGTTCCCAAAATTAGTTTGTGTTTTAAAAAACGTATTGAAGCTATCCACAAATTG
ATAAGTACTTGAAATCCAGCAAGTATATAGCATGGCCTTTCAGGGCTGGCAAGCCACGTTTGGTGGTGGC
GACCATCCTCCAAAATCGGATCTGGTTCGCGTGGATCTCGTTCGTGCATCTGTTGGATCCATGGAATTCct
cgagATGGGAAATTGTTGCTCTCATGGAAGAGATTGAGATGATAACAAAGAAGAACCAGGGCCGGAAAATG
GAGGCGGCGGTGTTGGTGCCTGAAAGCCTCTGTTAGAGCTTCTAAACACCCGCCAGCATCTCCTCCTCCT
GCAACCAACAAGGACCAATAGGACCTGTCTTAGGGCGACCAATGGAAGATGTAAGAGCTCATATACATT
GGGTAAGGAGCTAGGTCGTGGACAGTTTGGGGTGACTCATCTCTGCACGCAAAAGGCCACGGGGCTGCAAT
TCGCTTGCAAGACCATTGCTAAAAGGAAGCTCGTGAACAAAGAAGACATTGAGGATGTGAGAAGGGAGGTG
CAGATTATGCATCACTTGACCGGTGAGCCAAACATTGTGGAGCTTAAAGGAGCGTATGAGGATAAGCATTG
TGTGCATTTGGTTATGGAGCTTTGCGCGGGAGGTGAGTTGTTTCGACAGGATTATCGCAAAGGGACATTATT
CGGAGAGAGCTGCAGCCTCGTTACTACGGACGATTGTGCGAGATTATCCATACTTGCCATTCCATGGGGGTT
ATCCACAGGGACTTGAAGCCTGAGAACTTTTTGTTGCTTAGCAAGGATGAGAATTCCTCTGAAAGCCAC
CGACTTCGGGTTATCCGTGTTCTACAAACCAGGAGAGGTGTTCAAAGACATTGTGGGAAGTGCTTATTACA
TTGCACCAGAGGTGTTGAGGAGGAAGTATGGACCAGAGGCTGATATTTGGAGCATTGGTGTGATGTTGTAT
ATCCTCCTGTGTGGTGTTCACCTTTTTGGGCTGAGTCAGAGAATGGGATTTTCAATGCCATCCTAAGTGG
ACAGGTTGATTTTTCAAGCGATCCATGGCCAGTCATCTCACCACAGGCAAAAGACCTCGTTAGGAAGATGC
TCAACTCTGATCCAAAACAAAGATTAACCGCTGCTCAAGTTCTCAATCATCCATGGATCAAGGAGGATGGA
GAAGCACCGGATGTTCTCTTGACAATGCAGTGATGTCTAGGCTCAAGCAGTTCAAAGCAATGAACAACCTT
TAAGAAAGTTGCTTTACGGGTGATAGCCGGGTGCTTATCAGAGGAAGAAATCATGGGGTTAAAAGAGATGT
TCAAAGGAATGGACACTGACAACAGTGAACCATAACTCTTGAGGAACAAAGACAGGGACTTGCTAAGCAA
GGTACAAGGTTATCCGAATACGAAGTCCAGCAACTAATGGAAGCTGCTGATGCGGACGGTAATGGAACAAT
AGACTTGGGGAGTTTATTGCAGCTACAATGCACATCAACAGGCTCGACAGAGAAGAGCATCTCTACTCAG
CCTTCCAAACACTTTGACAAAGACAACAGTGGATATACAAACGGAAGAGCTAGAGCAAGCCCTTCGGGAG
TTTTGCATGAACGATGGCAGAGACATTAAGGAAATCATTTCTGAGGTTGATGGAGACAATGATGGGCGGAT
AAACTACGAGGCATTTGTGGCGATGATGAGAAAAGGAAACCCAGATCCTAATCCTAAGAAGCGGCGTGAAC
TATCATTCAAAGGTGGCGGtctagaCCCGGGAATGcatcaccatcaccatcacGGATCCTGA

```

GST-CPK34(D420A)-6His in pGEX vector; mutation in EF2, from GST to stop codon (TGA) is shown. CPK34(D420A) (**BOLD**) starts with ATG following GST and ends with a TGA downstream of a 6-His (blue lower case) coding site. XhoI and XbaI restriction sites (yellow lower case) are located between GST and CPK34(D420A), and between CPK34(D420A) and 6-His, respectively. Stop codon (TGA) after 6-His is highlighted as yellow.

```

ATGTCCCCTATACTAGGTTATTGGAAAATTAAGGGCCTTGTGCAACCCACTCGACTTCTTTTGGAAATATCT
TGAAGAAAAATATGAAGAGCATTGTATGAGCGCGATGAAGGTGATAAATGGCGAAAACAAAAAGTTTGAAT
TGGGTTTGGAGTTTCCCAATCTTCCTTATTATATTGATGGTGTATGTTAAATTAACACAGTCTATGGCCATC
ATACGTTATATAGCTGACAAGCACAACATGTTGGGTGGTTGTCCAAAAGAGCGTGCAGAGATTTCAATGCT
TGAAGGAGCGGTTTTGGATATTAGATACGGTGTTCGAGAATTGCATATAGTAAAGACTTTGAAACTCTCA
AAGTTGATTTTCTTAGCAAGCTACCTGAAATGCTGAAAATGTTTGAAGATCGTTTATGTCATAAAACATAT
TTAAATGGTGATCATGTAACCCATCCTGACTTCATGTTGTATGACGCTCTTGATGTTGTTTTATACATGGA
CCCAATGTGCCTGGATGCGTTCCCAAAATTAGTTTGTGTTTTAAAAAACGTATTGAAGCTATCCACAAATTG
ATAAGTACTTGAAATCCAGCAAGTATATAGCATGGCCTTTCAGGGCTGGCAAGCCACGTTTGGTGGTGGC

```

GACCATCCTCCAAAATCGGATCTGGTTCCGCGTGGATCTCGTCGTGCATCTGTTGGATCCATGGAATTCct
cgagATGGGAAATTGTTGCTCTCATGGAAGAGATT**CAGATGATAACAAAGAAGAACCGAGGCCGGAAAATG**
GAGGCGGCGGTGTTGGTGCCGCTGAAGCCTCTGTTAGAGCTTCTAAACACCCGCCAGCATCTCCTCCTCCT
GCAACCAAAACAAGGACCAATAGGACCTGTCTTAGGGCGACCAATGGAAGATGTAAAGAGCTCATATACATT
GGGTAAGGAGCTAGGTCGTGGACAGTTTTGGGGTGACTCATCTCTGCACGCAAAAGGCCACGGGGCTGCAAT
TCGCTTGCAAGACCATTGCTAAAAGGAAGCTCGTGAACAAAGAAGACATTGAGGATGTGAGAAGGGAGGTG
CAGATTATGCATCACTTGACCGGTAGCCAAACATTGTGGAGCTTAAAGGAGCGTATGAGGATAAGCATTCC
TGTGCATTTGGTTATGGAGCTTTGCGCGGGAGGTGAGTTGTTTCGACAGGATTATCGCAAAGGGACATTATT
CGGAGAGAGCTGCAGCCTCGTTACTACGGACGATTGTGCAGATTATCCATACTTGCCATTCCATGGGGGTT
ATCCACAGGGACTTGAAGCCTGAGAACTTTTTGTTGCTTAGCAAGGATGAGAATTCCTCTGAAAGCCAC
CGACTTCGGGTTATCCGTGTTCTACAAACCAGGAGAGGTGTTCAAAGACATTGTGGGAAGTGCTTATTACA
TTGCACCAGAGGTGTTGAGGAGGAAGTATGGACCAGAGGCTGATATTTGGAGCATTGGTGTGATGTTGTAT
ATCCTCCTGTGTGGTGTCCACCTTTTTGGGCTGAGTCAGAGAATGGGATTTTCAATGCCATCCTAAGTGG
ACAGGTTGATTTTTCAAGCGATCCATGGCCAGTCATCTCACCACAGGCAAAAGACCTCGTTAGGAAGATGC
TCAACTCTGATCCAAAACAAGATTAACCGCTGCTCAAGTTCTCAATCATCCATGGATCAAGGAGGATGGA
GAAGCACCGGATGTTCTCTTGACAATGCAGTGATGTCTAGGCTCAAGCAGTTCAAAGCAATGAACAACCTT
TAAGAAAGTTGCTTTACGGGTGATAGCCGGGTGCTTATCAGAGGAAGAAATCATGGGGTTAAAAGAGATGT
TCAAAGGAATGGACACTGACAACAGTGGAACCATAACTCTTGAGGAACTAAGACAGGGACTTGCTAAGCAA
GGTACAAGGTTATCCGAATACGAAGTCCAGCAACTAATGGAAGCCGCGGATGCGGCCGGTAATGGAACAAT
AGACTATGGGAGTTTATTGACAGCTACAATGCACATCAACAGGCTCGACAGAGAAGAGCATCTCTACTCAG
CCTTCCAACACTTTGACAAAGACAACAGTGGATATATCACAACGGAAGAGCTAGAGCAATCCCTTTGGGAG
TTTGGCATGAACGATGGCAGAGACATTAAGGAAATCATTCTGAGGTTGATGGAGACAATGATGGGCGGAT
AAACTACGAGGAATTTGTGGCGATGATGAGAAAAGGAAACCCAGATCCTAATCCTAAGAAGCGGCGTGAAC
TATCATTCAAAGGTGGCGGtctagaCCCGGGAATG**catcaccatcaccatcac**GGATCC**TGA**

GST-CPK34(N422A)-6His in pGEX vector; mutation in EF2, from GST to stop codon (TGA) is shown. CPK34(N422A) (**BOLD**) starts with ATG following GST and ends with a TGA downstream of a 6-His (**blue lower case**) coding site. XhoI and XbaI restriction sites (**yellow lower case**) are located between GST and CPK34(N422A), and between CPK34(N422A) and 6-His, respectively. Stop codon (**TGA**) after 6-His is highlighted as yellow.

ATGTCCCCTATACTAGGTTATTGGAAAATTAAGGGCCTTGTGCAACCCACTCGACTTCTTTTTGGAATATCT
 TGAAGAAAAATATGAAGAGCATTGTTGATGAGCGCGATGAAGGTGATAAATGGCGAAAACAAAAGTTTGAAT
 TGGGTTTGGAGTTTCCCAATCTTCCTTATTATATTGATGGTGTGATGTTAAATTAACACAGTCTATGGCCATC
 ATACGTTATATAGCTGACAAGCACAACATGTTGGGTGGTTGTCCAAAAGAGCGTGCAGAGATTTCAATGCT
 TGAAGGAGCGGTTTTGGATATTAGATACGGTGTTCGAGAATTGCATATAGTAAAGACTTTGAAACTCTCA
 AAGTTGATTTTTCTTAGCAAGCTACCTGAAATGCTGAAAATGTTTCGAAGATCGTTTATGTCATAAAACATAT
 TTAAATGGTGATCATGTAACCCATCCTGACTTCATGTTGTATGACGCTCTTGATGTTGTTTTATACATGGA
 CCAATGTGCCTGGATGCGTTCCCAAAATTAGTTTGTTTTTAAAAACGTATTGAAGCTATCCACAAATTG
 ATAAGTACTTGAAATCCAGCAAGTATATAGCATGGCCTTTGCAGGGCTGGCAAGCCACGTTTGGTGGTGGC
GACCATCCTCCAAAATCGGATCTGGTTCCGCGTGGATCTCGTCGTGCATCTGTTGGATCCATGGAATTCct
cgagATGGGAAATTGTTGCTCTCATGGAAGAGATT**CAGATGATAACAAAGAAGAACCGAGGCCGGAAAATG**
GAGGCGGCGGTGTTGGTGCCGCTGAAGCCTCTGTTAGAGCTTCTAAACACCCGCCAGCATCTCCTCCTCCT
GCAACCAAAACAAGGACCAATAGGACCTGTCTTAGGGCGACCAATGGAAGATGTAAAGAGCTCATATACATT
GGGTAAGGAGCTAGGTCGTGGACAGTTTTGGGGTGACTCATCTCTGCACGCAAAAGGCCACGGGGCTGCAAT
TCGCTTGCAAGACCATTGCTAAAAGGAAGCTCGTGAACAAAGAAGACATTGAGGATGTGAGAAGGGAGGTG
CAGATTATGCATCACTTGACCGGTAGCCAAACATTGTGGAGCTTAAAGGAGCGTATGAGGATAAGCATTCC
TGTGCATTTGGTTATGGAGCTTTGCGCGGGAGGTGAGTTGTTTCGACAGGATTATCGCAAAGGGACATTATT
CGGAGAGAGCTGCAGCCTCGTTACTACGGACGATTGTGCAGATTATCCATACTTGCCATTCCATGGGGGTT
ATCCACAGGGACTTGAAGCCTGAGAACTTTTTGTTGCTTAGCAAGGATGAGAATTCCTCTGAAAGCCAC
CGACTTCGGGTTATCCGTGTTCTACAAACCAGGAGAGGTGTTCAAAGACATTGTGGGAAGTGCTTATTACA
TTGCACCAGAGGTGTTGAGGAGGAAGTATGGACCAGAGGCTGATATTTGGAGCATTGGTGTGATGTTGTAT
ATCCTCCTGTGTGGTGTCCACCTTTTTGGGCTGAGTCAGAGAATGGGATTTTCAATGCCATCCTAAGTGG
ACAGGTTGATTTTTCAAGCGATCCATGGCCAGTCATCTCACCACAGGCAAAAGACCTCGTTAGGAAGATGC
TCAACTCTGATCCAAAACAAGATTAACCGCTGCTCAAGTTCTCAATCATCCATGGATCAAGGAGGATGGA

GAAGCACCGGATGTTCTCTTGACAATGCAGTGATGTCTAGGCTCAAGCAGTTCAAAGCAATGAACAACTT
 TAAGAAAGTTGCTTTACGGGTGATAGCCGGGTGCTTATCAGAGGAAGAAATCATGGGGTTAAAAGAGATGT
 TCAAAGGAATGGACACTGACAACAGTGGAACCATAACTCTTGAGGAACTAAGACAGGGACTTGCTAAGCAA
 GGTACAAGGTTATCCGAATACGAAGTCCAGCAACTAATGGAAGCCGCGGATGCGGACGGTGCTGGAACAAT
 AGACTATGGGGAGTTCATTGCAGCTACAATGCACATCAACAGGCTCGACAGAGAAGAGCATCTCTACTCAG
 CCTTCCAACACTTTGACAAAGACAACAGTGGATATATCACAACGGAAGAGCTAGAGCAAGCCCTTCGGGAG
 TTTGGCATGAACGATGGCAGAGACATTAAGGAAATCATTTCTGAGGTTGATGGAGACAATGATGGGCGGAT
 AAACATACGAGGAATTTGTGGCGATGATGAGAAAAGGAAACCAGATCCTAATCCTAAGAAGCGGCGTGAAC
 TATCATTCAAAGGTGGCGGtctagaCCCGGGAATGcatcaccatcaccatcacGGATCCTGA

GST-CPK34(D426A)-6His in pGEX vector; mutation in EF2, from GST to stop codon (TGA) is shown. CPK34(D426A) (**BOLD**) starts with ATG following GST and ends with a TGA downstream of a 6-His (blue lower case) coding site. XhoI and XbaI restriction sites (yellow lower case) are located between GST and CPK34(D426A), and between CPK34(D426A) and 6-His, respectively. Stop codon (TGA) after 6-His is highlighted as yellow.

ATGTCCCCTATACTAGGTTATTGGAAAATTAAGGGCCTTGTGCAACCCACTCGACTTCTTTTGGAAATATCT
 TGAAGAAAAATATGAAGAGCATTGTATGAGCGCGATGAAGGTGATAAATGGCGAAACAAAAAGTTTGAAT
 TGGGTTTGGAGTTTCCAATCTTCTTATTATATTGATGGTGATGTTAAATTAACACAGTCTATGGCCATC
 ATACGTTATATAGCTGACAAGCACAACATGTTGGGTGGTTGTCCAAAAGAGCGTGCAGAGATTTCAATGCT
 TGAAGGAGCGGTTTTGGATATTAGATACGGTGTTCGAGAATTGCATATAGTAAAGACTTTGAAACTCTCA
 AAGTTGATTTTCTTAGCAAGCTACCTGAAATGCTGAAAAATGTTTGAAGATCGTTTATGTCATAAAACATAT
 TTAATGGTGATCATGTAACCCATCTGACTTCATGTTGTATGACGCTCTTGATGTTGTTTTATACATGGA
 CCAATGTGCCTGGATGCGTTCCCAAATTAAGTTTGTGTTTTAAAAACGTATTGAAGCTATCCACAAATG
 ATAAGTACTTGAATCCAGCAAGTATATAGCATGGCCTTTGCAGGGCTGGCAAGCCACGTTTGGTGGTGGC
 GACCATCTCCAAAATCGGATCTGGTTCCGCGTGGATCTCGTTCGTGCATCTGTTGGATCCATGGAATTCt
 cgagATGGGAAATTTGTTGCTCTCATGGAAGAGATTAGATGATAACAAAGAAGAACCAGAGGCCGAAAATG
 GAGGCGGCGGTGTTGGTGCCGCTGAAGCCTCTGTTAGAGCTTCTAAACACCCGCCAGCATCTCCTCCTCCT
 GCAACCAAACAAGGACCAATAGGACCTGTCTTAGGGCGACCAATGGAAGATGTAAGAGCTCATATACATT
 GGGTAAGGAGCTAGGTCGTGGACAGTTTGGGGTGACTCATCTCTGCACGCAAAGGCCACGGGGCTGCAAT
 TCGCTTGCAAGACCATTGCTAAAAGGAAGCTCGTGAACAAAGAAGACATTGAGGATGTGAGAAGGGAGGTG
 CAGATTATGCATCACTTGACCGGTGAGCCAAACATTGTGGAGCTTAAAGGAGCGTATGAGGATAAGCATT
 TGTGCATTTGGTTATGGAGCTTTGCGCGGGAGGTGAGTTGTTTCGACAGGATTATCGCAAAGGGACATTATT
 CGGAGAGAGCTGCAGCCTCGTTACTACGGACGATTGTGCAGATTATCCATACTTGCCATTCCATGGGGGTT
 ATCCACAGGGACTTGAAGCCTGAGAACTTTTTGTTGCTTAGCAAGGATGAGAATCTCCTCTGAAAGCCAC
 CGATCTGGGTTATCCGTGTTCTACAACACGAGGAGGTTGTTCAAAGACATTGTGGGAATGCTTTATTACA
 TTGCACCAGAGGTGTTGAGGAGGAAGTATGGACAGAGGCTGATATTTGGAGCATTGGTGTCTTTGTAT
 ATCCTCCTGTGTGGTGTTCACCTTTTTGGGCTGAGTCAGAGAATGGGATTTTTCAATGCCATCCTAAGTGG
 ACAGGTTGATTTTTCAAGCGATCCATGGCCAGTCATCTCACCACAGGCAAAAAGACCTCGTTAGGAAGATGC
 TCAACTCTGATCCAAAACAAAGATTAACCGCTGCTCAAGTTCTCAATCATCCATGGATCAAGGAGGATGGA
 GAAGCACCGGATGTTCTCTTGACAATGCAGTGATGTCTAGGCTCAAGCAGTTCAAAGCAATGAACAACTT
 TAAGAAAGTTGCTTTACGGGTGATAGCCGGGTGCTTATCAGAGGAAGAAATCATGGGGTTAAAAGAGATGT
 TCAAAGGAATGGACACTGACAACAGTGGAACCATAACTCTTGAGGAACTAAGACAGGGACTTGCTAAGCAA
 GGTACAAGGTTATCCGAATACGAAGTCCAGCAACTAATGGAAGCCGCGGATGCGGACGGTAATGGAACAAT
 AGCCTATGGGGAGTTCATTGCAGCTACAATGCACATCAACAGGCTCGACAGAGAAGAGCATCTCTACTCAG
 CCTTCCAACACTTTGACAAAGACAACAGTGGATATATCACAACGGAAGAGCTAGAGCAAGCCCTTCGGGAG
 TTTGGCATGAACGATGGCAGAGACATTAAGGAAATCATTTCTGAGGTTGATGGAGACAATGATGGGCGGAT
 AAACATACGAGGAATTTGTGGCGATGATGAGAAAAGGAAACCAGATCCTAATCCTAAGAAGCGGCGTGAAC
 TATCATTCAAAGGTGGCGGtctagaCCCGGGAATGcatcaccatcaccatcacGGATCCTGA

GST-CPK34(N422D)-6His in pGEX vector; mutation in EF2, from GST to stop codon (TGA) is shown. CPK34(N422D) (**BOLD**) starts with ATG following GST and ends with a TGA downstream of a 6-His (blue lower case) coding site. XhoI and XbaI restriction sites (yellow lower case) are located between GST

and CPK34(N422D), and between CPK34(N422D) and 6-His, respectively. Stop codon (**TGA**) after 6-His is highlighted as yellow.

```

ATGTCCCCTATACTAGGTTATTGGAAAATTAAGGGCCTTGTGCAACCCACTCGACTTCTTTTGGAAATATCT
TGAAGAAAAATATGAAGAGCATTGTATGAGCGCGATGAAGGTGATAAATGGCGAAACAAAAAGTTTGAAT
TGGGTTTGGAGTTTCCCAATCTTCCTTATTATATTGATGGTGATGTTAAATTAACACAGTCTATGGCCATC
ATACGTTATATAGCTGACAAGCACAACATGTTGGGTGGTGTCCAAAAGAGCGTGCAGAGATTTCAATGCT
TGAAGGAGCGGTTTTGGATATTAGATACGGTGTTCGAGAATTGCATATAGTAAAGACTTTGAACTCTCA
AAGTTGATTTTCTTAGCAAGCTACCTGAAATGCTGAAAATGTTTGAAGATCGTTTATGTCATAAAACATAT
TTAAATGGTGATCATGTAACCCATCCTGACTTCTATGTTGTATGACGCTCTTGATGTTGTTTTATACATGGA
CCCAATGTGCCTGGATGCGTTCCCAAAATTAGTTTGTTCGAGAAACGTAATTGAAGCTATCCACAAATTG
ATAAGTACTTGAATCCAGCAAGTATATAGCATGGCCTTTGCAGGGCTGGCAAGCCACGTTTGGTGGTGGC
GACCATCTCCAAAATCGGATCTGGTTCCGCGTGGATCTCGTCTGCATCTGTTGGATCCATGGAATTCct
cgagATGGGAAATTGTTGCTCTCATGGAAGAGATTGAGATGATAACAAAGAAGAACCAGGCGCGGAAAATG
GAGGCGGCGGTGTTGGTGCCGCTGAAGCCTCTGTTAGAGCTTCTAAACACCCGCCAGCATCTCCTCCTCCT
GCAACCAACAAGGACCAATAGGACCTGTCTTAGGGCGACCAATGGAAGATGTAAAGAGCTCATATACATT
GGGTAAGGAGCTAGGTCGTGGACAGTTTTGGGGTACTCATCTCTGCACGAAAAGGCCACGGGGCTGCAAT
TCGCTTGCAAGACCATTGCTAAAAGGAAGCTCGTGAACAAAGAAGACATTGAGGATGTGAGAAGGGAGGTG
CAGATTATGCATCACTTGACCGGTGAGCCAAAACATTGTGGAGCTTAAAGGAGCGTATGAGGATAAGCATTTC
TGTGCATTTGGTTATGGAGCTTTGCGCGGGAGGTGAGTTGTTGACAGGATTATCGCAAAGGGACATTATT
CGGAGAGAGCTGCAGCCTCGTTACTACGGACGATTGTGCAGATTATCCATACTTGCCATTCCATGGGGTT
ATCCACAGGGACTTGAAGCCTGAGAACTTTTTGTTGCTTAGCAAGGATGAGAATTTCTCCTCTGAAAGCCAC
CGACTTCGGGTTATCCGTGTTCTACAACACAGGAGAGGTGTTCAAAGACATTGTTGGGAAGTCTTATTACA
TTGCACCAGAGGTGTTGAGGAGGAAGTATGGACCAGAGGCTGATATTTGGAGCATTGGTGTGATGTTGTAT
ATCCTCCTGTGTGGTGTTCACCTTTTTGGGCTGAGTCAGAGAATGGGATTTTTCAATGCCATCCTAAGTGG
ACAGGTTGATTTTTCAAGCGATCCATGGCCAGTCATCTCACCACAGGCAAAAAGACCTCGTTAGGAAGATGC
TCAACTCTGATCCAAAACAAAGATTAACCGCTGCTCAAGTTCTCAATCATCCATGGATCAAGGAGGATGGA
GAAGCACCGGATGTTCTCTTGACAATGCAGTGATGTCTAGGCTCAAGCAGTTCAAAGCAATGAACAACCTT
TAAGAAAGTTGCTTTACGGGTGATAGCCGGGTGCTTATCAGAGGAAGAAATCATGGGGTTAAAGAGATGT
TCAAAGGAATGGACACTGACAACAGTGGAACATAACTCTTGAGGAACTAAGACAGGGACTTGCTAAGCAA
GGTACAAGGTTATCCGAATACGAAGTCCAGCAACTAATGGAAGCCGCGGATGCGGACGGTGATGGTACCAT
AGACTATGGGGAGTTCATTGCAGCTACAATGCACATCAACAGGCTCGACAGAGAAGAGCATCTCTACTCAG
CCTTCCAACACTTTGACAAAGACAACAGTGGATATATACAACGGAAGAGCTAGAGCAAGCCCTTCGGGAG
TTTGGCATGAACGATGGCAGAGACATTAAGGAAATCATTTCTGAGGTTGATGGAGCAAGATGTTGGCGGAT
AAACTACGAGGAATTTGTGGCGATGATGAGAAAAGGAAACCCAGATCCTAATCCTAAGAAGCGGCGTGAAC
TATCATTCAAAGGTGGCGGtctagaCCCGGGAATGcatcaccatcaccatcacGGATCCTGA

```

GST-CPK34(E429D)-6His in pGEX vector; mutation in EF2, from GST to stop codon (TGA) is shown. CPK34(E429D) (**BOLD**) starts with ATG following GST and ends with a TGA downstream of a 6-His (**blue lower case**) coding site. XhoI and XbaI restriction sites (**yellow and lower case**) are located between GST and CPK34(E429D), and between CPK34(E429D) and 6-His, respectively. Stop codon (**TGA**) after 6-His is highlighted as yellow.

```

ATGTCCCCTATACTAGGTTATTGGAAAATTAAGGGCCTTGTGCAACCCACTCGACTTCTTTTGGAAATATCT
TGAAGAAAAATATGAAGAGCATTGTATGAGCGCGATGAAGGTGATAAATGGCGAAACAAAAAGTTTGAAT
TGGGTTTGGAGTTTCCCAATCTTCCTTATTATATTGATGGTGATGTTAAATTAACACAGTCTATGGCCATC
ATACGTTATATAGCTGACAAGCACAACATGTTGGGTGGTGTCCAAAAGAGCGTGCAGAGATTTCAATGCT
TGAAGGAGCGGTTTTGGATATTAGATACGGTGTTCGAGAATTGCATATAGTAAAGACTTTGAACTCTCA
AAGTTGATTTTCTTAGCAAGCTACCTGAAATGCTGAAAATGTTTGAAGATCGTTTATGTCATAAAACATAT
TTAAATGGTGATCATGTAACCCATCCTGACTTCTATGTTGTATGACGCTCTTGATGTTGTTTTATACATGGA
CCCAATGTGCCTGGATGCGTTCCCAAAATTAGTTTGTTCGAGAAACGTAATTGAAGCTATCCACAAATTG
ATAAGTACTTGAATCCAGCAAGTATATAGCATGGCCTTTGCAGGGCTGGCAAGCCACGTTTGGTGGTGGC
GACCATCTCCAAAATCGGATCTGGTTCCGCGTGGATCTCGTCTGCATCTGTTGGATCCATGGAATTCct
cgagATGGGAAATTGTTGCTCTCATGGAAGAGATTGAGATGATAACAAAGAAGAACCAGGCGCGGAAAATG
GAGGCGGCGGTGTTGGTGCCGCTGAAGCCTCTGTTAGAGCTTCTAAACACCCGCCAGCATCTCCTCCTCCT

```

GCAACCAAACAAGGACCAATAGGACCTGTCTTAGGGCGACCAATGGAAGATGTAAAGAGCTCATATACATT
 GGGTAAGGAGCTAGGTCGTGGACAGTTTGGGGTGACTCATCTCTGCACGCAAAGGCCACGGGGCTGCAAT
 TCGCTTGCAAGACCATTGCTAAAAGGAAGCTCGTGAAACAAAGAAGACATTGAGGATGTGAGAAGGGAGGTG
 CAGATTATGCATCACTTGACCGGTGAGCCAAACATTGTGGAGCTTAAAGGAGCGTATGAGGATAAGCATT
 TGTGCATTTGGTTATGGAGCTTTGCGCGGGAGGTGAGTTGTTTCGACAGGATTATCGCAAAGGGACATTATT
 CGGAGAGAGCTGCAGCCTCGTTACTACGGACGATTGTGCAGATTATCCATACTTGCCATTCCATGGGGGTT
 ATCCACAGGGACTTGAAGCCTGAGAACTTTTTGTTGCTTAGCAAGGATGAGAATTCTCCTCTGAAAGCCAC
 CGACTTCGGGTTATCCGTGTTCTACAAACCAGGAGAGGTGTTCAAAGACATTGTGGGAAGTGCTTATTACA
 TTGCACCAGAGGTGTTGAGGAGGAAGTATGGACCAGAGGCTGATATTTGGAGCATTGGTGTATGTTGTAT
 ATCCTCCTGTGTGGTGTTCACCTTTTTGGGCTGAGTCAGAGAATGGGATTTTCAATGCCATCCTAAGTGG
 ACAGGTTGATTTTTCAAGCGATCCATGGCCAGTCATCTCACCACAGGCAAAGACCTCGTTAGGAAGATGC
 TCAACTCTGATCCAAAACAAAGATTAACCGCTGCTCAAGTTCTCAATCATCCATGGATCAAGGAGGATGGA
 GAAGCACCGGATGTTTCTTGGACAATGCAGTGATGTCTAGGCTCAAGCAGTTCAAAGCAATGAACAACCTT
 TAAGAAAGTTGCTTTACGGGTGATAGCCGGGTGCTTATCAGAGGAAGAAATCATGGGGTTAAAAGAGATGT
 TCAAAGGAATGGACACTGACAACAGTGGAACCATAACTCTTGAGGAACTAAGACAGGGACTTGCTAAGCAA
 GGTACAAGGTTATCCGAATACGAAGTCCAGCAACTAATGGAAGCTGCTGATGCGGACGGTAATGGTACCAT
 AGACTATGGGGACTTTCATTGCAGCTACAATGCACATCAATCGATTAGACAGAGAAGAGCATCTCTACTCAG
 CCTTCCAACACTTTGACAAAGACAACAGTGGATATATCACAACGGAAGAGCTAGAGCAAGCCCTTCGGGAG
 TTTGGCATGAACGATGGCAGAGACATTAAGGAAATCATTCTGAGGTTGATGGAGACAATGATGGGGCGGAT
 AAACACGAGGAATTTGTGGCGATGATGAGAAAAGGAAACCAGATCCTAATCCTAAGAAGCGGCGTGAAC
 TATCATTCAAAGGTGGCGGtctagaCCCGGGAATGcatcaccatcaccatcacGGATCCTGA

GST-CPK34(N422D, E429D)-6His in pGEX vector; mutation in EF2, from GST to stop codon (TGA) is shown.

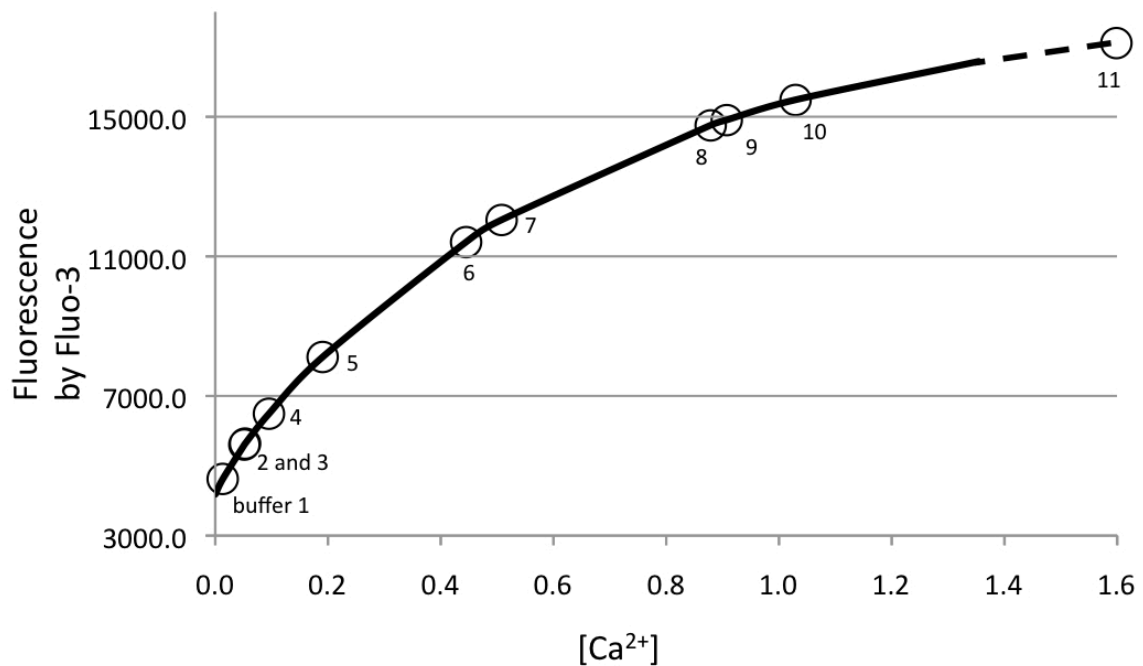
CPK34(N422D, E429D) (**BOLD**) starts with ATG following GST and ends with a TGA downstream of a 6-His (blue lower case) coding site. XhoI and XbaI restriction sites (yellow lower case) are located between GST and CPK34(N422D, E429D), and between CPK34(N422D, E429D) and 6-His, respectively. Stop codon (TGA) after 6-His is highlighted as yellow.

ATGTCCCCTATACTAGGTTATTGGAAAATTAAGGGCCTTGTGCAACCCACTCGACTTCTTTTGGAAATATCT
 TGAAGAAAAATATGAAGAGCATTGTATGAGCGCGATGAAGGTGATAAATGGCGAAACAAAAGTTTGAAT
 TGGGTTTGGAGTTTCCAATCTTCTTATTATATTGATGGTGATGTTAAATTAACACAGTCTATGGCCATC
 ATACGTTATATAGCTGACAAGCACAACATGTTGGGTGGTGTCCAAAAGAGCGTGCAGAGATTTCAATGCT
 TGAAGGAGCGGTTTTGGATATTAGATACGGTGTTCGAGAATTGCATATAGTAAAGACTTTGAAACTCTCA
 AAGTTGATTTCTTAGCAAGCTACCTGAAATGCTGAAAATGTTTCAAGATCGTTTATGTCATAAAACATAT
 TAAAATGGTGATCATGTAACCCATCTGACTTCATGTTGATGACGCTCTTGATGTTGTTTTATACATGGA
 CCCAATGTGCCTGGATGCGTTCCTCAAAATAGTTTGTGTTTTAAAAACGTATTGAAGCTATCCCAAAATG
 ATAAGTACTTGAATCCAGCAAGTATATAGCATGGCCTTTGCAGGGCTGGCAAGCCACGTTTGGTGGTGGC
 GACCATCTCCAAAATCGGATCTGGTTCGCGTGGATCTCGTCTGTCATCTGTTGGATCCATGGAATTCct
 cgagATGGGAAATTTGTTGCTCTCATGGAAGAGATTGAGATGATAACAAAGAAGAACCAGAGGCCGAAAATG
 GAGGCGGCGGTGTTGGTGCCGCTGAAGCCTCTGTTAGAGCTTCTAAACACCCGCCAGCATCTCCTCCTCCT
 GCAACCAAACAAGGACCAATAGGACCTGTCTTAGGGCGACCAATGGAAGATGTAAAGAGCTCATATACATT
 GGGTAAGGAGCTAGGTCGTGGACAGTTTGGGGTGACTCATCTCTGCACGCAAAGGCCACGGGGCTGCAAT
 TCGCTTGCAAGACCATTGCTAAAAGGAAGCTCGTGAAACAAAGAAGACATTGAGGATGTGAGAAGGGAGGTG
 CAGATTATGCATCACTTGACCGGTGAGCCAAACATTGTGGAGCTTAAAGGAGCGTATGAGGATAAGCATT
 TGTGCATTTGGTTATGGAGCTTTGCGCGGGAGGTGAGTTGTTTCGACAGGATTATCGCAAAGGGACATTATT
 CGGAGAGAGCTGCAGCCTCGTTACTACGGACGATTGTGCAGATTATCCATACTTGCCATTCCATGGGGGTT
 ATCCACAGGGACTTGAAGCCTGAGAACTTTTTGTTGCTTAGCAAGGATGAGAATTCTCCTCTGAAAGCCAC
 CGACTTCGGGTTATCCGTGTTCTACAAACCAGGAGAGGTGTTCAAAGACATTGTGGGAAGTGCTTATTACA
 TTGCACCAGAGGTGTTGAGGAGGAAGTATGGACCAGAGGCTGATATTTGGAGCATTGGTGTATGTTGTAT
 ATCCTCCTGTGTGGTGTTCACCTTTTTGGGCTGAGTCAGAGAATGGGATTTTCAATGCCATCCTAAGTGG
 ACAGGTTGATTTTTCAAGCGATCCATGGCCAGTCATCTCACCACAGGCAAAGACCTCGTTAGGAAGATGC
 TCAACTCTGATCCAAAACAAAGATTAACCGCTGCTCAAGTTCTCAATCATCCATGGATCAAGGAGGATGGA
 GAAGCACCGGATGTTTCTTGGACAATGCAGTGATGTCTAGGCTCAAGCAGTTCAAAGCAATGAACAACCTT
 TAAGAAAGTTGCTTTACGGGTGATAGCCGGGTGCTTATCAGAGGAAGAAATCATGGGGTTAAAAGAGATGT

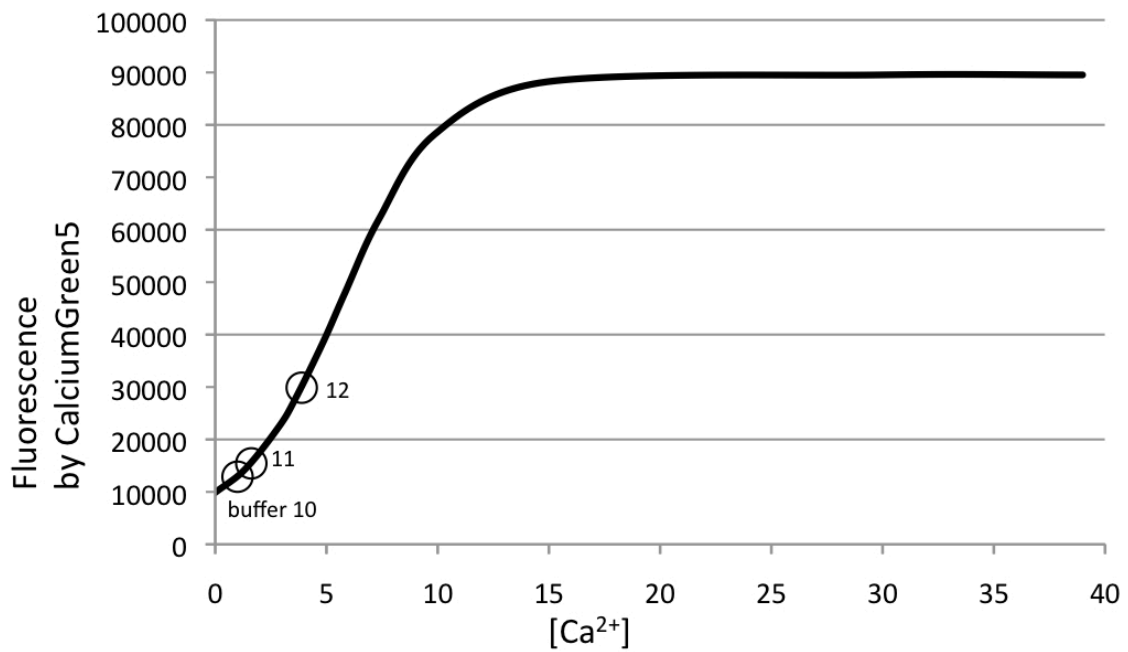
TCAAAGGAATGGACACTGACAACAGTGGAAACCATAACTCTTGAGGAACTAAGACAGGGACTTGCTAAGCAA
 GGTACAAGTTATCCGAATACGAAGTCCAGCAACTAATGGAAGCCGCGGATGCGGACGGTATGGTACCAT
 AGACTATGGGGACTTCATTGCAGCTACAATGCACATCAATCGATTAGACAGAGAAGAGCATCTCTACTCAG
 CCTTCCAACACTTTTGACAAAGACAACAGTGGATATATCACAACCGGAAGAGCTAGAGCAAGCCCTTCGGGAG
 TTTGGCATGAACGATGGCAGAGACATTAAGGAAATCATTCTGAGGTTGATGGAGACAATGATGGGCGGAT
 AAACCTACGAGGAATTTGTGGCGATGATGAGAAAAGGAAACCCAGATCCTAATCCTAAGAAGCGGGCGTGAAC
 TATCATTCAAAGGTGGCGgtctagaCCCGGGAATGcatcaccatcaccatcacGGATCC**TGA**

GST-CPK34(EF2 5A's)-6His in pGEX vector. from GST to stop codon (TGA) is shown.
 CPK34(EF2 5A's) (BOLD) starts with ATG following GST (blue) and ends with a TGA downstream of a
 6-His (blue lower case) coding site. XhoI and XbaI restriction sites (yellow lower case) are located
 between GST and CPK34, and between CPK34 and 6-His, respectively. Stop codon (TGA) after 6-His is
 highlighted as yellow.

ATGTCCCCTATACTAGGTTATTGGAAAATTAAGGGCCTTGTGCAACCCACTCGACTTCTTTTGGAAATATCT
 TGAAGAAAAATATGAAGAGCATTGTATGAGCGCGATGAAGGTGATAAATGGCGAAACAAAAAGTTTGAAT
 TGGGTTTGGAGTTTCCAATCTTCCTTATTATATTGATGGTATGTTAAATTAACACAGTCTATGGCCATC
 ATACGTTATATAGCTGACAAGCACAACATGTTGGGTGGTTGTCCAAAAGAGCGTGCAGAGATTTCAATGCT
 TGAAGGAGCGGTTTTGGATATTAGATACGGTGTTCGAGAATTGCATATAGTAAAGACTTTGAAACTCTCA
 AAGTTGATTTTCTTAGCAAGCTACCTGAAATGCTGAAAATGTTTGAAGATCGTTTATGTCATAAAACATAT
 TTAATGGTGATCATGTAACCCATCCTGACTTCATGTTGTATGACGCTCTTGATGTTGTTTTATACATGGA
 CCCAATGTGCCTGGATGCGTTCCCAAAATTAGTTTGTTTTAAAAAACGTATTGAAGCTATCCACAAATTG
 ATAAGTACTTGAATCCAGCAAGTATATAGCATGGCCTTTCAGGGCTGGCAAGCCACGTTTGGTGGTGGC
 GACCATCTCCAAAATCGGATCTGGTTCGCGTGGATCTCGTCTGTCATCTGTTGGATCCATGGAATTCct
 cgagATGGGAAATTGTTGCTCTCATGGAAGAGATTAGATGATAACAAAGAAGAACCAGAGCCGAAAAATG
 GAGCGGGGTTGTTGGTGCCGCTGAAGCCTCTGTTAGAGCTTCTAAACACCCGCCAGCATCTCCTCCTCCT
 GCAACCAAAACAAGGACCAATAGGACCTGTCTTAGGGCGACCAATGGAAGATGTAAAGAGCTCATATACATT
 GGGTAAGGAGCTAGGTCGTGGACAGTTTGGGGTACTCATCTCTGCACGCAAAAGGCCACGGGGCTGCAAT
 TCGCTTGCAAGACCATTGCTAAAAGGAAGCTCGTGAACAAAGAAGACATTGAGGATGTGAGAAGGGAGGTG
 CAGATTATGCATCACTTGACCGGTGAGCCAAACATTGTGGAGCTTAAAGGAGCGTATGAGGATAAGCATT
 TGTGCATTTGGTTATGGAGCTTTGCGCGGGAGGTGAGTTGTTGACAGGATTATCGAAAGGGACATTATT
 CGGAGAGAGCTGCAGCCTCGTTACTACGGACGATTGTGCAGATTATCCATACTTGCCATTCCATGGGGGTT
 ATCCACAGGGACTTGAAGCCTGAGAACTTTTTGTTGCTTAGCAAGGATGAGAATTCTCCTCTGAAAGCCAC
 CGACTTCGGGTTATCCGTGTTCTACAAACCAGGAGAGGTGTTCAAAGACATTGTGGGAAGTGCTTATTACA
 TTGACACCAGAGGTGTTGAGGAGGAAGTATGGACCAGAGGCTGATATTTGGAGCATTGGTGCATGTTGTAT
 ATCCTCCTGTGTGGTGTTCACCTTTTTGGGCTGAGTCAGAGAATGGGATTTTCAATGCCATCCTAAGTGG
 ACAGGTTGATTTTTCAAGCGATCCATGGCCAGTCATCTCACCACAGGCAAAAGACCTCGTTAGGAAGATGC
 TCAACTCTGATCCAAAACAAGATTAACCGCTGCTCAAGTTCTCAATCATCCATGGATCAAGGAGGATGGA
 GAAGCACCGGATGTTTCTTGGACAATGCAGTGTGCTAGGCTCAAGCAGTTCAAAGCAATGAACAACCTT
 TAAGAAAGTTGCTTTACGGGTGATAGCCGGGTGCTTATCAGAGGAAGAAATCATGGGGTTAAAGAGATGT
 TCAAAGGAATGGACACTGACAACAGTGGAAACCATAACTCTTGAGGAACTAAGACAGGGACTTGCTAAGCAA
 GGTACAAGTTATCCGAATACGAAGTCCAGCAACTAATGGAAGCcGCgGcTGCgGcCGGTgcTGAACAAT
 AGcCTATGGGGcGTTTATTGCAGCTACAATGCACATCAACAGGCTCGACAGAGAAGAGCATCTCTACTCAG
 CCTTCCAACACTTTTGACAAAGACAACAGTGGATATATCACAACCGGAAGAGCTAGAGCAAGCCCTTCGGGAG
 TTTGGCATGAACGATGGCAGAGACATTAAGGAAATCATTCTGAGGTTGATGGAGACAATGATGGGCGGAT
 AAACCTACGAGGAATTTGTGGCGATGATGAGAAAAGGAAACCCAGATCCTAATCCTAAGAAGCGGGCGTGAAC
 TATCATTCAAAGGTGGCggctctagaCCCGGGAATGcatcaccatcaccatcacGGATCC**TGA**



Appendix B. Calcium calibration curve with Fluo-3. Circles are the buffers from #1 to #11 from the left. The calcium concentration of buffer #2 and #3 are tightly superimposed shown as one circle. Among the buffers calibrated, buffer #1, 7, 8, 9, 10, and 11 were chosen to use in kinase assays. Calibrated concentration of each buffer is listed in Appendix D.



Appendix C. Calcium calibration curve with Calcium Green 5. Circles are the buffers from #10 to #12 from the left. Calibrated concentration of each buffer is listed in Appendix D.

Buffer #	Fluorescence by Fluo-3	Calibrated [Ca ²⁺], μ M	Fluorescence by CG-5	Calibrated [Ca ²⁺], μ M
1	4626	0.01		
2	5610	0.05		
3	5639	0.05		
4	6494	0.10		
5	8119	0.19		
6	11411	0.45		
7	12045	0.51		
8	14755	0.88		
9	14906	0.91		
10	15484	1.03*	12892	0.99
11	17114	1.60	15433	1.61
12			29868	3.88
13**				100

Appendix D. Calcium concentration measurement using two calcium dyes, Fluo-3 and Calcium Green 5. *1.03 μ M is used as a concentration for buffer 10. **Buffer 13 is not calibrated, 100 μ M is used as a concentration for buffer 13. Eight buffers in bold were used for kinase activity assay.